



UNIVERSITÀ
DI SIENA
1240

Department of Biotechnology, Chemistry and Pharmacy

Ph.D. in Chemical and Pharmaceutical Sciences

Cycle XXXIV

Course coordinator

Prof. Maurizio Taddei

CHIM/08

**Investigation of *in vitro* and *in vivo* pharmacokinetics and
biological evaluation of pharmacologically active
compounds**

Author

Federica Poggialini

Supervisor

Prof. Elena Dreassi

A.A. 2020/2021

To Professor Maurizio Botta

Acknowledgments

“Finding a drug involves a complex combination of many disciplines...

Only a good collaboration can drive the work to its final goal”

(Professor Maurizio Botta)

Although this thesis is presented and ascribed to me, it could not have been achieved without the valuable contribution and support of many people. I would like to thank those who allowed all this to happen, Professor Maurizio Botta, and Professor Elena Dreassi, my supervisor, who helped me in the most difficult months of my Ph.D. I grew up within the research group of Professor Botta and I have to thank my colleagues for the contribution given to me in human and scientific terms. A specific thanks to Dr. Palombi and Dr. Borgini and the rest of Botta's research group involved in the synthesis and characterization of the compounds reported in the first two chapters of the thesis.

I would also like to thank all the collaborators who contributed to the realization of the projects presented in this thesis, such as Vismederi S.r.l. and Accurange S.r.l. and Professor M. Zazzi (University of Siena), for evaluating the antiviral activity of Methyl-Arylidene Structure (MAS) compounds, and Lead Discovery Siena S.r.l. for the facilities provided. The project discussed in the first chapter of this thesis was partially supported by the European Union's Horizon 2020 Research and Innovation Programme under ZIKAlliance Grant Agreement no. 734548 and by PRO-CREO project PANVIR.NET.

IRBM S.p.A. and Promidis S.r.l. in the figure of Dr. Ferrante, Professor Summa, and Dr. di Fabio have made a precious contribution to the development of NO-donors/largazole hybrids, while Professor Marco Lolli (University of Torino) and Professor Maria Frosini (University of Siena) have been involved in the characterization of compounds and in the *in vitro* NO release assay, respectively.

I would also like to thank Professor Per Artursson, from the Department of Pharmacy at the University of Uppsala, for having hosted me for five months in his research group and allowed me to collaborate in the project described in the third chapter of the thesis.

AstraZeneca, especially in the figure of the Chief Scientist & Head of Oligonucleotide discovery Dr. Shalini Andersson, Dr. Deepak Kumar Bhatt, and all other scientists who contributed to the synthesis, purification, and characterization of ASOs, and for their precious contribution given to the project. Professor Jan Kihlberg and his research group from the Department of Chemistry at Uppsala University, for the synthesis of the CPP used in the experiments, and Dr. Varun Maturi and Dr. Madlen Hubert, from the Department of Pharmacy at the University of Uppsala, for the constant support provided.

Last but not least, all the scientists with whom I have had the pleasure of collaborating in these years of Ph.D. in various projects reported in the papers at the end of this thesis.

Abstract

The first part of this thesis deals with the evaluation of *in vitro* and *in vivo* pharmacokinetics of novel broad-spectrum antiviral compounds active against enveloped viruses. Due to the relevant role that viral infections play in causing death worldwide, and the lack of antiviral compounds and vaccines for most viruses, the identification of promising broad-spectrum antiviral compounds represents a relevant opportunity for improving the efficacy of antiviral therapies. The design and synthesis of new series of antiviral compounds with 1H-pyrrol-methylene thioxodihydropyrimidine structure, has been realized by Professor Maurizio Botta's research group, at the University of Siena. Compounds' antiviral activity has been evaluated on several enveloped viruses, such as ZIKAV, DENV-2 and five influenza strains including the pandemic strain H7N9. The selectivity against enveloped viruses, time of addition and binding experiments confirmed their ability to intercalate in the viral envelope membrane, oxidize phospholipids and alter the fluidity of the lipid bilayer, compromising the efficacy of the virus-cell fusion step and preventing viral entry. With the aim of investigating the *in vitro* ADME properties, the most active compounds were selected to assay their chemical-physical properties and early select the most promising lead candidate. Thus, membrane permeability, binding to human serum albumin, and stability in human plasma and microsomes have been assayed. Finally, the lead candidate was selected to evaluate preliminary *in vivo* pharmacokinetic parameters; after formulation studies, the compound was administrated intravenously (*iv*) at the dose of 25 mg/kg and 12.5 mg/kg.

The second chapter of this Ph.D. thesis concerns the investigation of the *in vitro* biological profile of nitric oxide-donor largazole prodrugs. Two hybrid analogues of largazole, as dual HDAC inhibitor and nitric oxide (NO) donors potentially useful as anticancer agents, have been designed and synthesized thanks to the collaboration between Professor Maurizio Botta's research group and IRBM. Largazole is a natural product identified as the most potent and selective Class-I deacetylase (HDAC) inhibitor, that showed a broad-spectrum growth-inhibitory activity against epithelial and fibroblastic tumor cell lines and a low cytotoxicity profile. Over the last decades, dual nitric oxide (NO) donors/HDAC inhibitors

have been developed as novel anticancer chemical entities, potentially more efficacious than selective HDAC inhibitors, owing to the capability of NO to specifically modulate the function of some HDAC isoforms and to overcome tumor cell resistance to conventional treatments. Thus, after the synthesis, the characterization of derivatives compounds and the *in vitro* NO release assay performed by Professor Maria Frosini using the Griess method, biological evaluation of their antiproliferative activities against U-2OS (human osteosarcoma cells), Caco-2 (human colorectal adenocarcinoma cells), and IMR-32 (human neuroblastoma cells) have been conducted. To further explain the additive antiproliferative effect of NO-donor compounds vs largazole, their stabilities both in human plasma and in cell culture medium were assessed.

The third and last chapter of this Ph.D. thesis deals with the project I participated in during my exchange period at the research group of Professor Per Artursson, who hosted me for 5 months, at Uppsala University. In collaboration with AstraZeneca, a series of antisense oligonucleotide (ASO) conjugates, targeting *MALAT1* chosen as a model target, were used to assess and validate their silencing efficiency and enhance/overcome endosomal escape. For these studies, four ASO-conjugates were synthesized and purified by AstraZeneca. The *MALAT1* silencing efficiencies of lipophilic ASO-conjugates and a peptide-ASO have been determined in the presence and absence of a cyclic cell permeation peptide (CPP) in two human embryonic kidney (HEK293) cell lines of which one overexpressing the target G-protein coupled receptor selected for the study. The CPP used in our experiments to investigate the ability to enhance endosomal escape has been synthesized by Professor Jan Kihlberg's group at Uppsala University. For this purpose, the expression levels of the *MALAT1* gene mRNA were measured using qPCR in a time (0-24-48 hrs) and concentration (0.5-2.5-5 μ M of ASOs and 5-10-15 μ M of CPP)-dependent manner.

Index

Acknowledgments	4
Abstract	7
Index of Figure.....	14
Index of Table.....	16
Index of Scheme	17
Chapter 1.....	18
Introduction.....	18
Viral Infections	18
Enveloped Viruses	20
The Envelope Membrane	21
Virus Life Cycle.....	23
Entry pathway.....	26
Pharmacological strategies against enveloped viruses.....	31
Influenza Viruses	38
Structure.....	40
Replicative cycle.....	41
Tissue tropism	42
Antiviral drugs.....	43
Flaviviruses	44
Structure.....	44
Flavivirus life cycle.....	45
Zika virus (ZIKV).....	46
Dengue Virus (DENV)	47
Vaccines for Flaviviruses.....	48
Anti-Flavivirus drugs	50
Methyl-Arylidene Structure (MAS) Compounds.....	53
Aim of the work.....	56
State of art.....	58
Structure-activity relationship (SAR).....	58
Modifications on part A of the scaffold.....	58
Modifications on part B of the scaffold.....	60

Modifications on part C of the scaffold	61
Mechanism of Action (MoA)	61
Experimental Section	65
Biological evaluation	65
Influenza virus.....	65
ZIKA & Dengue Virus	65
<i>In vitro</i> ADME profiling.....	66
Solubility	66
Permeability: PAMPA Assay	66
Metabolic stability	68
Plasma stability	68
HPLC-UV-MS method	69
Albumin binding	70
<i>In vivo</i> preliminary pharmacokinetic (PK) studies	71
Formulation.....	71
PK & BD at 25 mg/kg and 12.5 mg/kg doses	72
Results and Discussion	73
Biological evaluation	73
Influenza virus.....	73
ZIKA Virus	75
Double rounds of infection: ZIKV and DENV	76
<i>In vitro</i> ADME profiling.....	77
Solubility	77
Permeability	77
Metabolic stability	78
Plasma stability	80
Albumin binding	80
<i>In vivo</i> preliminary pharmacokinetic (PK) studies	82
Conclusions	86
Chapter 2	87
Introduction	87
Histone Deacetylases.....	87
HDACs & Cancer	92

The dual role of Sirtuins in cancer progression.....	95
HDACs inhibitors	97
Naturally occurring HDAC inhibitors.....	99
Largazole.....	101
Nitric Oxide.....	104
NO & Cancer: a bimodal effect	105
Dual NO donors/HDAC inhibitors	110
Aim of the work.....	113
Experimental Section.....	114
Synthesis of NO-donors/largazole hybrids	114
Biological Evaluation	114
In vitro determination of NO release by Griess method	114
Cytotoxicity Assay.....	115
Chemical and Metabolic Stability Assay	116
HPLC/UV-MS Method.....	116
Results and Discussion	118
Synthesis of NO-donors/largazole hybrids	118
NO release by Griess method.....	119
Antiproliferative Activity.....	119
Chemical and Metabolic Stability	121
Conclusions	123
Chapter 3.....	125
Introduction.....	125
RNA-target therapy.....	125
Antisense Oligonucleotides.....	129
Chemicals and backbones modifications.....	131
Delivery challenges	134
Cellular uptake and trafficking.....	138
Mechanism of Action	140
Pharmacokinetics of therapeutic oligonucleotides	142
<i>MALAT1</i> : a long non-coding RNA.....	143
Molecular Function of <i>MALAT1</i>	145
Aim of the work.....	148

Experimental Section	149
Biological evaluation	149
Cell Culture	149
Stimulation with ASOs conjugates	149
RNA extraction & quantification	151
RT-PCR and qPCR assays	152
Results and Discussion	154
Conclusions	163
Appendix I	165
Appendix II	167
Bibliography	168

Index of Figure

Figure 1.....	19
Figure 2.....	20
Figure 3.....	22
Figure 4.....	24
Figure 5.....	26
Figure 6.....	28
Figure 7.....	34
Figure 8.....	37
Figure 9.....	39
Figure 10.....	41
Figure 11.....	47
Figure 12.....	51
Figure 13.....	53
Figure 14.....	53
Figure 15.....	54
Figure 16.....	55
Figure 17.....	56
Figure 18.....	59
Figure 19.....	60
Figure 20.....	61
Figure 21.....	61
Figure 22.....	63
Figure 23.....	64
Figure 24.....	64
Figure 25.....	79
Figure 26.....	80
Figure 27.....	83
Figure 28.....	84
Figure 29.....	85
Figure 30.....	87
Figure 31.....	90
Figure 32.....	93
Figure 33.....	100
Figure 34.....	101
Figure 35.....	104
Figure 36.....	106
Figure 37.....	113
Figure 38.....	119
Figure 39.....	126
Figure 40.....	132

Figure 41 133
Figure 42 135
Figure 43 141
Figure 44 144
Figure 45 147
Figure 46 148
Figure 47 154
Figure 48 155
Figure 49 156
Figure 50 157
Figure 51 158
Figure 52 159
Figure 53 161

Index of Table

Table 1	30
Table 2	58
Table 3	62
Table 4	69
Table 5	70
Table 6	74
Table 7	75
Table 8	76
Table 9	77
Table 10	78
Table 11	78
Table 12	81
Table 13	83
Table 14	98
Table 15	109
Table 16	120
Table 17	121

Index of Scheme

Scheme 1 112
Scheme 2 114
Scheme 3 118

Chapter 1

Introduction

Viral Infections

According to the *World Health Organization's* (WHO) ranking, viral infections are at the 4th position as the most deadly diseases.¹ Nowadays, although several signs of progress have been successfully made in the attempt to fight and eradicate viral infections such as the ones caused by HIV (Human Immunodeficiency Virus) and HCV (Hepatitis C Virus), vaccines and innovative antiviral strategies are still missing for the whole of viruses.² Since March 2020 when WHO declared Covid-19 a pandemic, public opinion and media attention have been focused on emerging and re-emerging infectious diseases which still afflict the world's population. Dealing with emerging infectious diseases (EIDs) can be distinguished almost 4 different categories (Figure 1):

1. **Emerging diagnosis** of old infectious;
2. **Newly emerging** infectious diseases;
3. **Re-emerging** infectious diseases;
4. **Emerging resistance** of infectious pathogens to therapeutic approaches.

Factors that mostly contributed to this emergence are correlated to human activities such as deforestation, change in air quality, and climate that alter the ecology of the microbial world facilitating the spread of infectious diseases.³ The greater part of emerging or re-emerging viruses are zoonoses. According to WHO, zoonosis is an infection or a disease that naturally can be transmitted from vertebrate animals to humans, representing a large amount of new and existing diseases in humans.⁴ Moreover, it has been demonstrated that the passage among different species is easier for enveloped viruses than for the non-enveloped ones, probably due to the mechanism that allows virus entry: the fusion between viral and cell membrane. Enveloped viruses are characterized by the presence of an outer lipidic membrane covering the capsid that protects the pathogen from enzymatic degradation and makes it less susceptible to host immune defenses.⁵

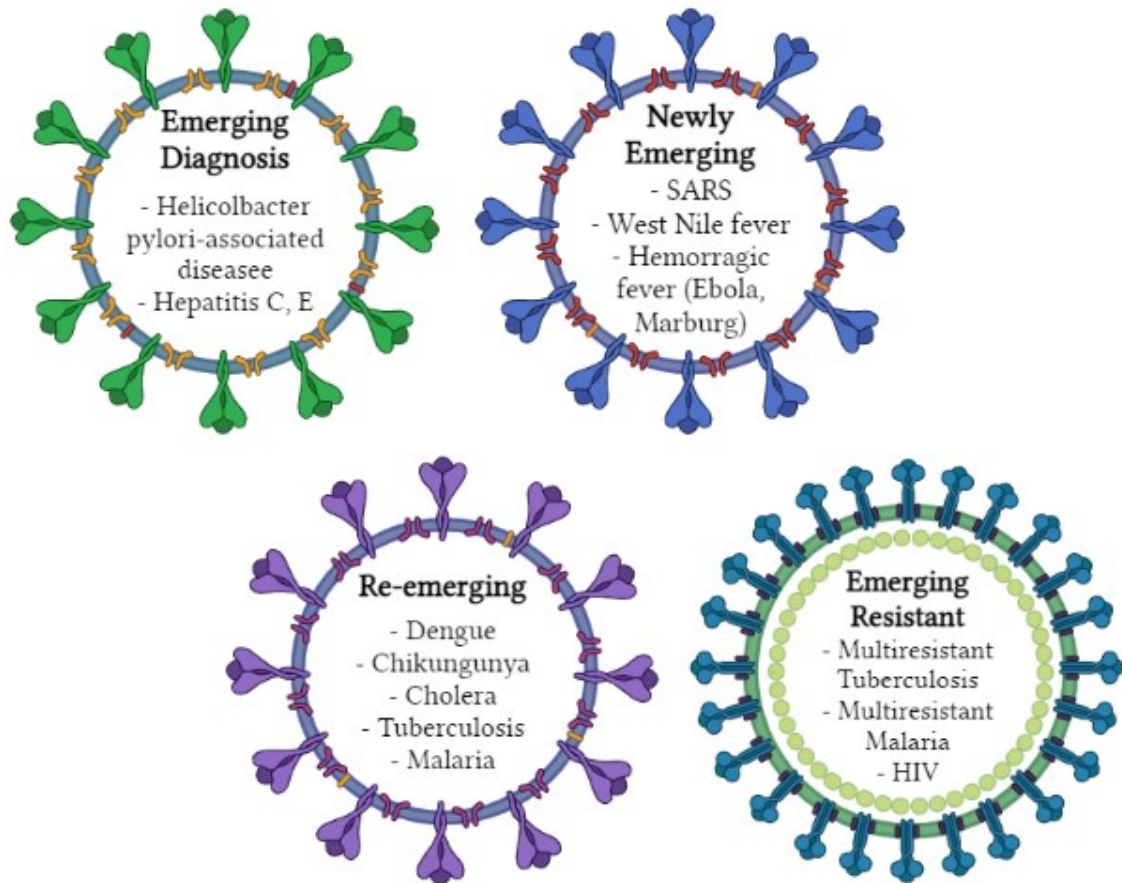


Figure 1

Emerging Infectious Diseases (EIDs). EIDs can be distinguished into four categories as Emerging Diagnosis, Newly Emerging, Re-emerging, and Emerging Resistance.

Unfortunately, the still lack of vaccines or efficacious therapy for a large number of viral infections emphasizes the urgent need to develop new broad-spectrum antiviral compounds that can act on a wide type of viruses targeting fundamental steps of their life cycle rather than specific viral proteins, leading to the death of viral pathogen.² Otherwise, the development of new antiviral compounds is a complicated process that has to deal with the age-old problem of drug resistance: in fact, viruses rapidly undergo mutations necessary to resist the activity of the most commonly used antiviral compounds. These mutations usually occur both after a first viral exposition to an antiviral drug, both previously due to natural variability to which viruses are exposed.⁶ Another strategy to fight viral infection is represented by the development of molecules able to hit a specific viral target that can be common to several species such as the viral envelope.

Enveloped Viruses

Viruses are small obligate parasites characterized by a diameter between 20 and 300 nanometers, able to infect plants, animals, and humans. As obligate parasites they are not capable to produce energy and replicate by themselves; to live and propagate, viruses require to infect cells by altering their physiological functions and exploiting their complex metabolic and biosynthetic system for propagation.

Since 1892 when viruses were discovered, about 5000 viruses are known to date. Viruses can be classified into several types considering the morphology, the chemical composition (positive or antisense, single, or double-strand), the genetic material (DNA or RNA) encapsulated inside the capsid, the protein shell that protects nucleic acids from enzymatic degradation. They can also be distinguished into naked viruses and enveloped viruses (Figure 2).

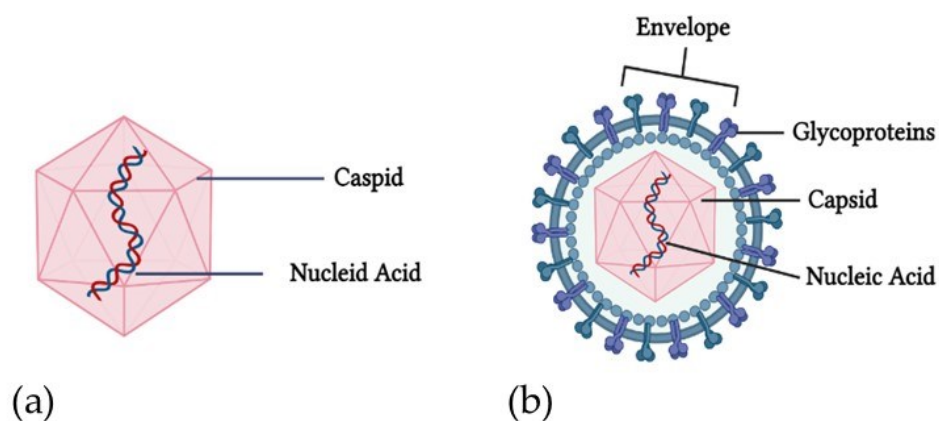


Figure 2

Structures of viruses. Viruses can be distinguished into two major categories: (a) Naked Nucleocapsid Virus, (b) Enveloped Virus.

As mentioned above, new-emerging and pre-existing infectious diseases are mainly caused by envelope viruses classified in the Emerging Infectious Diseases/Pathogens by the US National Institute of Allergy and Infectious Diseases (NIAID) such as Severe Acute Respiratory syndrome-Coronavirus 2 (SARS-CoV-2), Ebola virus (EBOV), West Nile (WNV), Dengue virus (DENV), Hepatitis C, HIV, Zika virus (ZIKAV). Thus, the envelope membrane represents an ideal and promising target for developing new broad-spectrum antivirals (BSAs) to fight the spread of viral infections.^{5,7}

The Envelope Membrane

The viral envelope is the outer shell surrounding the protein capsid and protecting genetic material, primarily made of lipids that viruses get from the host's membrane during the budding process; this external lipidic membrane is enriched with glycoproteins that act as anchor binding specific receptors on cell's membranes and facilitating the entrance of the budded virus into new cells.⁸ Viruses dress up with one or more lipidic bilayers from the host membrane during the budding, one of the most important steps in the viral life cycle. The lipidic composition of the envelope membrane differs significantly from virus to virus; in fact, lipids are not randomly combined to form the envelope, but viruses can select specific lipidic domains, called lipid rafts and enriched with cholesterol, glycerophospholipids, and sphingolipids that best suit with them. The relevance of those specialized lipidic domains appears when several studies have confirmed that viruses such as EBOV, measles, and Influenza virus exploit lipid rafts to get off infected cells. Regarding HIV-1 and HIV-2, their envelopes are significantly different from each other and from the host membrane from which they originate; in fact, has been demonstrated a relevant increase in cholesterol concentration compared to that of phospholipids. This probably leads to having a more stable viral membrane.⁵

As shown in Figure 3, other relevant components of viral envelope are cell membrane-derived proteins and glycoproteins:

- *Envelope proteins (E)*, exposed on the outer surface, are virus-encoded engaged in the binding process to specific cell receptors that enhance the virus's capability to spread and evade the immune system;
- *Membrane proteins (M)*, typically inserted in the external layer of the envelope and characterized by a hydrophobic trans-membrane (TM) domain, represent about 30% of all viral proteins, playing a crucial role in viral energy metabolism, signal transduction, and immune protection;
- *Spike proteins (S)*, highly glycosylated, are characterized by the presence of a large trans-membrane fusion protein made up of 1160-1400 amino acids. Unlike envelope and membrane proteins primarily implicated in virus assembly, S proteins play a

fundamental role in the process of host cells penetration and viral infection initiation and propagation.^{9,10}

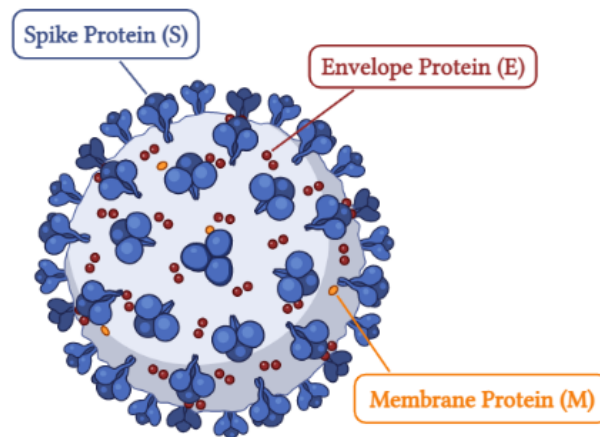


Figure 3

Viral proteins. In addition to lipids, the enveloped membrane is composed of proteins: Envelope Protein (E), Membrane Protein (M), and Spike Protein (S); each plays a specific role in the viral life cycle and spread of infection.

The ongoing health emergency due to Covid-19 and the emergence of several new variants of coronavirus, has sparked renewed interest in the key role played by spike protein in the spread of infection; in fact, SARS-CoV-2 can enter host cells thanks to a binding made between spike protein and angiotensin-converting enzyme 2 (ACE-2) particularly overexpressed in lung cells. Glycosylation of viral proteins, carried out in the glycosyltransferase enzymes in the secretory pathway of ER-Golgi complex of host cells, represents an essential step for making virions suitable to interact with host cells and escape from the immune system. For example, EBOV glycoproteins are covered by N- and O-bound glycans that create a central structure covered by the oligosaccharides prejudicing the interaction with neutralizing antibodies, and an external region with the binding site for the receptors. As for lipidic composition, also for what regards glycoproteins, there is a lot of heterogeneity on the surface of different viruses: gp120 and gp41 in HIV-1 bind host receptors; in SARS-CoV-2 spike proteins are responsible for binding to ACE-2; in influenzas virus hemagglutinin and neuraminidase promotes the binding with sialic acid on the surface of host cells; in DENV envelope protein carries out the step of attachment and fusion with human cells.

In conclusion, the envelope membrane displays key-role in several processes:

- hiding capsid antigens from circulating antibodies and acquiring part of the host membrane allows enveloped viruses to escape from the immune system better than non-enveloped ones;
- acting as a sort of viral adaptation facilitates cell entry by endocytosis and exit by budding which doesn't compromise the cellular integrity useful for another replicative cycle;
- expressing several types of viral receptors, allowing viruses to infect different cells and tissues.⁵

Virus Life Cycle

Viruses are obligate intracellular parasites that require to enter inside target cells to propagate the infection. Several steps involved in this process occurring inside cells are classified under the name of "virus life cycle" which can be distinguished into three major stages: *entry*, *genome replication*, and *exit*.

Naked viruses can enter cells through two different ways after the viral capsid binding to host cell receptors: a receptor-mediated endocytosis process or the creation of channels in the host membrane that allows viral genetic material to be injected into cells. After that, genome replication occurs inside the cellular nucleus, and at the end of their life cycle, non-enveloped viruses are released out of cells thanks to membrane lysis.

Regarding enveloped viruses, their life cycle is more complex (Figure 4). The initial step of virus infection is called *binding*; this represents the first contact between the virus and the host cell, occurring through the binding to viral receptors or extracellular attachment factors, usually glycoconjugates (i.e., glycoproteins, glycolipids, proteoglycans), involved in cell-cell interaction, ion transport, and essential elements for recognition and binding to the cell membrane. Virus-cell interactions through attachment factors show an electrostatic and non-specific nature. For instance, heparan sulphate is the common attachment factor for herpes virus, DENV, papillomavirus, and adeno-associated viruses. Virus receptors, as a consequence of the binding to the virus particles, favour the virus particles' penetration into cells in a more specific way. HIV-1 infects CD4⁺-expressing T lymphocytes after the interaction of gp120 to CD4⁺, influenza virus receptors bind sialic acid in a strong specific

manner, and SARS-CoV-2 infects cells thanks to spike protein that promote the binding to ACE-2. The more specific is the binding, the greater will be the tissue tropism that determines the nature of the disease and the endocytotic path that the virus will follow.

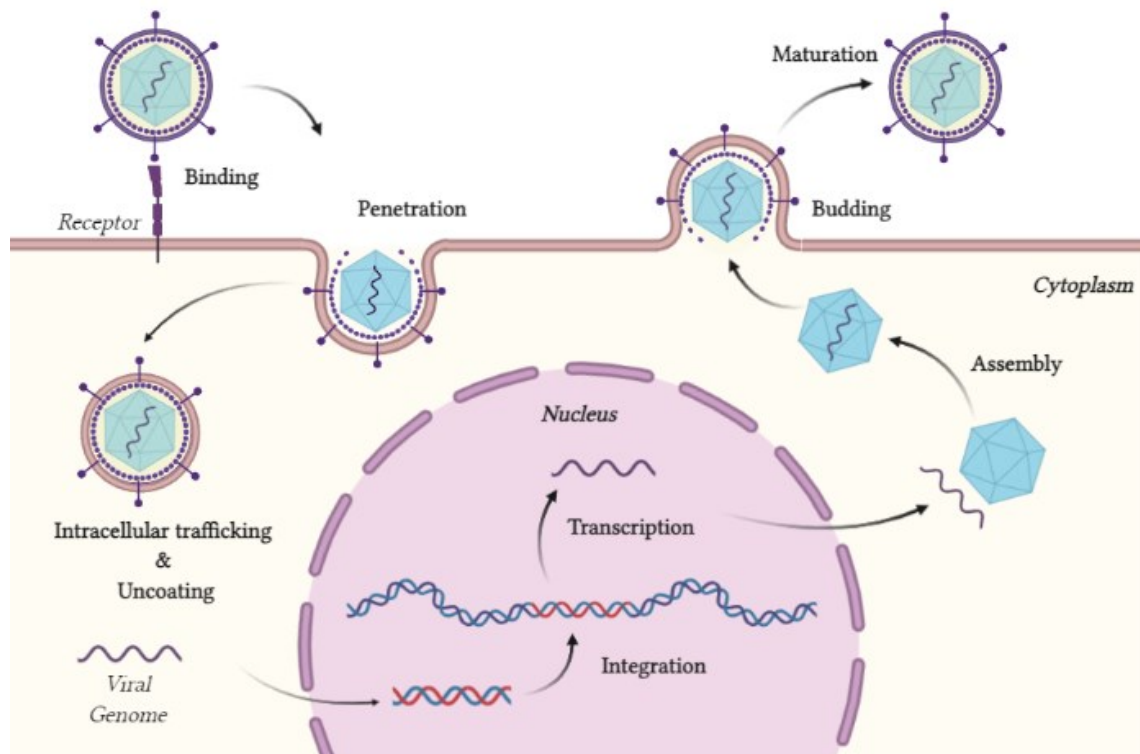


Figure 4

Viral life cycle. Enveloped viruses need to perform several steps during their life cycle to enter inside cells, replicate their genomic material and spread infection after releasing cells. The cycle can be distinguished into three fundamental phases: entry, genome replication, exit.

Following the assessment of the binding between virus and target cells, the next step consists of the **penetration** into the cytoplasm. This process differs from naked to enveloped viruses; if on one hand, naked viruses exploit only a receptor-mediated endocytotic mechanism for penetration, enveloped ones can pass through cell membrane exploiting two different mechanisms:

- *Direct fusion:* the fusion between the viral envelope and cell membrane allows a rapid viral capsid delivery into the cytoplasm (e.g., Retrovirus penetrates using this mechanism);
- *Receptor-mediated endocytosis:* after the initial binding of viral particles to specific receptors on cell surface, a coated pit is formed on the plasma membrane facilitating the trigger of endocytosis and leading to endosome formation in which virus

particles are located. After that, viruses have to reach the cytoplasm breaking down from endosomes using several mechanisms which will be elucidated later. Enveloped viruses escape from the early endosome thanks to a fusion between the viral envelope and the endosomal membrane triggered by acid pH that causes conformational change and the consequent activation of the fusion peptide embedded on the glycoproteins provoking the endosome disruption; non-enveloped virus, on the contrary, easily leave endosome thanks to a lytic mechanism induced by capsid proteins.

Completed the *entry* step, the most important step for enveloped viruses that will be discussed in a more detailed way in the next chapter, viruses undergo a process called *intracellular trafficking*. This step allows pathogens to reach their appropriate cellular site for starting genome replication. If a virus replicates in the cytoplasm, a microtubule-mediated transport routes the viral nucleocapsid to the site for replication, if the virus replicates in the nucleus the same transport system allows the penetration of the nuclear membrane and the achievement of the perinuclear area. During the previous step, virus particles are driven to the specific replication sites, but before starting this important passage, they require to release their genomic material (DNA or RNA) in the perinuclear space through the *uncoating* process. If viruses replicate in the nucleus, the viral genome enters via a nuclear pore causing a partial disruption or some morphological changes (adenovirus and herpes virus, respectively) allowing the entrance of DNA into the nucleus. Here, *viral gene expression* and *genome replication* happen with different strategies among the virus families, but always depend on host translation machinery, the ribosomes, for their protein synthesis. Finally, the virus life cycle gets with the *exit* process which can be distinguished into 3 fundamental steps: the *assembly* where capsid proteins and viral genome reassemble themselves; the *budding* process, triggered by a peptide motif named late (L) domain, is typically used by enveloped viruses to leave infected cells through endocytosis; the *maturation* process, essential to confer infectivity to viral particles, is the last one that occurs extracellularly after release.¹¹

Entry pathway

Several studies by electron microscopy, cryo-EM, and light microscopy have been conducted to elucidate the mechanisms used by enveloped viruses in the entry step. Few viruses can fuse their envelope with the cellular membrane after the initial attachment of glycoproteins to cell receptors. An example is represented by HIV-1 which penetrates membrane cellular after an initial interaction between gp120 and CD4 which induces conformational changes allowing chemokines CCR5 or CXCR4 interaction that finally induce conformational changes of gp41 to the fusion protein. Viruses take advantage of different endocytotic mechanisms typically used by cells to uptake fluids, solutes, and small particles. As reported in Figure 5, several pathways are used by cells for the up-taking process, and some of them are exploited by viruses as well for the entry step.¹²

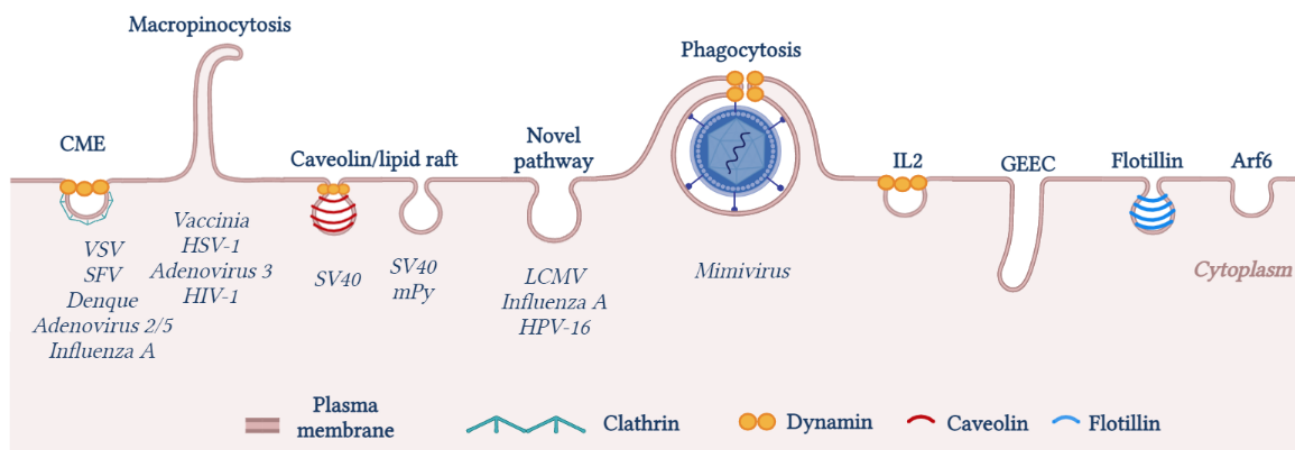


Figure 5

Endocytotic mechanism. Multiple mechanisms are involved in the entry pathway of several viruses: clathrin-mediated endocytosis (CME), micropinocytosis, caveolar/lipid raft mediated endocytosis, as well as several novel mechanisms. Only in a few cell types can be found a phagocytotic mechanism used for taking up large particles. Moreover, other pathways are used by cells to carry specific cellular cargo, but not yet used by a virus such as IL-2, the GEEC pathway, flotillin- and ADP-ribosylation factor 6 (Arf6)-dependent pathways.

The most common paths used in the entry step are clathrin-mediated endocytosis (CEM), caveolar/lipid rafts-mediated endocytosis, and macropinocytosis. Vesicular Stomatitis virus (VSV), Semliki Forest virus (SFV), Dengue virus (DENV), Adenovirus 2/5, and Influenza A typically exploit the CME mechanism, literally moving along the membrane until they find

a clathrin coat formed on the plasma membrane. After interaction with specific attachment factors, the load is released to the endosomal network consisting of early endosomes (EEs) that evolve in mature endosomes (MEs) and finally into late endosomes (LEs). CME of viruses is a rapid process; in fact, less than 2 minutes are required by load material to reach the EEs after internalization through the CEM pathway, and just after 30-60 minutes they reach MEs, LEs, and finally the lysosomes in the perinuclear space where viruses will be released for the next step of their life cycle. The complex maturation process from EEs to LEs involves a series of changes in the endosomes and induces viral proteins to start the fusion. Binding to receptors, low pH exposition, and the consequent activation of protease are the most common changes that occur in LEs and trigger viral proteins.¹³ While, herpesviruses and retroviruses begin their entry step binding to the receptor, fusing their membranes with the host plasma membrane at physiological pH, influenza, alphaviruses, and flaviviruses required only low pH to activate their fusion proteins. The gradual acidification in LEs until values below 5 is caused by variation in subunit composition of the vacuolar-type H⁺-ATPase (V-ATPase) and several isoforms of chloride channels.^{14,15} The maturation process consists of the intermediate formation of a hybrid endosome (ME) characterized by Rab5 and Rab7 domains of both early and late endosomes, which undergo further acidification allowing the changeover to mature LEs. The evolutionary process from EEs to LEs results in the final activation of viral proteins that is relevant for the Influenza A virus which uses this pathway for entry. Other enveloped viruses, such as respiratory syndrome coronavirus (SARS-CoV) and Middle East respiratory syndrome coronavirus (MERS-CoV) trigger the binding to receptors followed by protease activation, always at low pH. Between viral proteins can be distinguished three different classes depending on the way used to prime them:

- Class I represented by influenza virus protein HA;
- Class II typified by flavivirus protein E;
- Class III embodied by rhabdovirus glycoprotein G.

For class I and II proteins, the prime step is mandatory; in fact, they have to be converted into a competent state fusion through a proteolytic cleavage that generates the receptor-binding domain *N*-terminal fragment, and the fusogenic fragment *C*-terminal (HA₁ and HA₂

in influenza virus, respectively) composed by a hydrophobic fusion peptide and a transmembrane domain.¹⁶ After that, the fusogenic conformational changes occur in an irreversible exothermic way leading to a low energy conformation which, thanks to the high energy released, can overcome the hydration forces that usually reject the lipid heads when two membranes become closer less than 3 nm avoiding their spontaneous fusion. Fusion is characterized by sequential steps (Figure 6). After the virus has approached the host cells, viral proteins undergo conformational changes that allow the creation of a bridge between the two membranes that collapsing leads to the formation of two membrane fragments that come together resulting in distortions.

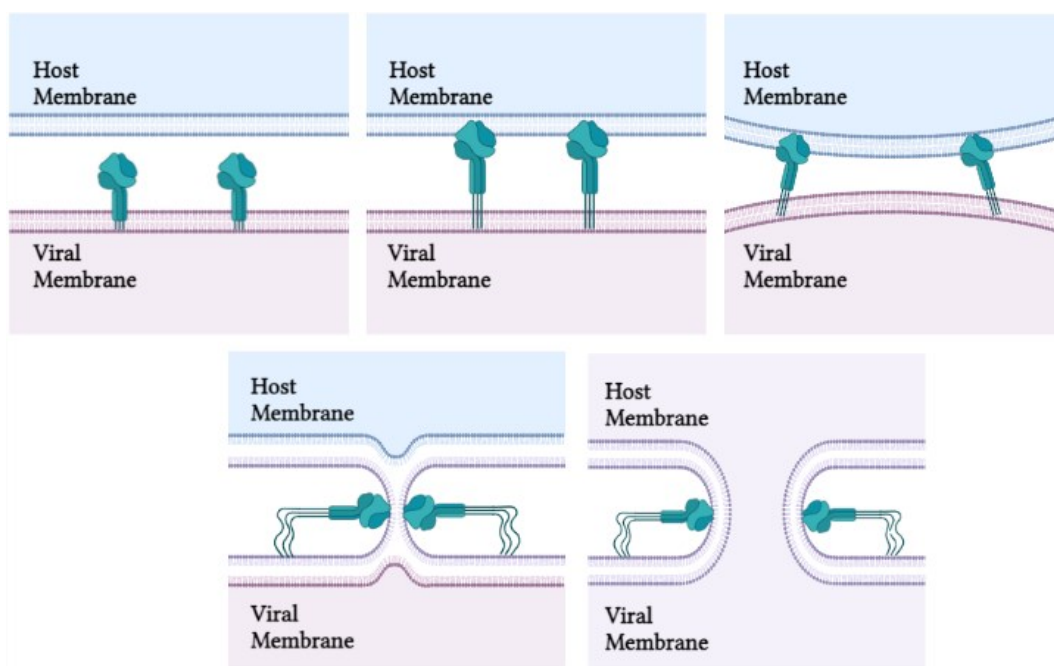


Figure 6

Representation of fusion process. When the host membrane and viral membrane come closer, the viral proteins open up to form a bridge between both membranes. Then, the bridge collapses, and membranes undergo a consequent distortion leading to the final formation of the hemifusion stalk which forms a transient fusion pore stabilized irreversibly by a final protein refolding.

Finally, the hemifusion stem forms a transient fusion pore which will be made irreversible by a final protein refolding. Through this pathway, viruses can penetrate the cytoplasm and start their replication cycles.^{5,12}

Caveolar/lipid-rafts are small membrane domains characterized by high percentages of cholesterol and sphingolipids, typically found in plasma as well as intracellular membranes and extracellular vesicles. They are considered fundamental for the maintenance of several

cellular functions such as endocytosis, vesicle formation, receptor activation, and intracellular trafficking of lipids and proteins. At the same time, caveolar/lipid-rafts display a key role in essential steps in the viral life cycle, such as entry and budding. The distinctive characteristic of the caveolar/lipid rafts-mediated endocytosis pathway is the formation of primary endosomes due to cholesterol and lipid rafts and driven by tyrosine kinase and phosphatases. The process is triggered by the receptor-virus attachment leading to an accumulation of viral particles that promote the development of the membrane curvature and consequently endocytosis. After internalization, the process follows the endosomal network from EEs to LEs slowly and asynchronously, allowing viruses to complete their penetration step in 6-12 hrs. Among the different viruses which use the caveolar/lipid rafts-dependent mechanism, mouse Polyomavirus (mPy) and Simian virus 40 (SV40), belonging to the polyomavirus family, are the most studied examples. Using gangliosides as receptors they can interact with cellular membranes inducing the endocytotic mechanism and the intracellular pathways. SV40 entry by caveolar-mediated mechanism has been studied for several years, but recently has been discovered an alternative pathway caveolar, clathrin, dynamin-II, and Arf6 independent, but still cholesterol-sensitive and tyrosine kinase driven.¹⁷ Unlike the two previous pathways, macropinocytosis is a nonspecific endocytotic mechanism that does not require binding to specific cellular receptors. Macropinocytosis is a transient actin-dependent mechanism induced by growth factors, that allows the internalization of fluids in large vacuoles, called macropinosomes. When membrane ruffles fold back onto the cellular membrane, the fluid-filled vacuoles are formed in irregular sizes and shapes. Several particles can also induce ruffling and stimulate the macropinocytotic internalization process, such as necrotic cells, bacteria, and viruses. Moreover, micropinocytosis requires several cellular components to happen. The activation step, for example, involves cellular lipids, kinases, GTPases, myosins, actin modulatory factors, and fusion-fission factors.

Macropinocytosis is exploited by several families of viruses as a direct route of internalization; Vaccinia Virus, Adenovirus 3, Herpes Simplex Virus 1 (HSV-1), and Human Immunodeficiency Virus (HIV-1).

Virus	Receptor	Trigger
Clathrin-mediated endocytosis (CME)		
Vesicular stomatitis virus	LDL receptors and family members	pH<6.4 Early endosome
Influenza A virus	Sialic acid-containing glycoconjugates	pH<5.4 Early endosome
Macropinocytosis		
Vaccinia virus	Heparan sulphate	Low pH and macropinosomes
Respiratory syncytial virus	Heparan sulphate	Macropinosomes
Ebolavirus	Host lectins (e.g., DC-SIGN)	Cathepsins (B, C) and macropinosomes
Kaposi sarcoma virus	Heparan sulphate, Proteoglycan, Integrins $\alpha 3$ ($\beta 1$, $\alpha V\beta 3$ and $\alpha V\beta 5$)	Macropinosomes
SARS-CoV	ACE-2	Macropinosomes
Other mechanisms		
Poliovirus	Poliovirus receptor	Early endosomes
Lymphocytic choriomeningitis virus	A-Dystroglycan	pH<6.3 Late endosomes
SARS-CoV	ACE-2	pH<6.2

Table 1

Pathways of enveloped virus entry into cells. Different mechanisms are exploited by enveloped viruses for penetrating plasma membranes and spreading an infection; after the initial interaction with the specific attachment factors, the entry mechanisms progress through a membrane fusion step.

The first one is probably the best example of virus entry by macropinocytosis: the interaction between virus and cells leads to the formation of large blads on the plasma membrane that through a retraction process uptake virions and fluids. Additionally, the enrichment of vaccinia's membrane of phosphatidylserine, essential for the clearance of apoptotic debris through micropinocytosis, suggests that this virus can act as an apoptotic body inducing an endocytotic response.¹² As previously described, can be distinguished several mechanisms

used by viruses to penetrate membranes and enter into cells; Table 1 summarizes the principal entry mechanisms exploited by enveloped viruses to enter inside cells, underling also which receptors are involved and the intracellular conditions necessary for the fusion step.

Pharmacological strategies against enveloped viruses

Several families of enveloped viruses are recognized to be able to provoke severe infection diseases; can be distinguished herpes virus (HSV-1 and HSV-2) cytomegalovirus (HCMV), hepadnavirus (HBV), flavivirus (ZIKV, DENV, WNV, and YFV), retrovirus (HIV) and Orthomyxovirus (Influenza A and B). Among the strategies used to counteract viral infections, vaccination remains one of the most efficient ways in preventing and fighting the advance of viruses. The currently available vaccines against viruses are mainly made of inactivated viruses or attenuated ones and display a significant efficacy in the control of infectious diseases.¹⁸ To date, no effective antiviral strategy is available to combat viruses responsible for serious chronic diseases such as Hepatitis B (HBV), so the development of a specific and potent vaccine has represented a milestone step in the prevention of this disease. In contrast, for infectious diseases such as Hepatitis C (HCV) or tropical diseases caused by the Dengue virus, which can cause 390 million cases of infection every year, no vaccine is yet available.¹⁹

Recently, the ongoing global pandemic of Covid-19 displays the urgent request for novel antiviral compounds and at the same time underlines the strategical role that vaccines can play in preventing severe infectious diseases. Several laboratories all around the world are working on the development of new Covid-19 vaccines, but actually, only Pfizer/BioNTech, AstraZeneca-SK Bio, Serum Institute of India, Janssen/Johnson & Johnson, and Moderna vaccines have been approved for emergency use and listed on WHO Emergency Use Listing (EUL).²⁰

Currently, there are three main types of Covid-19 vaccines:

- *mRNA vaccines*, a promising alternative to more traditional ones due to their high potency and safe administration, contain viral material that helps our cells to

recognize and fight the S-protein found on the surface of the Covid-19 virus-producing T-lymphocytes and B-lymphocytes that will remember that kind of virus in a future infection avoiding severe infectious diseases. Both Pfizer-BioNTech and Moderna vaccines use this technology;²¹

- **Protein subunit vaccines** contain only isolated specific proteins from viral pathogens, like harmless S-protein, that stimulate the human immune system to produce antibodies and defensive with blood cells that will fight the virus;
- **Vector vaccines** use a modified version of a different virus, called a viral vector, to deliver the genetic material of the Covid-19 virus into human cells. Herein new S-protein copies will be created and displayed on the cellular surface, and the immune system will be stimulated to produce antibodies and white blood cells. AstraZeneca-SK Bio and Janssen/Johnson & Johnson are vector vaccines.

As previously described, the entry step of enveloped viruses represents a crucial passage in the process of spreading infection involving cellular factors, viral proteins, fluidity, and the curvature of the cellular membranes. All these different stages can be hit and blocked using molecules acting like inhibitors of the specific envelope component. Targeting the envelope membrane and preventing the viral entrance are considered good strategies to fight viral infections, thus allowing the interference with a site that does not undergo evolutionary processes due to viral resistance mechanisms, since the viral envelope is not synthesized following the instructions reported in the viral genome. As clearly described in Figure 7, can be distinguished several types of entry inhibitors targeting viral envelope:

Antibodies: from the earliest use of antibodies for the treatment of viral infections at the beginning of the 20th century, great progress has been made by researchers in the attempt to establish new therapies for the prevention and treatment of viral diseases. Antibodies are a key component of human immune responses to pathogens, and thanks to their unique maturation process, they can fight viral infections in a highly specific way. In the last two decades, more than 60 new recombinant monoclonal antibodies have been developed for human use both for newly emerging as well as the long known viral pathogens. *Influenza virus* infections usually cause mild illness and can be treated with neuraminidase inhibitors

able to stop the release of mature viral particles; otherwise, the influenza virus can escape from immune response thanks to some changes occurring in their structure called antigenic drift. *MHAA4549A* (Genentech, Inc.) is a human IgG1 mAb that binding hemagglutinins inhibits the hemagglutinin-mediated membrane fusion in the endosome. *CR6261* (Crucell Holland BV and the National Institute of Allergy and Infectious Diseases) is a human IgM+ isolated from a healthy vaccinated patient that acts by blocking conformational rearrangements occurring during membrane fusion. *Human Immunodeficiency Virus (HIV)* still represents a great challenge for researchers involved in the attempt to find out an effective vaccine; otherwise, the recent identification of neutralizing antibodies isolated from memory B cells of infected patients is becoming a viable approach for the prevention and treatment of HIV infection and AIDS. *VRC01* (NIAID) is a mAb able to fight several HIV-1 strains binding the CD4-binding site of HIV gp120. *4E10*, *2F5*, and *2G12* (Rockefeller University) are broadly neutralizing mAb specific for gp41 due to their capability to recognize the highly conserved membrane external domain. *Respiratory Syncytial Virus (RSV)* is a common respiratory virus that usually causes mild, cold-like symptoms; at the end of the 90s, FDA approved *Palivizumab*, a humanized IgG1-isoform mAb used for prophylaxis in children at high risk of severe RSV disease. The outbreak of *Ebola* and *Zika* between 2014 and 2016 emphasized the urgent need to develop new countermeasures against emerging infectious diseases. *ZMapp* (NIAID) is a cocktail of three mAbs that received special approval for compassionate use during the Ebola epidemic, while *Z23* and *Z3L1* are potent ZIKV-specific neutralizing mAbs isolated from a single patient.²² The impact of the *SARS-CoV-2* pandemic is unprecedented; although monoclonal antibodies have not yet received authorization from the European Medicines Agency (EMA), in Italy some of them have been exceptionally and temporarily approved (*Bamlanivimab*, *Casirivimab-Imdevimab*, and *Sotrovimab*). Meanwhile from the Monoclonal Antibody Discovery (MAD) Lab under the supervision of Professor Rappuoli, have been identified more than 400 neutralizing antibodies from 14 COVID-19 convalescent patients; some of the most potent mAbs recognize the spike protein receptor-binding domain, while others recognize the S1 domain, the spike protein trimer, and the S2 subunit. Among them has

been identified the most potent monoclonal antibody, which has been engineered to reduce the risk of antibody-dependent enhancement (ADE) and prolong half-life.²³

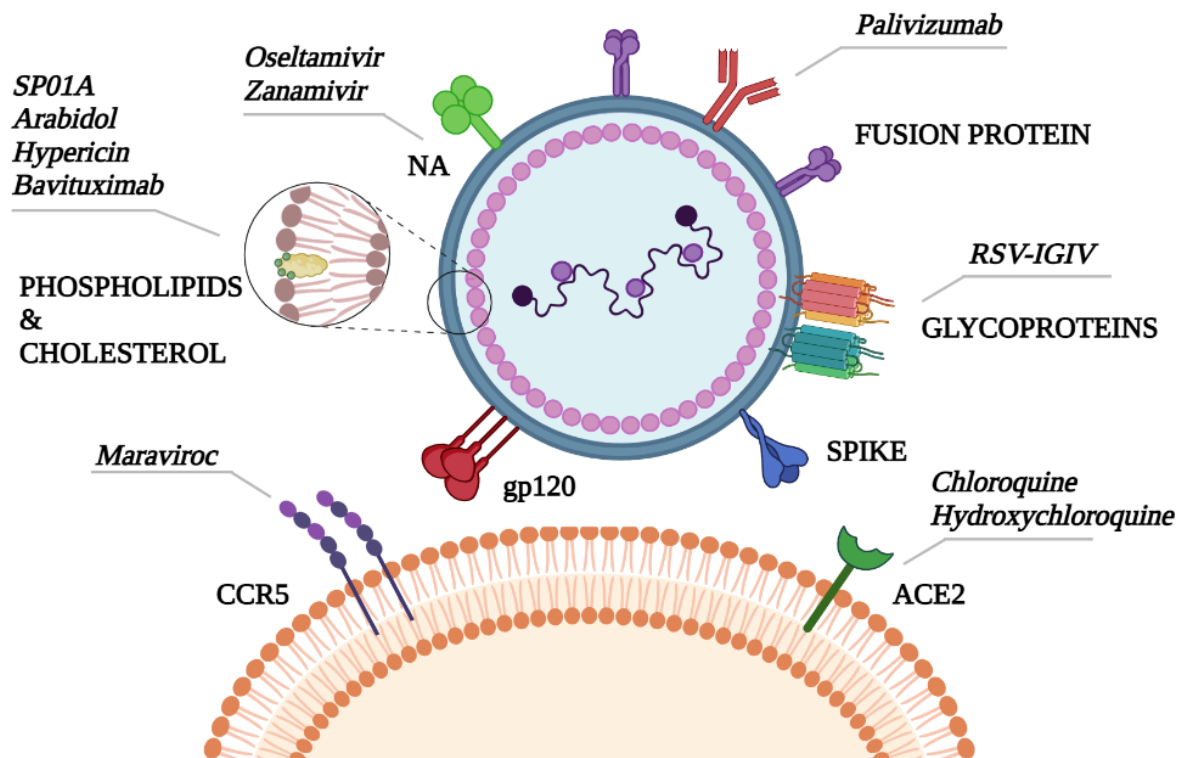


Figure 7

Entry inhibitors targeting viral envelope. mAbs targeting lipids, glycoproteins, receptors, and a large number of small molecules are capable to interfere with viral attachment factors or perturb membrane fluidity and curvature.

Virolitic antiviral peptides (AVPs): small, hydrophobic, or amphipathic molecules able to interact with the viral lipidic membrane, they are characterized by a low half-life and poor oral biodistribution, but otherwise, their mechanism of action is unique. The most famous example of AVP is *Enfuvirtide*, a fusion inhibitor used for HIV-infected people unresponsive to HAART. Its chemical structure is quite similar to the amino acid sequence found in the C-terminal portion of gp41. C5A is a peptide acting at nanomolar concentrations *in vitro* by inhibiting the entry step of different enveloped viruses (HCV, WNV, DENV, HIV) without cytotoxicity; apparently, its mechanism of action seems to involve the viral membrane and not the host one. MP7-NH2 is a mastoparan-derived peptide active against a large number of enveloped viruses thanks to the formation of an amphipathic α -helix when interacting with lipids leading to its perpendicular insertions into the membrane. C34 is an AVP sharing with *Enfuvirtide* a sequence of 24 residues; it blocks the entry step of HIV preventing the

transition to the 6HB structure but when combined with cholesterol, its efficacy increases 50 folders than alone. *NK-lysins* are peptides well known in the antimicrobial and antitumoral field thanks to their ability to interact with lipid membranes; for the same reason, recently have been re-evaluated for their capability to bind phosphatidylserine (PS) at low pH. This mechanism of action can be exploited to inhibit the fusion step of enveloped viruses requiring acid pH to trigger the viral protein that mediates the fusion. Another peptide identified as a broad-spectrum antiviral compound is CPXV012; it seems to act selectively thanks to the interaction between its cationic residues with the anionic ones of membranes, while its hydrophobic region helps to penetrate the envelope.⁵

Inhibitors of the fusion and host cell receptors: able to prevent the viral entry and block the integration of viral genome into the host one, they represent an important class of anti-HIV drugs useful in limiting the development of mutation and drug resistance. Several studies have underlined the use of small molecules as inhibitors of binding glycoprotein gp120 can block the attachment step of the virus to the CD4 receptor. In 2007 FDA approved the first CCR5 antagonist, Maraviroc a potent antiviral compound able to block the binding between MIP-1 β and CCR5 receptor. Thanks to its interaction with the hydrophobic domain of CCR5, Maraviroc provokes allosteric modifications that preclude the interaction between CCR5 and gp120. Despite the mechanism of action limiting the outcome of mechanisms of resistance, some viruses can interact with CCR5 receptors even in presence of Maraviroc thanks to the binding to the CCR5 N-terminal domain.²⁴ Regarding the treatment of Influenza diseases, hemagglutinins (HA) and neuraminidases (NA) represent crucial targets to hit and block the first step of the viral life cycle and the release of mature virions from infected cells, respectively. Various natural compounds have been identified as HA inhibitors (e.g., Rutin, Quercetin, Xylopin, and Theaflavins); one of the most potent natural HAI is Neoehinulin B active against a panel of influenza virus strains including amantadine- and oseltamivir-resistant strains, can bind to influenza envelope HA, disrupting its interaction with the sialic acid receptor.²⁵ NA inhibitors, such as Zanamivir and Oseltamivir, are sialic acid analogues acting as potent antiviral compounds able to fight both Influenza A and B preventing the release and spread of virions from the cell surface.²⁶ To fight the current COVID-19 pandemic, efforts have been intensified to exploit the

potential antiviral effect against SARS-CoV-2 among those already used for other diseases. Chloroquine and Hydroxychloroquine are two examples of this effort; both apparently can inhibit the fusion step of SARS-CoV-2 thanks to the increment of endosomal pH; while Chloroquine can also inhibit glycosylation of ACE-2 receptors preventing the initial attachment, both can inhibit the final release of mature virions from the cell surface.⁵

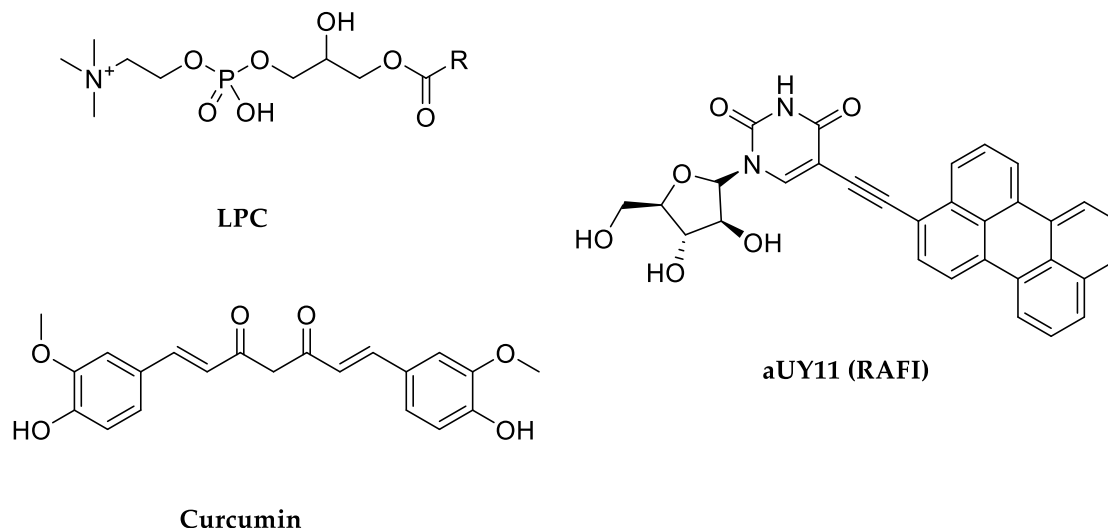
Compounds targeting the enveloped membranes: able to hit the lipids of envelope membrane in several ways so that the fusion with the host cell membrane, these kinds of compounds represent a new strategy for developing broad-spectrum antiviral compounds. Regarding enveloped membranes, one of the most important parameters for allowing the curvature transition from positive to negative during the fusion step is their fluidity. The membrane curvature depends on how lipids (each characterized by different head groups size, number of unsaturations, and length of alkyl chains) are packed together and on proteins interacting into the bilayer. While cholesterol and other cone-shaped lipids promote a negatively curved membrane enhancing fusion, inverted cone-shaped lipids, e.g., lysolipids, favor a positive membrane curvature not allowing the fusion step due to an increase in energy barrier. Among new compounds targeting enveloped membranes, can be distinguished polyunsaturated ER-targeting liposomes (PERLs), SP01A, lysolipids, and rigid amphipathic fusion inhibitors (RAFIs).

PERLs were designed as drug-delivery systems but only later were found to inhibit HIV, HBV, and HCV replication probably due to their ability to interact and reduce the amount of cholesterol within enveloped membranes.

With a similar mechanism of action, SP01A, a compound patented by Samaritan Pharmaceuticals Inc., was shown to be active against HIV inhibiting the lipid rafts system and reducing viral plasma levels.

For what concerns lysolipids and RAFIs, they are classified as stabilizing compounds of positive membrane curvature; if lysolipids (e.g., lysophosphatidylcholine LPC) induce a positive charge when creeping into membranes and seem to act in a late phase of entry step limiting the opening of pores, RAFIs are characterized by a bulky hydrophilic head and a rigid planar hydrophobic tail which are thought to fight the negative charge of the membrane curvature.

COMPOUNDS MODIFYING THE MEMBRANE CURVATURE



COMPOUNDS OXIDIZING UNSATURATED LIPIDS

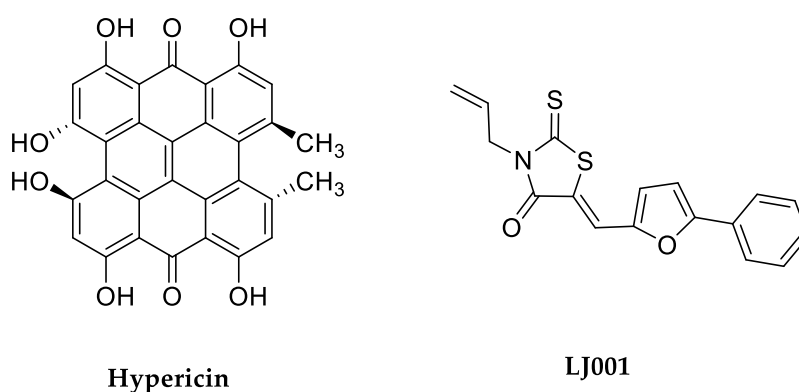


Figure 8

Chemical structure of antiviral compounds. Herein are reported some examples of drugs pharmacologically active against several enveloped viruses, targeting membrane lipids and preventing the entry step.

Their sub-nanomolar activity against HSV, Influenza virus, VSV, and HCV suggest a second mechanism of action, probably due to their capability to catch the light, generate ROS which oxidizes phospholipids and make enveloped membrane rigid. Interestingly, this secondary mechanism of action seems not to affect the host membrane as demonstrated by the non-correlation between antiviral activity and cytotoxicity. Moreover, Curcumin has always been studied as an antioxidant, anti-inflammatory, and antitumoral compound, but only recently has been discovered its antiviral activity against several enveloped viruses, i.g.,

ZIKAV, HCV, Influenza virus, through a mechanism affecting membrane fluidity. On the other hand, curcumin has been demonstrated to have no more antiviral activity when tested *in vivo*, probably due to its low bioavailability, and to behave like pan-assay interference compounds (PAINS).

Unsaturated lipids are another target to hit to alter membrane stability and fluidity. Compounds able to catch energy from light and transfer to oxygen atoms to obtain highly reactive species, such as ROS and singlet oxygen ($^1\text{O}_2$), leading to the final oxidation of unsaturated lipids, can be exploited for their antiviral activity, even if their use is limited by the important side effects that cause, such as damage to nucleic acids and proteins. Hypericin is a natural photodynamic anthraquinone mostly studied for antidepressive, antimicrobial, and antitumoral activity; recently has been proven its antiviral activity against enveloped viruses (HIV, HTLV, CMV) thanks to *in vitro* studies that have shown an activity directly correlated to the exposure of light, due to a major amount of reactive species of oxygen (ROS) produced and increased oxidation. J001 (Figure 8) is an amphiphilic thiazolidine active against enveloped viruses, able to interact with the entry process by altering the fluidity and functionality of enveloped lipid membrane; several studies suggested that its mechanism of action deals with the insertion of hydroperoxy groups (-OOH) into the hydrophobic tails of lipids leading to a modification of membrane curvature from positive to negative.

Influenza Viruses

Among the respiratory viral infections, Influenza causes around 400 000 deaths globally each year. Influenza virus is an enveloped, single-stranded, negative-sense RNA virus belonging to the *Orthomyxoviridae* family. Influenza viruses can alter periodically their nucleic acid leading to new waves of infections. Typically, RNA viruses are characterized by high spontaneous mutation if compared to DNA ones due to their lack of DNA polymerase I whose role is to correct errors in the DNA synthesis; so, mutations involving outer coat proteins allow the virus to spread infection in a highly contagious way and to cause acute respiratory syndrome. Moreover, if two different influenza viruses simultaneously infect the same host, they can recombine to create a new virus characterized

by RNA fragments from both the parent viruses. These mechanisms let the influenza virus to overcome the host's immune system.^{27,28} The fragmented nature of influenza RNA that allows the combination of two different viruses into a new one, and the fact that Influenza A can infect both humans and animals, are the cause of sporadic pandemic outbreaks due to influenza A virus variants of zoonotic origin. In the 20th and 21st centuries severe influenza pandemics happened (Figure 9); the first and most devastating, called Spanish flu, occurred in 1918 caused by influenza A H1N1; then a very similar H1N1 strain restarted circulation at the end of the 1970s without degenerate into a pandemic, while in 2009 a novel H1N1 pandemic was provoked by an antigenically different strain. At the beginning of 1957 in East Asia, influenza A H2N2 virus, which originated from an avian influenza A virus, emerged causing Asian flu, while in 1969 in Hong Kong H3N2 influenza A virus comprised of genes from an avian strain, caused a new pandemic.²⁹

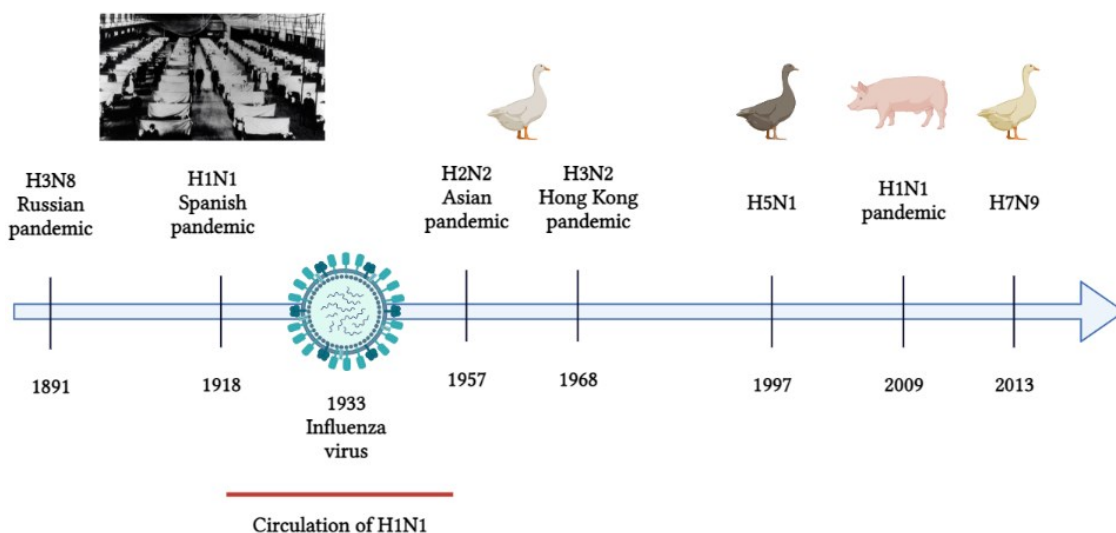


Figure 9

Influenza pandemics. Timeline of influenza virus circulation from the 1890s through the 20th and 21st centuries.

To date, four types of influenza virus are known: *Influenza virus A, B, C, and D*. They are classified following a standard nomenclature internationally accepted:

- The antigenic type (A-B-C-D);
- The host of origin (i.e., equine, swine) if not human;
- The location, the isolate number, and the year of the collection;

- For Influenza A are also specified the hemagglutinin and neuraminidase antigen (e.g., influenza A(H1N1 or H5N1) virus);
- When influenza viruses typically circulating in swine infect humans, the variants are identified with a letter “v” (i.e., influenza A(H3N2)v virus).

Despite the availability of vaccines and potent antiviral drugs, seasonal epidemics occur every autumn and winter usually caused by human Influenza A and B. Although less frequently, global pandemics also occur when a new influenza A virus comes up having the ability to spread infections among people. Regarding Influenza A viruses can be distinguished 18 and 11 different hemagglutinin and neuraminidase subtypes, respectively. For what concerns Influenza B viruses, primarily are divided into two lineages: B/Yamagata and B/Victoria, but at the same time they can be classified into clades and sub-clades.³⁰

Structure

Influenza viruses are characterized by a segmented genome containing negative-sense single-stranded RNA: Influenza A and B contain eight RNA segments, instead of Influenza C and D seven. Using an electron microscope is impossible to distinguish Influenza A from B, due to their common aspect being spherical or filamentous. Looking at the lipid enveloped membrane of Influenza A can be easily identified glycoproteins HA and NA projecting out and ion channels (M2) traversing by. Moreover, matrix 1 proteins (M1), underneath the envelope, protect and enclose the virion core. The eight virions inside the core, encode for several viral proteins, such as heterotrimeric RNA-dependent RNA polymerase, hemagglutinin (HA), neuraminidase (NA), the matrix proteins (M1 and M2), nucleoprotein (NP), and non-structural proteins (NS1 and NS2). Influenza B virus is quite similar to the A, even if differs in the presence of NB and BM2 instead of M2. More differences can be identified in influenza virus C and D: both with seven segmented RNA, are characterized by the presence of the sole spike surface glycoprotein, the hemagglutinin-esterase-fusion protein (HEF), instead of the typical HA and NA of influenza A and B.³¹

Replicative cycle

Influenza viruses begin their replicative life cycle thanks to their HA molecules, expressed on the viral envelope, that trigger the binding process to surface glycoconjugates containing sialic acid (N-acetylneuraminic acid) residues on the host cell surface (Figure 10).

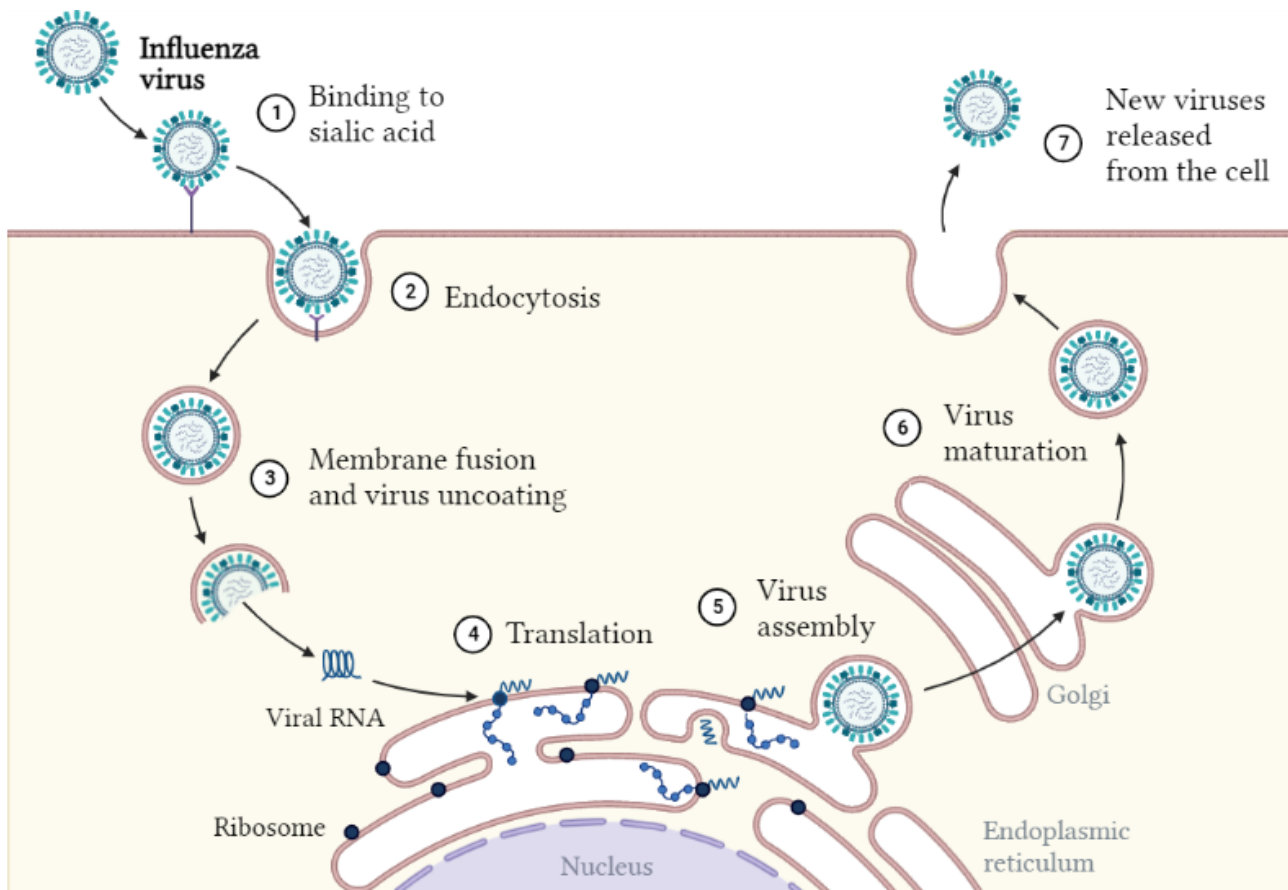


Figure 10

Influenza replicative cycle. After the entry step triggered by the binding between HA and sialic acid residues expressed on the host cells surface (1), an endocytotic mechanism brings the virus inside cells (2). The virus traffics to the late endosomes where membrane fusion is triggered by low pH that induce conformational changes in HA allowing the formation of the fusion pore and the virus released into the cytoplasm (3). After the translation step, occurs into the nucleus through RNA viral polymerases (4), all viral proteins are synthesized and in the Golgi apparatus all the elements are packed into the new infectious virions (5-6). Finally, new viruses are released from host cells (7).

Looking at the HA crystal structure can be appreciated that the protein consists of two regions cleaved by serine protease during the viral infection to be functional: HA₁, which contains the receptor-binding site for sialic acid, and HA₂ that mediates the fusion. The endocytotic mechanism can also occur in a clathrin-dependent way, including dynamin and Epsin-1 proteins, or by macropinocytosis.³² Once inside cells, the virus is trafficked in the

late endosome, where M2 ion channels are activated by the low pH and play a relevant role during the entry step. M2 is a protein whose transmembrane domains act as channels allowing the entrance of hydrogen ions into the virion ensuring the right grade of acidification that disrupts protein-protein interactions and allows the release of the genome in the cytoplasm.³³ The transcription and the replication of the influenza virus take place in the nucleus. The viral genome is a negative-sense strand of RNA, so to be transcribed, it is necessary to transform into positive-sense RNA which acts as a primer used by the viral RNA polymerase for starting transcription and replication. cRNA can be synthesized starting from vRNA and afterward transformed by polymerases into the new vRNA of virus progeny. From the mRNA primer all-new viral proteins are synthesized and in the Golgi apparatus are transported to undergo the last translational modifications. Since influenza is an enveloped virus, requires creating its external membrane starting from the host cell's plasma membrane; after that virus particles are released from the apical side of host cells. For this reason, HA, NA, and M2 move towards the apical side of the plasma membrane. A crucial part of the budding step is represented by the cleavage of sialic acid residues from glycoproteins and glycolipids made by NA; without this final act, new virions would not be released from infected plasma membrane cells.³⁴

Tissue tropism

Defined as the ability of a virus to infect a specific organ, tissue tropism contributes in a significant manner to maximizing the infection in a specific region of the infected organ. Influenza virus infects the human respiratory tract thanks to the interaction between HA proteins and the specific receptors expressed on the host epithelial cell membranes. Although the exact nature of these receptors is not yet clarified, Influenza virus binds in a specific way glycosylated oligosaccharides with sialic acid residues. Sialic acid is a nine-carbon monosaccharide whose carbon-2 can bind carbon-3, -6, or -8 of galactose to form α -2,3, α -2,6, and α -2,8 linkages. Influenza virus mostly targets α -2,3 and α -2,6 receptors, both expressed in the epithelial cells of the respiratory tract. As seen before, HA needs to be activated by the cleavage of human proteases, most abundant in the respiratory tract. Also, NA has a key role in the early step of the viral infection because they break down the mucins

allowing the virus not to remain entrapped in the respiratory mucus, and facilitating infection.³⁵⁻³⁷

Antiviral drugs

Although vaccines remain the best solution to control and reduce the influenza impact, continuous reformulation of components and an annual immunization are needed to be effective against influenza infection. Among the antiviral drugs used against Influenza virus, amantadine was the first synthetic compound able to prevent the entrance of H⁺ ions into the virions within endosomes, avoiding the process of uncoating. Amantadine, and its derivative Rimantadine, act by blocking the M2 protein. From the 2004-2005 influenza season, the use of these drugs was no more recommended, mainly due to the circulation of new resistant influenza virus strains. Even if amantadine and rimantadine have been used for both prophylaxis and treatment of Influenza A infections, their activity was limited to this virus strain and was characterized by poor tolerability and central nervous system side effects. Actually, in practice, only neuraminidase inhibitors (NAIs) are prescribed for the prevention and therapy of influenza infections. The first NAIs synthesized were DANA (2-deoxy-2,3-didehydro-*N*-acetylneuraminic acid) and FANA (2-deoxy-2,3-dehydro-*N*-trifluoroacetylneuraminic acid). Both served as lead compounds for the development of the NAIs used for the treatment of Influenza A and B infections: Zanamivir and Oseltamivir. These compounds are characterized by high inhibitory activity ($IC_{50} \leq 1$ ng/mL) against viral NA and can block virus replication both *in vitro* and *in vivo*; used for therapy and prophylaxis, are well tolerated, and administrated by inhalation (10 mg twice a day) and orally (75 or 150 mg twice daily), respectively. In the last decades, several attempts were made to achieve the control and prevention of influenza infections. Antibodies against haemagglutinin (HA) and several drugs targeting different passages of the viral replicative cycle have been studied and tested. Among these attempts, only baloxavir marbolix (BAM) and favipiravir (FP) have reached the market.

BAM is a prodrug orally administrated within 48 hrs of clinical manifestations. The liver, intestine, and blood metabolize BAM to release the baloxavir acid (BXA), the active compound. BXA inhibits the endonuclease activity of the viral polymerase acid protein (PA)

in order to prevent the “cap snatching”, the mechanism typically used by the virus to modify the mRNA transcription process used by host cells, allowing the viral RNAs synthesis. Also, FP is a prodrug, a nucleoside derivative activated by intracellular phosphoribosylation after oral administration; its mechanism of action consists of the inhibition of the viral RNA-dependent RNA polymerase (RdRp). In fact, the biggest advantage is its extended activity to several RNA viruses (i.e., arenaviruses, hantaviruses, flaviviruses, respiratory syncytial virus, and noroviruses). Although FP is characterized by good safety and tolerability profile, potential teratogenic effects have been collected in all animals treated.^{38,39}

Flaviviruses

Flaviviruses, belonging to the *Flaviviridae* family, are single-stranded RNA viruses transmitted by mosquitos and ticks, able to cause from mild febrile illnesses to severe haemorrhagic manifestations in humans. The major vector-borne diseases are caused by flaviviruses, such as yellow fever virus (YFV), Dengue virus (DENV), Zika virus (ZIKV), Japanese encephalitis virus (JEV), West Nile virus (WNV), and hepatitis C virus (HCV). The unique characteristics of vectors, the ideal habitats created by poor urbanization plans, environmental changes and the geographical expansion of vectors are factors promoting the epidemic potential of these viruses. Moreover, most of them are zoonotic which means that infections can spread between animals and humans, so their capability to infect a wide array of animals increase their potential as animals can constitute important stable reservoirs and contribute to the introduction of new viral species and transmission among humans.⁴⁰⁻⁴²

Structure

Mature flaviviruses are small (about 50 nm in diameter) spherical particles composed of a single-stranded positive-sense genomic RNA protected by a protein capsid and a host lipidic envelope. The viral genome encodes three structural (E, prM and C) and seven non-structural (NS1, NS2A/B, NS3, NS4A, 2K, NS4B, and NS5) proteins essential for viral replication. The envelope protein (E), involved in the entry step of the replicative virus cycle, is made of a three-domain structure (E-DI, E-DII, E-DIII) connected to the membrane with

a helical stem and two transmembrane domains. Usually, most of the E proteins undergo post-translation modifications with the addition of carbohydrates. PrM is integrated with the viral envelope in the early step of virion morphogenesis; the cleavage to M is made by a host serine protease, meanwhile immature virions move through the trans-Golgi apparatus, in order to allow the formation of the infectious mature form of the virion. The viral capsid protein (C) is a small helical protein able to bind both viral nucleic acids and host lipids, allowing the right incorporation of the viral genome inside virions. This step is also regulated by the cleavage of the polyprotein by the non-structural proteins NS2B and NS3.⁴⁰

Flavivirus life cycle

The flavivirus replication cycle begins when mature virions penetrate the host cell through several interactions such as the binding between asparagine-linked sugars on structural proteins and C-type lectins including DC-SIGN, the interaction of the E protein charged surface with glycosaminoglycans, of viral lipid envelope with proteins of the T-cell immunoglobulin domain and mucin domain (TIM) and Tyro3, Axl and Mert family of phosphatidylserine receptors. DC-SIGN (dendritic-cell-specific ICAM-grabbing non-integrin), GRP78/BiP (glucose-regulating protein 78) and CD 14-associated molecules have been proposed as primary receptors used by DENV in the early step of the infection process; in fact, the mannose-specific lectin DC-SIGN seems to interact with carbohydrate residues of DENV E protein. Heparin and other glycosaminoglycans have been identified as low-affinity co-receptors for DENV, WNV, and JEV. The first step in the replicative life cycle is governed by a class II viral fusion, transmembrane E protein present on the virion surface. Some virus attachment factors (i.e., TAM or integrin receptors) can bind virions, transduce signals into cells, and potentially augment the infection. Like other enveloped viruses, flaviviruses entry step follows a clathrin-mediated endocytotic mechanism, so they are encapsulated in early and late endosomes where the virus membrane fusion occurs in low pH conditions and is triggered by conformational changes in the E protein leading to the formation of E protein trimers and penetration of E-DII fusion loop into the host membrane and the folding of the helical stem towards the external surface of the new E protein trimer. The fusion mechanism involves the hemifusion stalk, as seen before for enveloped viruses

in general, allowing the fusion between the outlet leaflets of the viral and host membrane and the following formation of the pore.^{40,43} Although the clathrin-mediated endocytosis represents the main way used by this virus to penetrate membrane host cells, some experiments conducted on DENV showed its ability to infect cells using different routes for entering inside cells, such as macropinocytosis or other mechanisms, depending on the cell host and virus serotype.⁴⁴ After the fusion step, the uncoating process takes place and the release of the viral genome occurs followed by the beginning of the RNA replication on intracellular membranes. On the endoplasmic reticulum surface, structural proteins and the new synthesized RNA are assembled in the new immature virions. Although the formation of the nucleocapsid (NC) is one of the earliest events of the viral assembly process, in flavivirus-infected cells NCs are rarely found. The immature virions formed are transported to the plasmatic membrane by the Golgi apparatus and then the virions maturation occurs. The host furin proteases cleave the prM protein before particles are released from cells and the E protein undergoes a major rearrangement leading to the complete maturation of virions.

Zika virus (ZIKV)

Zika virus (ZIKV) is a newly emerging virus belonging to the Flaviviridae family, isolated for the first time in Uganda in the 1940s from the serum of Rhesus monkey and pool of *Aedes Africanus* mosquitoes. ZIKV is a positive-sense single-stranded RNA characterized by two noncoding regions (3' and 5') and a long open frame encoding for a polyprotein which can be cleavage into capsid (C), envelope (E), precursor of membrane (prM), and non-structural proteins. Even if more than 80% of cases are asymptomatic mild clinical manifestations can occur (fever, headache, conjunctivitis, arthritis, retroorbital pain, vertigo, myalgia, digestive disorders, and cervical lymphadenopathy) but also more severe symptomatology like Guillain-Barré syndrome and meningoencephalitis, leukopenia, fetal malformations, and optical lesions. With an incubation period of about 2-7 days, ZIKV infection is transmitted by the bite of infected female mosquitoes of the *Aedes* species. Although the infection remained restricted to Africa and Asia until 2007, as can be seen in Figure 11, cases of ZIKV

infection have been reported in the US and South America (mostly in Brazil, with the 2015 health emergency that caused more than 1.5 million of infection).^{45,46}

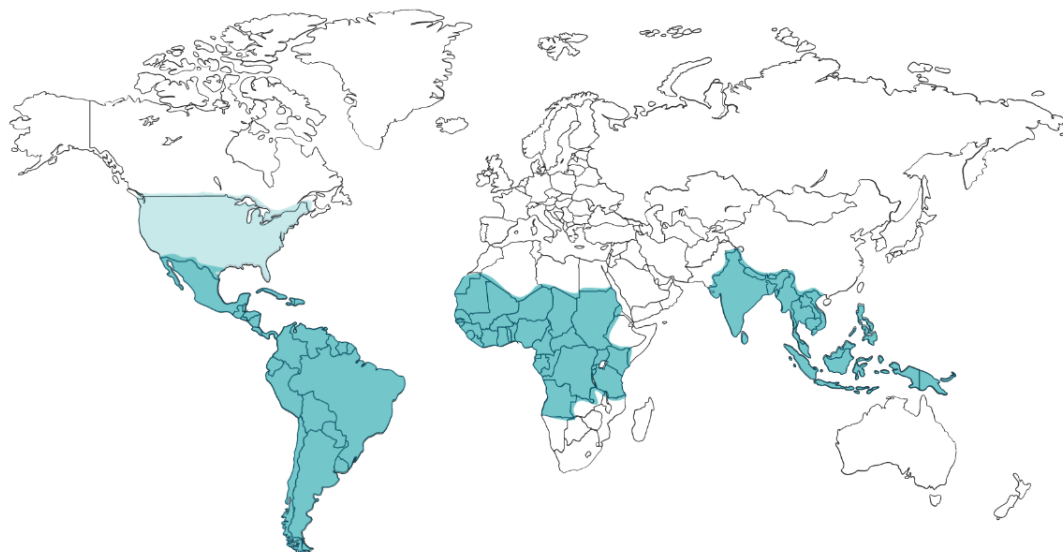


Figure 11

World map of areas with risk of ZIKV. Outbreaks of Zika virus disease have been recorded in Africa, the Americas, Asia, and the Pacific Ocean.

Two lineages of ZIKV are known: African and Asian. Although the main way of transmission is the bite of female mosquitos, further perinatal and sexual transmission are described. Viral RNA has been detected in breast milk, placental tissue and amniotic fluid suggesting the danger of infection in pregnant women. Unfortunately, the relationship between infected mothers and infants with microcephaly cannot be regarded as casual, even if has not been clarified how ZIKV can overpass the placenta and reach the microcephalic fetal brain tissue.⁴⁷

Dengue Virus (DENV)

Dengue is one of the most common infectious tropical diseases affecting humans. DENV is an epidemic in Africa, the Americas, South-East Asia, Western Pacific, and the Eastern Mediterranean area. Responsible for almost half a billion human infections yearly, was first reported in 1780 in India, whereas the virologically epidemic occurred in India in the 1960s. DENV is a single positive-stranded RNA flavivirus, characterized by four major serotypes (DENV-1, DENV-2, DENV-3, DENV-4). The four serotypes are enveloped spherical particles whose genome encodes for ten proteins: the structural proteins (M, E, C)

and the non-structural ones (NS1, NS2A, NS2B, NS3, NS4B and NS5). After the entry step common to the other flaviviruses, the fusion between viral and host plasma membrane, the endocytotic mechanism by which virions are entrapped into endosomes and the consequent pH-dependent release of the viral genome into the host cytoplasm, allow the RNA replication and the release of new mature virions able to spread infection.

The structural protein E plays a crucial role in the host-virus interaction in the early step of entry; it is expressed on the surface of DENV and, among its three domains (DI-DIII), the third one is directly responsible for binding host receptors. The NS proteins are mostly involved in the RNA replication process; NS1 is a glycoprotein that can be detected into infected patients' blood from the beginning of symptoms suggesting to have a crucial role in the pathogenesis of Dengue infection.⁴⁸

Clinically, according to WHO 1997 dengue guideline, DENV infection can be distinguished into classical dengue fever (DF), dengue haemorrhagic fever (DHF), and dengue shock syndrome (DSS). DF is characterized by an acute febrile illness with bone and muscular pains, headaches, leukopenia, and rash. DHF has four clinical stages from severe fever to hepatomegaly and circulatory failure. The principal way of infection is represented by the bite of the female *Aedes aegypti* mosquito, which after 4-10 days of virus incubation can transmit the infection.⁴⁹

Vaccines for Flaviviruses

Worldwide flavivirus infections cause suffering in humans. The best strategy to fight against virus epidemics/pandemics is represented by the development of vaccines. Among vaccines can be distinguished several different types:

1. *Live attenuated vaccines* are designed to stimulate long-term immune protection. Although the advantages of effectiveness and low cost, the safety profile of these vaccines needs to be carefully evaluated. TV003, a four full-length DENV serotype vaccine in clinical trials, shows after a single dose a significant antibody response. This vaccine has been developed by incorporating prM and E proteins from the other three serotypes into DENV2, and its effectiveness and safety have been demonstrated

in phase I trials. Using the same strategy, a live attenuated ZIKV vaccine has also been developed.

2. *17D Vaccine* was studied and developed for YFV infections. The effectiveness of this vaccine has been proven to be due to stimulating the innate and adaptive antibody responses, with the final result of neutralizing YFV E protein. Moreover, the 17D vaccine showed the ability to control the number of cytokines in human body, leading to the regulation of anti- and pro-inflammatory mechanisms.
3. *Inactivated vaccines* are made from inactivated antigenic material from a bacterium or a virus. Pathogens are cultured and then inactivated chemically or with heating. Nevertheless the safety profile and the simplicity of production, the immune response is relatively low and short.
4. *Molecularly engineered vaccines* have been developed to overcome the traditional limits of vaccines, such as poor safety, too high immunogenicity, or a short immune response. They use a genetic recombinant technology based on the use of genetic engineering or molecular cloning methods for the isolation of a pathogen target gene, that into a eukaryotic system allows the development of the specific antigen used to produce vaccines. Among engineered vaccines can be distinguished:
 - *Recombinant vaccines*: Dengvaxia is a tetravalent vaccine developed by Sanofi Pasteur starting from the 17D vaccine vector backbone in which has been inserted the specific DENV-1,2,3, or 4 genes. From phase III trials has been demonstrated that the vaccine induces an antibody response, especially in people previously infected by DENV.
 - *Molecularly cloned vaccines*: the use of known attenuated viruses as effective vectors is another way to develop a vaccine. Measles virus and adenoviruses are commonly used as vectors in vaccines development. Measles virus is used for WNV and DENV studies, to let the vector express E proteins of Flaviviruses and get an immune response by the antibody production after administration. In addition, a ZIKV vaccine has been developed with the same technique using an adenovirus for the stimulation of E protein expression and

the production of IgG *in vivo*, trying to protect the foetus through the placental barrier.

- *DNA vaccines*: known as naked vaccines because of the lack of vector or other chemical carriers, this technique is based on the idea to inject engineered DNA sequences encoding antigens to induce a direct stimulation of host cells to start the immune response. A ZIKV vaccine has been designed using a DNA backbone for encoding prM and E ZIKV proteins; *in vivo* results underlined the high titer antibodies produced. In the same way, GLS-5700 was assembled.
- *mRNA vaccines*: IgEsig-prM-E-LNP is an mRNA vaccine synthesized by the introduction of modified nucleoside 1-methylpseudouridine and nucleoside-modified ZIKV prM and E genes and encapsulated into lipid nanoparticles. Due to the ability of mRNA vaccines to modify genes, many attempts have been made to use this technology to solve the ADE (Antibody-dependent enhancement) reaction typical of flaviviruses.⁵⁰

Anti-Flavivirus drugs

Another strategy to fight Flavivirus infection is represented by the development of drugs targeting essential proteins strictly involved in the viral life cycle and regulating entry, replication, assembly, and maturation processes. The structural E protein represents an ideal target for an antiviral drug; with its three domains connected by a polypeptide linker, E protein plays a key role in the viral maturation process. The rearrangement process E protein undergoes, can be altered by using small molecules able to inhibit furin protease that usually cleaves E protein before it arrives in the Golgi apparatus so that the membrane fusion and the synthesis of new virions are stopped. MI-1148 (Figure 12. a) is a furin protease inhibitor characterized by high efficacy in blocking flavivirus maturation.

Non-structural proteins such as NS1, NS3 and NS5 can also be selected as a target for the development of new antiviral drugs. Recent studies have underlined the progress obtained by targeting hydrophobic channels and the lipidic concentration in the microenvironment. Nicotinic acid and methyl- β -cyclodextrin act in this way, enhancing the lipidic amount

during the replication process and reducing the secretion of NS1. NS3 is a trypsin-like serine protease involved in RNA replication and protein folding.

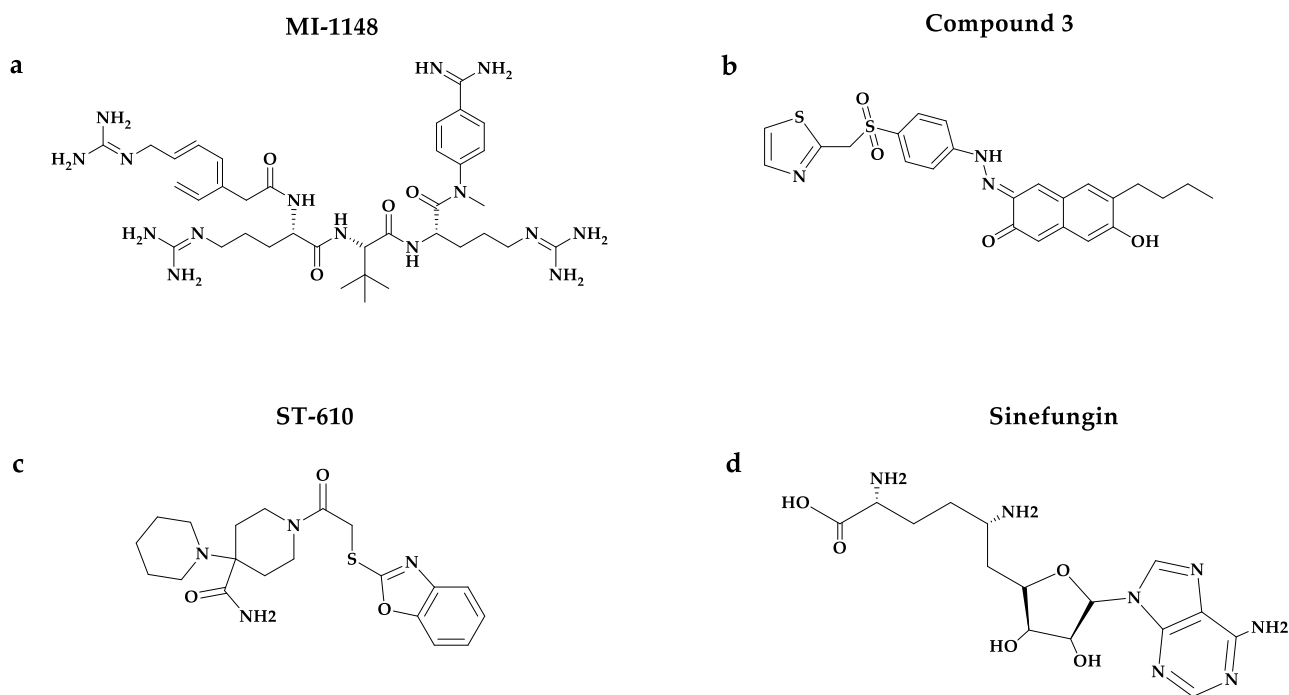


Figure 12

Chemical structure of anti-flavivirus compounds. (a) 4-(guanidinomethyl)-phenylacetyl-Arg-Tle-Arg-4-aminoboenzylamide (MI-1148); (b) Compound 3; (c) ST-610; (d) Sinefungin.

The development of an allosteric inhibitor, compound 3 (Figure 12. b), allows blocking the protein-protein interaction between NS2B and NS3, while the new approach of design drugs like ST-610 (Figure 12. c) can inhibit helicase functions preventing ATP hydrolysis. MTase and RdRp of the N-terminal and C-terminal of NS5 are essential for guaranteeing viral genome stability, translation, and escape from immune response; for that reason are considered potential targets for developing new antiviral compounds. Sinefungin (Figure 12. d) is a natural compound acting as a potent inhibitor blocking both N7 and 2'-O-methylation reactions. NSC12155 is another MTase inhibitor active against WNV, DENV and JEV, binding the SAM cofactor site of the MTase.⁵⁰

Although targeting viral components like structural and non-structural proteins could be probably the most used strategy to fight viral infection, an alternative and effective way is represented by the inhibition of crucial host cellular molecules involved in the replicative cycle of the viruses. Metabolic pathways such as fatty acid and cholesterol biosynthesis are

perfect targets to hit with new antiviral drugs, due to their role in the synthesis of complex lipids like those enriched during viral infections and the active biogenesis and cholesterol accumulation in the replicative complexes formed during the invagination process of the ER membrane. Molecules able to interfere in different pathways and steps of lipid synthesis, display inhibitory activity against ZIKV infection by blocking the biotransformation of sphingomyelin to ceramide, against ZIKV, DENV and WNV inhibiting the acetyl-CoA carboxylase (ACC) or the uptake, transport, and synthesis of cholesterol. Some FDA-approved drugs against Flaviviruses include this latter group: imipramine commonly used as an antidepressant can interfere with cholesterol transport inhibiting ZIKV, DENV, and WNV infection, ezetimibe is active against DENV infections due to its capability to block the NPC1L1 cholesterol transporter, and statins active as broad anti-flavivirus spectrum thank to the inhibition of the HMGCR enzyme involved in the cholesterol synthesis.⁵¹

Methyl-Arylidene Structure (MAS) Compounds

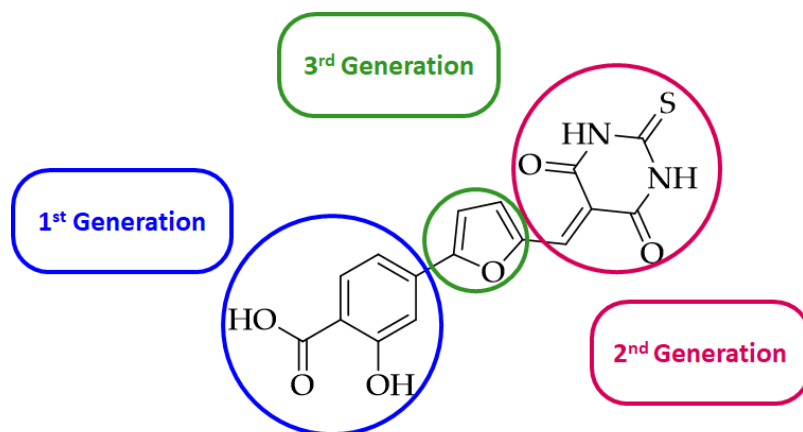


Figure 13

General structure of MAS compounds and modification sites for the first, second, and third generations.

Thanks to the efforts of Maurizio Botta's research group in the study and development of new antiviral drugs, MAS compounds were identified (Figure 13).

The first steps leading to the development of the first generation of compounds involved the use of a virtual screening protocol on over 200 000 compounds (Asinex gold collection) with the final score to discover new HIV-1 integrase protein inhibitors.^{52,53} The screening parameters used, were: Lipinski's rules of five, the pharmacophoric model based on the interaction with the target binding site, and the interaction energy.

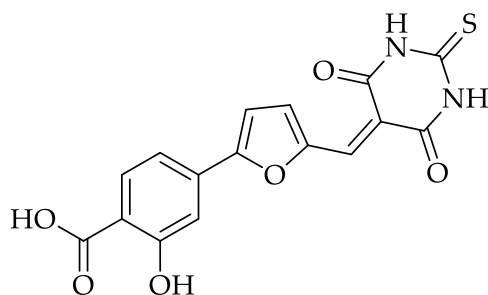


Figure 14

Chemical structure of hit compound 1.

After the computational screening and the subsequent biological evaluation, compound 1 (Figure 14) was chosen as the hit compound due to its inhibitory efficacy; in fact, compound 1 showed interesting activity both in the enzymatic assay on integrase protein (IC_{50} 8.9 μ M) and in HIV-1 replicative assay (EC_{50} 30.0 μ M), and a cytotoxic value of 60.0 μ M. The focus

on docking studies and other biological evaluations of the 1st generation compounds underlined the necessity to maintain the acidic moiety for a good activity profile. Indeed, when the salicylic group was replaced with 2-methyl-3-nitrophenyl, the inhibitory activity decreased leading to increased IC₅₀ and EC₅₀ values, 58.04 μM, and >17 μM, respectively. Additionally, the replacement of furan with thiophene ring or the introduction of substituents in position 3 caused the activity reduction, while this trend has never appreciated if the substitution of the thiobarbituric group with other heterocyclic moieties occurred.

The 2nd generation can be distinguished into three different series of salicylic acid derivatives (Figure 15) synthesized considering structure-activity relationship (SAR) studies previously conducted.⁵⁴

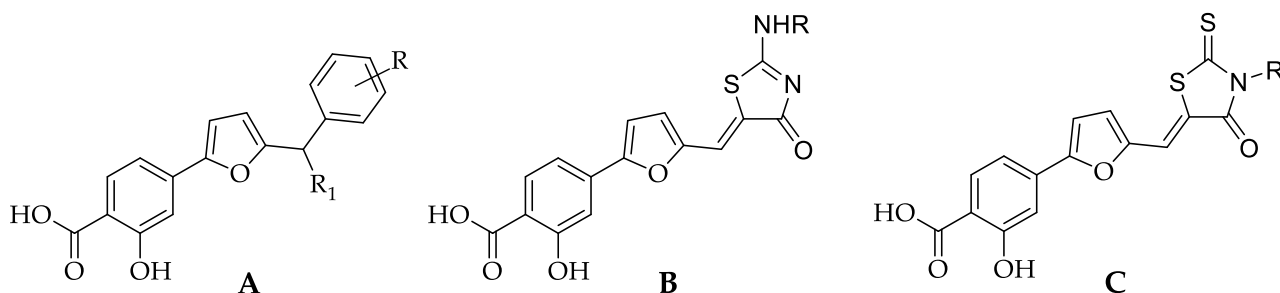


Figure 15

Chemical structure of 2nd generation derivatives, classified in series A, B, and C.

Serie A compounds are chemically characterized by the presence of the benzyl moiety replacing the thiobarbituric heterocycle; regarding the activity against HIV-1, all compounds showed an important lost efficacy. For this reason, no more efforts have been conducted in developing this series. Anyway, the replacement of the thiobarbituric acid moiety revealed a good strategy when 5-membered heterocyclic rings were introduced leading to the development of the series B derivatives. Responding to the aminothiazole structure, these compounds were moderately active against HIV-1 integrase but particularly efficient in inhibiting the HIV-1 replication cycle with sub-micromolar EC₅₀ values.⁵⁵ It has been hypothesized a different mechanism of action (MoA), so a time addition experiment was conducted to evaluate how the addition of an antiviral compound at different time points can interact within the viral replicative cycle steps. The results showed a possible

interaction in the entry step, proposing gp120 as the target of these series of compounds. This hypothesis was disproved by the ELISA competitive assay proving that these compounds were able to displace CD4 from gp120 only at 20 μ M. By the way, data suggested that compounds hit the entry step of the viral replication cycle without compromising the gp120 activity. The series C rhodanine derivatives inhibited HIV-1 and HSV-1/2 replication at nanomolar concentrations with a low cytotoxic profile (Selectivity Index > 100). These compounds were characterized by a gradual loss of antiviral activity when incubated in presence of a complete medium containing fetal bovine serum (FBS). Experiments were conducted in presence of increasing concentrations of bovine serum albumin (BSA) and a linear correlation between BSA concentrations and reduction of activity was found until a complete loss at the higher concentration of BSA. In order to overcome the interaction between rhodanine derivatives and serum albumin, was chosen a topical administration in gel formulation.⁵⁶

In the 3rd generation of MAS compounds we chose to explore the heterocyclic moiety replacing the furan ring with a pyrrole one (Figure 16).

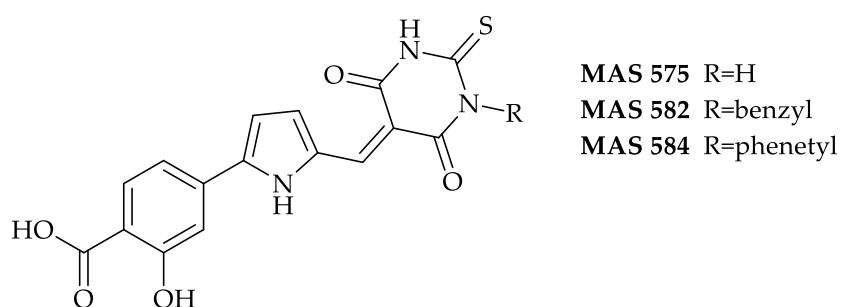


Figure 16

Chemical structure of 3rd generation of MAS compounds.

MAS 582 and MAS 584 have the thiobarbituric nitrogen substituted with a benzyl and a phenethyl moiety, respectively. For MAS 575 was evaluated the ability to reduce infection testing on HIV-1 integrase protein. Results obtained were comparable to hit compound 1 values. Also for MAS 575, the incubation in the presence of serum led to a marked decrease of activity as seen previously for 2nd generation compounds.

Aim of the work

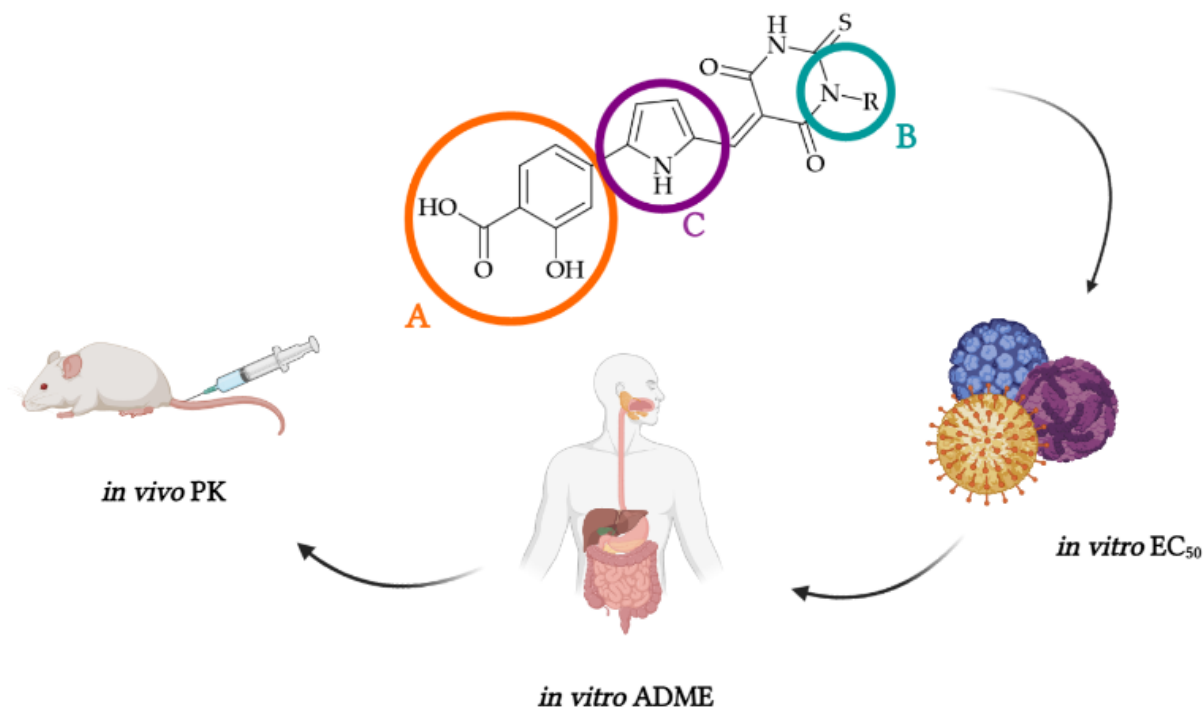


Figure 17

Graphical abstract of the project.

This Ph.D. work aimed to investigate preclinical ADME properties of new broad-spectrum compounds synthesized through three main types of modification (Figure 17) and characterized by promising antiviral profiles. The notable difference between IC₅₀ and EC₅₀ values found for the 3rd generation MAS, and the similarity with other broad-spectrum antivirals already published, led us to screen compounds on a panel of enveloped and non-enveloped viruses. Results underlined the ability of these compounds to selectively inhibit enveloped virus replication (e.g., Influenza virus strains, ZIKV and DENV-2), with any activity against non-enveloped ones. Due to these important findings, our purpose was to evaluate the mechanism of action.

The investigation of *in vitro* ADME properties has been focused on the evaluation of water solubility, plasma, and metabolic stability, binding affinity to human serum albumin (HAS), and permeation through plasma membrane with a PAMPA assay. Among different derivatives, the MAS compound with the best pharmacodynamic profile was identified and

selected for preliminary *in vivo* PK studies. The appropriate formulation for the selected MAS compound was chosen and the administrations in healthy mice at doses of 12.5 mg/kg and 25 mg/kg were performed.

(Cagno V. et al. 2018 PLoS ONE 13; (12): e0208333)

Structure-activity relationship (SAR)

Starting from the activities against enveloped and non-enveloped viruses (Table 2), MAS 584 was chosen as the hit-compound for developing new derivatives through modification on parts A, B and C of the scaffold, as seen previously in the graphical abstract (Figure 17).

Type of virus	Virus	EC ₅₀ (nM)	CC ₅₀ (nM)	S.I.
Enveloped	HSV-2 Acy R	83.4	> 300	> 3597
	HSV-1	454	> 300	> 660.8
	HSV-2	86.9	> 300	> 3452
	HCMV	118	36.3	308.7
	RSV	315	241	765
	VSV	144	> 300	> 2631
	H1N1	1241	> 300	> 77
	ZIKV	43.3	> 111	> 2563
	HIV AD8	251	> 300	> 1195
	HIV NL4-3	64	> 300	> 4687
Non-enveloped	HPV-16	Na	> 300	Nd
	Ad5	Na	> 300	Nd
	HRoV	Na	> 300	Nd

Table 2

Antiviral activity of MAS 584 on enveloped and non-enveloped viruses. S.I.: selectivity index; Na: not active;

Nd: not determined.

Modifications on part A of the scaffold

The first issue was to overcome the reduction of antiviral activity when compounds were incubated in presence of serum. Initially, the salicylic acid moiety of compounds was

supposed to be responsible for binding the human serum albumin (HSA)⁵⁷ and thus the efficacy in inhibiting viral replication. For this reason, chemical modifications on region A of the scaffold were conducted (Figure 18).

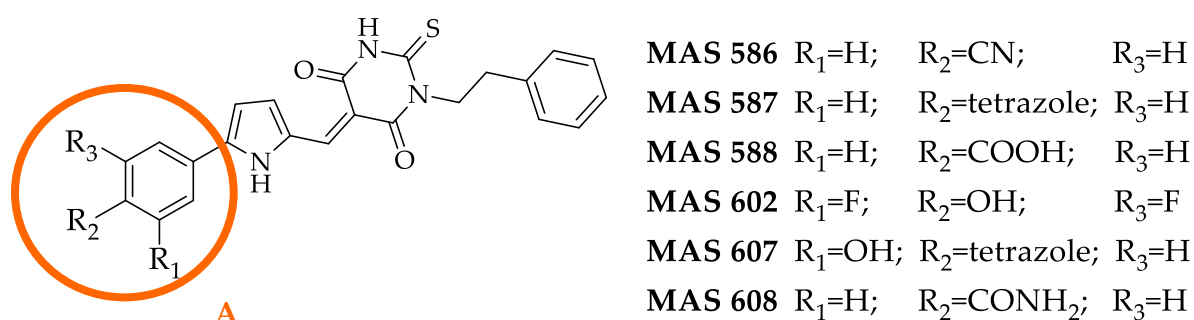


Figure 18

Chemical modifications on A part of the scaffold.

To investigate if the salicylic acid moiety was essential for the antiviral activity was substituted with the benzonitrile group (**MAS 586**) and the benzoic acid (**MAS 588**). The classical strategy used in medicinal chemistry to introduce carboxylic acid's bioisosteres was applied in order to improve the physico-chemical properties without compromising the antiviral activity.⁵⁸

The tetrazole moiety was selected as bioisostere of the carboxylic acid group due to the improved bioavailability, metabolic stability, and potency.⁵⁹ The introduction of the tetrazole group instead of the salicylic group (**MAS 587**) was also an attempt to reduce the interaction with HSA and maintain the pKa values around 5. Moreover, a derivative with the hydroxyl group in ortho position (**MAS 607**) was synthesized. Another moiety able to act as a lipophilic bioisostere of carboxyl acid is the 2,6-difluorophenol group; thus **MAS 602** was developed in order to evaluate if the fluorine atoms, nearly small and capable of bonding as hydrogen, may replace and mimic the carboxylate carbonyl oxygen. Another attempt to investigate SAR has been represented by the use of amide structure (**MAS 608**) due to their capability to be both donor and acceptor hydrogen bonds.

Modifications on part B of the scaffold

Modifications on part B of the scaffold had the final scope to investigate the effect on the compounds' antiviral efficacy due to the introduction of polar and apolar substituents or to the different lengths of the alkyl chain bound to the thiobarbituric nitrogen (Figure 19).

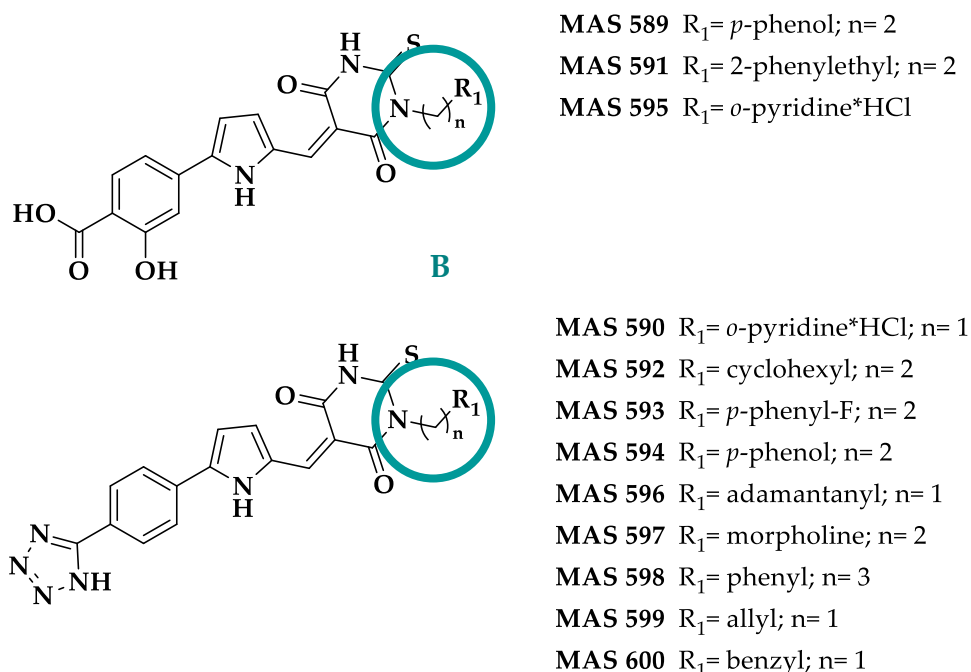


Figure 19

Chemical modifications on part B of the scaffold.

Polar groups like-hydroxyphenyl (MAS 589 and MAS 594) or 2-pyridinyl groups (MAS 595 and MAS 590) were introduced to enhance the water solubility on both the salicylic acid and the tetrazole derivatives. The introduction of the morpholine moiety in MAS 597 was made due to its capability to generate protonated compounds at pH 7.4 and thus increase the solubility of the compound. Another approach to increase solubility, permeability and metabolic stability was represented by the introduction of the fluorine atom in *para* position of the phenyl ring in MAS 593.⁶⁰

In order to maintain the amphiphilic character of MAS compounds, considering their activity against enveloped viruses, polar groups like 2-phenylethyl (MAS 591), cyclohexyl (MAS 592) and allyl (MAS 599) groups were also introduced.

Considering the efficacy of adamantine and rimantadine in blocking Influenza A replicative cycle, the last attempt was to replace the phenyl moiety with 1-adamantanyl group (MAS 596).

Modifications on part C of the scaffold

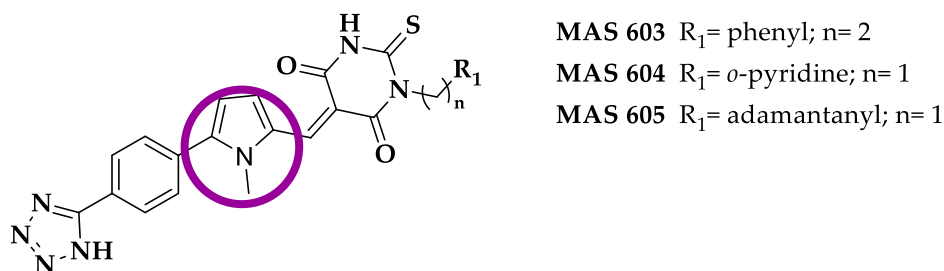


Figure 20

Chemical modifications on part C of the scaffold.

The introduction of a methyl group on the pyrrole nitrogen gave rise to three new MAS compounds (Figure 20): MAS 603, MAS 604, and MAS 605. The principal aim of this type of substitution was to further extend the SAR around the pyrrole ring and potentially increase the passive permeability of these compounds.

Mechanism of Action (MoA)

The mechanism of action was investigated using the arylidene derivative **25**, a 2nd generation MAS, as a probe (Figure 21).

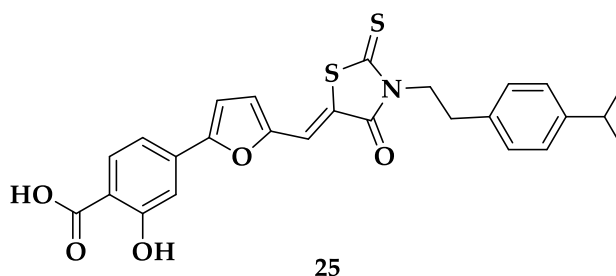


Figure 21

Chemical structure of derivative 25 characterized by a broad-spectrum antiviral activity.

As reported in Table 3, compound **25** is a potent broad-spectrum antiviral compound active especially on enveloped viruses, while on non-enveloped ones was found to be inactive.

Type of virus	Virus	EC ₅₀ (nM)	CC ₅₀ (μM)
Enveloped	HSV-1	2.18	2.09
	HSV-2	1.60	2.09
	HCMV	4.22	5.24
	RSV	54.8	17.04
	ZIKV	69.6	8.85
	IAV	66.1	135.7
	VSV	13.2	24.84
Non-enveloped	HPV-16	Na	94.23
	Ad5	Na	94.23
	HROV	Na	156.1

Table 3

Antiviral activity of compound 25 on enveloped and non-enveloped viruses. Na: not active.

The hypothesis suggested was the possible interaction between this compound and the viral envelope. Aiming to investigate the mechanism of action (MoA), compound **25** was used for a time of addition assay in order to determine if the antiviral activity was due to the interaction between compound **25** and cells before (PRE-TREATMENT CELLS), during (DURING INFECTION) viral infection, or if the activity could be explained with direct interaction with the virus (PRE-TREATMENT VIRUS). As represented in Figure 22. A, the tested compound resulted inactive in pre-treatment cells due to a lack of interaction with non-infected cells (red). A reduction of viral titers was observed during infection and when the compound was incubated with the virus before adding to cells. Respectively, EC₅₀ values were 0.147 μM and 6.55 nM, suggesting that viral enveloped and plasma membrane can compete for the compound.

In Figure 22. B, are reported data obtained from the post-treatment assay, where compound **25** was added at increasing concentrations to infected cells after the removal of inoculum. Finally, the percentage of infectious virus was titrated with a plaque assay. The low EC₅₀ value, 33.9 nM, suggested the capability of this compound to inhibit multiple cycles of infection.

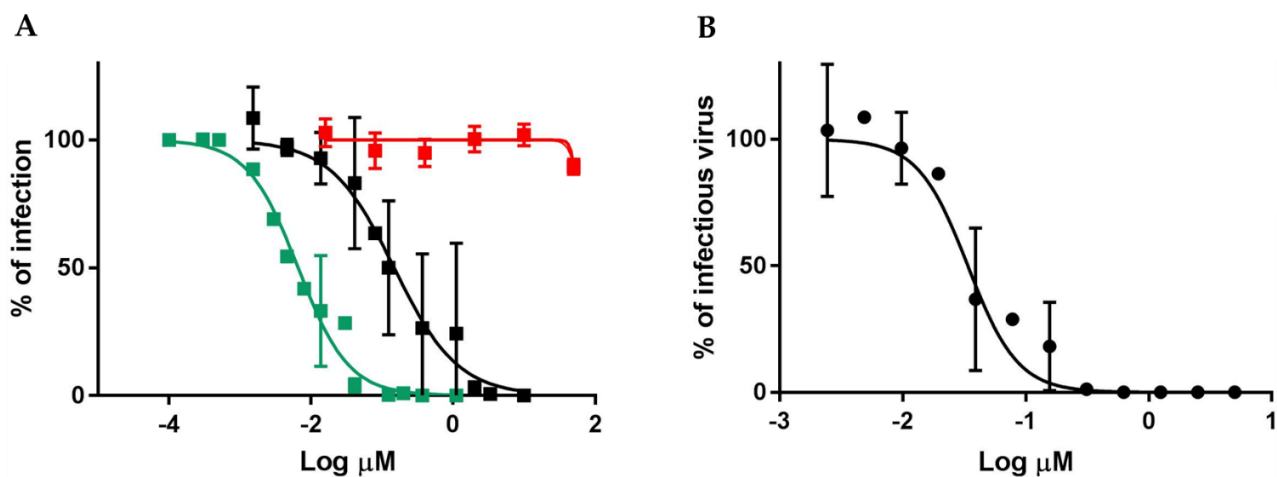


Figure 22

Time of addition and viral yield reduction assay. A) Compound 25 was added before virus infection (pre-treatment cells, red) or simultaneously (during infection, black) on cells, or after an incubation time with the virus (pre-treatment virus, green). B) Cells infected with HSV-2 (MOI 0.01), were treated with increasing concentrations of compound 25.

To further elucidate the MoA, compound **25** was incubated at different concentrations with the virus; the mixture was titrated on cells and viral titer was evaluated in a plaquing efficiency assay. Results obtained suggested a permanent virucidal activity.

Moreover was investigated if the irreversible effect could be revealed at different passages of the viral replicative cycle and if compound **25** disrupted physically the virus preventing the entry step. Thus binding assays were conducted (Figure 23. A-B-C) demonstrating that the compound did not modify the virus capability to bind cell membrane surface receptors, like heparin and act as an attachment inhibitor. Otherwise, in the entry assay was observed a reduction of the amount of virus entered inside cells (Figure 23.D). With immunofluorescence assay was localized the virus signal inside endosomes (Figure 23. E), supporting the idea that an amount of virus able to penetrate cell membrane remained entrapped inside endosomes, probably due to impaired fusion.

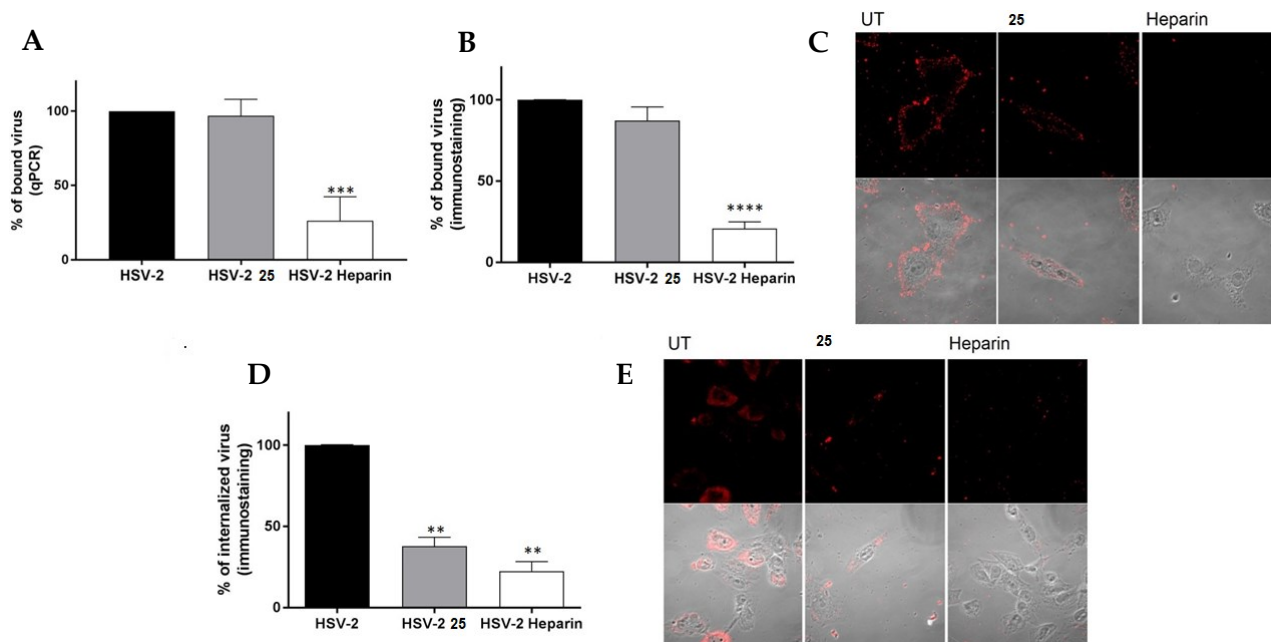


Figure 23

Binding and entry assay. HSV-2 was incubated with compound 25 and then added on Vero cells. Subsequently, cells were subjected to qPCR (A), immunostaining (B), or IF (C); HSV-2 was incubated with compound 25 and then added on Vero cells. Finally, cells were fixed and subjected to ICC (D) or IF (E). For both experiments, heparin was used as a positive control, being an attachment inhibitor.

Due to the high affinity of arylidene compounds and lipids, has been suggested the capability of these compounds to intercalate inside enveloped lipid membrane and provoke peroxidation of viral phospholipids leading to altered fusion with host membranes during the entry step.

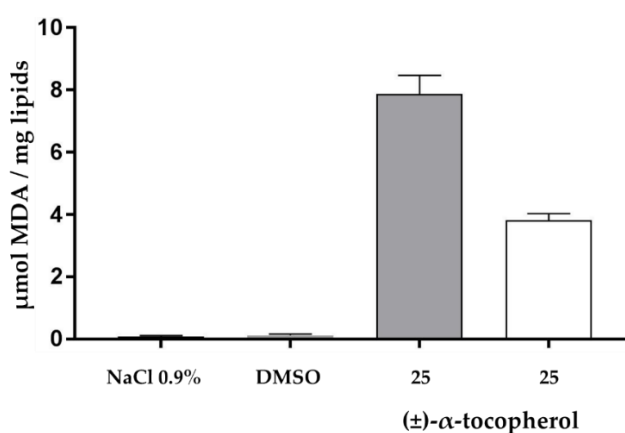


Figure 24

Lipoperoxidation assay. MDA produced from the linoleic acid peroxidation after exposure to compound 25 in the presence and the absence of (±)-α-tocopherol.

Thus, an *in vitro* lipoperoxidation assay was developed using linolenic acid as a reference lipid substrate, incorporated in DPPC liposomes; the grade of lipid peroxidation was evaluated following the amount of malondialdehyde (MDA) as a probe of lipid degradation. Adding compound **25**, the production of MDA increased, while in presence of the antioxidant (\pm)- α -tocopherol, the MDA quantity was halved (Figure 24).

Experimental Section

Biological evaluation

MAS compounds have been assayed on different enveloped viruses. Prof. M. Van Hemert's research group performed tests on ZIKV, Vismederi group tested derivatives on influenza virus strains, Accurange group performed the MTT assay on MDCK cells, and Professor M. Zazzi's research group investigated the double cycle of infection.

Influenza virus

Activity tests were conducted throughout the microneutralization test on MDCK (Madin-Darby Canine Kidney cells) infected by influenza A-H1N1, strain A/Michigan/45/2015; A-H3N2, strain A/Hong Kong/4801/2014; A-H7N9, strain A/Anhui/1/2013; BB, B/Brisbane/60/2008; BP, B/Utah/90/2014. This method was chosen for its capability to study how live viruses can infect and replicate in cells, inducing cytopathic effects (CPE) in the presence of MAS compounds. From the microneutralization test have been obtained the endpoint concentration for each compound assayed, which means the lowest concentration able to neutralize the virus.

ZIKA & Dengue Virus

MAS compounds' antiviral activity was also tested on ZIKV in Vero cells, using reduction cytopathic effect (CPE) in the multi-cycle assay. The antiviral activity of some MAS compounds has been further investigated with ELISA assay on ZIKV and DENV-2 (Table 7). When DENV-2 was matured on insect cell line, compounds did not inhibit the virus at the first round of infection, conversely, when HUH-7 cells were used for virus maturation,

MAS exploited their potent inhibitory action blocking the virus at the first round of infection.

***In vitro* ADME profiling**

Assessment of ADME (Absorption, Distribution, Metabolism, and Excretion) profile of new chemical entities is critical both to screen large libraries of molecules and identify a chemical lead compound and, during the further lead optimization, to investigate and elucidate the Structure-Activity Relationships (SAR). Improvements in ADME properties of compounds also reflect an increase in their PK properties.

MAS 575-584-587-596-602-604 have been selected to analyze their physicochemical properties and assess ADME profiles. These compounds were selected for their chemical diversity and antiviral activities.

Solubility

The MAS 2nd generation derivatives have previously been subjected to aqueous solubility studies. Each solid compound was added to Milli-Q water (1 mg/mL) and maintained under agitation for 24 hrs. The resulting suspension was filtered and the concentration of solubilized compounds was determined by UV/LC-MS method. The quantification was obtained by comparison with the appropriate calibration curve in methanol at different concentrations of compound. Results reported low aqueous solubility, ranging from 0.1 to 0.88 µg/mL.⁵⁶

Moving from these results has been decided to value a predicted solubility with QikProp software.

Permeability: PAMPA Assay

The PAMPA assay, firstly proposed by Kansy in 1998,⁶¹ is a high-throughput *in vitro* assay capable of assessing the transcellular permeability of potential drugs. It is used in pharmaceutical research to simulate intestinal absorption, providing information on permeability by passive diffusion not influenced by active transport.

To carry out the assay, specific 96-well multiscreen plates equipped with 0.45 μm polyvinylidene fluoride membranes (PVDF) were used, all supplied by Merck Millipore. A solution of anhydrous KH_2PO_4 phosphate buffer (PBS) at a final concentration of 10 mM was prepared at physiological pH.

The pH was adjusted with NaOH 1 N to 7.4 with the aid of a pH meter.

An L- α -phosphatidylcholine (PC) solution, used to mimic the phospholipid bilayer of cell membranes, was made at the final concentration of 1% w/v in N-Dodecane. Before using, a complete dissolution was reached incubating the PC solution for 15' in an ultrasonic bath.

Stock solutions in DMSO were made for each tested compound at the final concentration of 1 mM.

Donor solutions (DS) have been prepared from the stock ones, diluting until the final concentration of 500 μM with PBS. To allow the complete solution of compounds, DS were incubated at RT under stirring overnight and then filtrated using 0.45 μm disposable nylon filters.

Acceptor solutions (AS) were made using the same proportion of solvents present in DS (1:1 v/v DMSO/PBS 10 mM pH 7.4).

300 μL of AS were added to the acceptor plate, 10 μL of PC solution were deposited on the donor plate and, over the lipidic membrane, 150 μL of DS were added. Overlapping both plates avoiding bubble creation, the sandwich was incubated for 5 hrs at RT under gentle shaking.

At the time point, samples from both acceptor and donor wells have been collected and analysed with HPLC-UV/MS method, mentioned below. Experiments have been conducted in triplicate and all material used for them was purposed by Sigma Aldrich.

P_{app} value was calculated with the following formula:

$$P_{app} = \frac{(Vd \times Va)}{(Vd + Va) \times A \times t} \times [-\ln(1 - r)]$$

Where:

- Vd is the DS volume;
- Va is the AS volume;

- A is the filter area;
- r is the ratio between drug concentration in AS and DS.

Metabolic stability

Drug metabolism represents how our body interacts with exogenous molecules using numerous enzymatic reactions to increase the clearance and allow an easier elimination of these compounds. Biostrafomations of pharmaceutical substances are carried out by several enzymes responsible, mainly present in the liver.

HLM Pooled Male Donors 20 mg/mL Human Liver Microsomes used for the assay were provided by BD Gentest-Biosciences (San Jose, California). The NADPH solution, prepared freshly, was obtained by dissolving NADPH tetrasodium salt in a 48 mM aqueous solution of MgCl₂, all purchased by Sigma Aldrich.

The metabolic stability assay was performed in 2 mL vials (Safe-Lock Tubes, Eppendorf) in presence of 482.5 μ L of 10 mM PBS pH 7.4 and 2.5 μ L of the 10 mM compound stock solution in DMSO. Placing the vials on ice, 5 μ L of HLM and 10 μ L of NADPH are added and samples were incubated at 37°C under stirring for 1 hour in a thermostatically controlled bath.

After the incubation period, the metabolization process was stopped by adding 1 mL of ACN to each vial and then samples were centrifuged for 15' at 5000 rpm using a 5804-centrifuge provided by Eppendorf.

Exactly 1 mL of supernatant for each sample was brought to dryness under a flow of N₂. Resuspending each sample with 100 μ L of MeOH and following vortexing, sonication, and centrifugation at 5000 rpm for 5', the amount of metabolite formed was quantified using the HPLC-UV-MS method described below.

Plasma stability

Determination of drugs stability in plasma is fundamental as pharmacologically active compounds, except for pro-drugs, which undergo a massive degradation due to plasma esterases, generally show a poor *in vivo* efficacy.

Stock solutions in DMSO were made for each tested compound at the final concentration of 2 mM. A solution of HEPES buffer was prepared at the final concentration of 25 mM (140 mM NaCl) and pH was adjusted with NaOH to a physiological value.

The assay was performed in 2 mL vials (Safe-Lock Tubes, Eppendorf) adding 100 μ L of 2 mM compound solution, 900 μ L of HEPES buffer and finally, 1000 μ L of human plasma previously thawed and centrifuged at 5000 rpm for 5'. The solutions were then mixed and incubated at room temperature for the following time points: t'0, 5', 15', 30' 60' 480', 180', and 1440'. At each time point, 50 μ L of solutions were taken from each sample and treated with 450 μ L of ACN to denature proteins and block their action. These final solutions were centrifuged and the supernatant was recovered and analysed using the HPLC-UV-MS method, described below. Human plasma and all the other reagents were supplied by Sigma Aldrich.

HPLC-UV-MS method

All the quantitative analyses seen in the previous chapters have been performed with an LC-DAD-MS system consisting of an Agilent 1260 Infinity HPLC-DAD interfaced with an Agilent 6130 MSD. The system consists of a solvent degasser, an injection valve with a variable volume of 1 to 100 μ L, a binary pump system, a diode array UV detector, a thermostatically controlled column housing and an autosampler.

Time (min)	H ₂ O/CH ₃ COONH ₄ 0.1% w/v (%)	ACN/MeOH 1:1 v/v (%)
0.3	100	0
5.0	5	95
9.0	5	95
10.0	100	0

Table 4

Chromatographic gradient used HPLC-LC-MS.

The instrument is interfaced with an Agilent 6130 single quadrupole MSD analyser. Chromatographic separations were performed using a Phenomenex Kinetex column (C18, 30 x 2.1 mm, particle size at 2.6 μ m) at a flow rate of 0.4 mL/min. Chromatograms were

recorded at wavelengths of 240 and 290 nm using a gradient with ACN/MeOH mobile phase (1:1 v/v) and H₂O/CH₃COONH₄ 0.1% w/v (Table 4).

Albumin binding

Albumin represents the most abundant plasma protein, almost 60%, followed by globulins present in smaller quantities, around 35%. Hydrophobic drugs can interact with albumin via Van der Waals forces and hydrogen bonds and form a drug/protein complex resulting in a plasma equilibrium between the protein-bound drug and the free drug.

A 100 mM stock solution in DMSO is prepared for each compound. For each compound assayed, working solutions (WS) have been made by diluting with 1 mM PBS (pH 7.4) the stock ones until the final concentration of 1 mM, 40 μ M, and 2 μ M.

A stock solution of 1 mM of human serum albumin (HAS), purchased by Sigma Aldrich, was made by dissolving the protein in 1 mM PBS (pH 7.4); then the HSA stock solution was diluted until the final concentration of 20 μ M to obtain the working HSA solution.

Black 96-well plate was assembled as reported in the following Table 5:

Well	1	2	3	4	5	6	7	8	9	10	11	12
	CPD WS 2 μ M				CPD WS 40 μ M				CPD WS 1 mM			
PBS (μ L)	90	80	50	0	90	75	50	0	90	80	50	0
CPD (μ L)	10	20	50	100	10	25	50	100	10	20	50	100
HSA 20 μ M (μ L)	100	100	100	100	100	100	100	100	100	100	100	100
C _f CPD (μ M)	0.1	0.2	0.5	1	2	5	10	20	50	100	250	500

Table 5

Black 96-well plate set-up for albumin binding assay.

The experiments have been conducted in duplicate in the presence of a constant HSA concentration and in absence of the protein for the negative control (blank), which allowed us to exclude any interference caused by fluorescence phenomena of the analyte itself. After

30' of incubation, plates were read on the spectrofluorometer with excitation energy at 295 nm and emission energy from 300 to 450 nm with 2 nm intervals and constant temperature. Once all the fluorescence data have been collected, those corresponding to the wavelength associated with the maximum emission were considered, the mean value of these data was calculated and the fluorescence value of the blank/control was then subtracted from this. The percentage of fluorescence reduction (*quenching*) was plotted as a function of the total concentration of the compound in each well. Results have been expressed as Kd values (μM). The albumin binding assay has been performed recording the fluorescence intensity with the Perkin Elmer EnVision Multilabel Reader 2014 spectrofluorometer, with EnVision Manager software version 1.13.

***In vivo* preliminary pharmacokinetic (PK) studies**

Formulation

Given the acidic behaviour of MAS compounds, due to the NH of tetrazole and thiobarbituric moiety, able to exist in the deprotonated form when at pH 8 and pH 6-9, respectively, an alkaline buffer with pH 8 was chosen as the administrative medium to allow an easier conversion of **MAS 596** into a more soluble salt. Unfortunately, the use of a basic buffer was not enough to allow the complete solubilization of the selected compound; other experiments were conducted to find out the right composition and percentage of co-solvents.

In the first attempt, 0.5 mg of sample were dissolved using 5% DMSO, 5% tween, 20% PEG-400, and 70% TRIS buffer at pH 8.

For the second one, tween was not used while the other co-solvents were retained but in different percentages: 5% DMSO, 45% PEG-400, and 50% TRIS buffer pH 8.

For the third experiment, PEG-400 was replaced by Tween-80 and EtOH; MAS 596 was dissolved with 5% DMSO, 5% Tween-80, 10% EtOH, and 80% of TRIS buffer pH 8.

The three previous attempts resulted in incomplete solubilization of MAS 596 or the formation of a gel, none adapt for *iv* administration.

Thus a fourth experiment was done by dissolving 20% of DMSO stock solution in presence of 80% of a triamine solution.

The formulation consisted of three amino acids (aspartic acid, glutamic acid, and histidine) at 15 mM concentration solubilized in TRIS buffer 10 mM at pH 8.^{62,63} The formulation was made starting from the addition of an aliquot of 20% DMSO stock solution and then the solution of the three amino acids (80%) for a final volume to be injected of 200 μ L. With this protocol, the compound was perfectly soluble.

PK & BD at 25 mg/kg and 12.5 mg/kg doses

The animal model used for the pharmacokinetic (PK) and tissue distribution (TD) studies were male Balb/c mice, provided by Charles River (Milan, Italy), with an average weight of 25 g. Animals were kept in a controlled environment, at a temperature of 22°C, subjected to alternating cycles of light and darkness every 12 hrs and with free access to water and food. All procedures used in this study were reviewed and approved by the Animal Welfare Board (OPBA) of the University of Siena and the Italian Ministry of Health.

The most promising compound (**MAS 596**), selected from biological and ADME data, was administered intravenously at doses of 25 and 12.5 mg/kg.

At the predetermined time points of 5, 60, 120 and 180 minutes after administration, animals were sacrificed under anesthesia; plasma and organs were collected for the determination of the PK properties.

MAS 596 extraction was performed on 200 μ L of plasma or 200 mg of tissue (lung, liver, and kidney) by homogenizing samples for 3 min with a mixture of ACN-MeOH-DMSO in a 5:4:1 ratio (1500 μ L) containing **MAS 604** (10 μ g/mL) as an internal standard (I.S.).

After centrifugation for 20 min at 6000 rpm and filtration, samples were analysed by the HPLC method reported above.

Quantitative analysis of **MAS 596** was obtained by making appropriate calibration lines in the solvent, plasma, and tissue (always in the presence of internal standard).

Biological evaluation

Influenza virus

As reported in Table 6, MAS derivatives obtained from the modification of the salicylic acid moiety (A) seem not to enhance the antiviral activity against influenza pandemic strain. **MAS 584**, **MAS 587** (its tetrazole analogue) and **MAS 588** displayed a good efficacy profile on influenza A and B, but not on pandemic strain H7N9.

The nitrile derivate **MAS 586** showed better antiviral activity against pandemic strain than on Influenza A and B. **MAS 602** improved the activity against influenza A and B, probably due to the presence of fluorine atoms.

Any changes in the antiviral activity were observed regarding the modification of the length of the alkyl chain connecting the thiobarbituric nitrogen and the phenyl ring (**MAS 582**), while in the tetrazole analogues (**MAS 600** and **MAS 598**) the end-point concentration on pandemic strain decreased.

Other modifications on part B of the scaffold, such as the introduction of polar groups (**MAS 589**, **593**, **595**, **597**) provoked a visible reduction in the antiviral activity, while the introduction of lipophilic moiety maintained a good antiviral profile per **MAS 591** and **MAS 599**. Among these derivatives, **MAS 592** and **MAS 596** showed the best result, especially **MAS 596** with a relevant broad antiviral activity on all influenza strains assayed and a nanomolar activity on pandemic' one.

Moreover, the attempt to further extend the SAR around the pyrrole ring made by N-pyrrole methylation, lead to **MAS 603** and **MAS 604** with improved antiviral activity on all influenza strains assayed than the non-methylated compound, **MAS 587**, and **MAS 590**, respectively.

MAS CPD	End-point conc. H1N1 (μ M)	End-point conc. H3N2 (μ M)	End-point conc. BB (μ M)	End-point conc. BP (μ M)	End-point conc. H7N9 (μ M)	MDCK cells CC ₅₀ (μ M) 24hrs
575	Nd	Nd	Nd	Nd	Nd	Nd
582	1.99	3.98	7.96	7.96	15.9	221
584	1.16	2.32	1.16	4.64	9.28	266
586	4.33	34.6	4.33	8.65	1.08	256
587	1.88	0.47	1.88	3.76	15	222
588	0.44	0.447	0.447	0.89	14.3	243
589	1.72	6.88	6.88	13.7	13.7	200
590	7.48	29.9	29.9	60	14.9	195
591	1.85	0.92	0.92	3.70	14.8	196
592	0.49	0.49	0.99	0.49	0.99	259
593	7.89	7.89	7.89	7.89	7.89	189
594	66	8.30	66	Na	33	249
595	Na	Na	Na	Na	31	264
596	0.089	0.044	0.044	0.39	0.044	191
597	33	66	Na	Na	Na	221
598	1.65	6.6	0.82	3.30	0.21	240
599	2.44	1.22	2.45	9.79	1.22	296
600	1.16	1.17	0.145	1.17	0.58	173
602	0.79	1.58	0.099	0.099	1.58	67
603	1.73	1.84	0.11	0.11	1.84	26
604	0.127	2.02	0.127	0.127	8.10	202
605	Nd	Nd	Nd	Nd	Nd	Nd
607	Nd	Nd	Nd	Nd	Nd	Nd
608	Nd	Nd	Nd	Nd	Nd	Nd

Table 6

Antiviral activity of MAS compounds on influenza virus strains. Na: not active. Nd: not determined.

ZIKA Virus

As reported in Table 7, compounds **MAS 582** and **MAS 584**, obtained from modification A, were not active, while **MAS 588** resulted to be cytotoxic. The introduction of the p-nitrile moiety (**MAS 586**) allowed to restore activity in an acceptable values range and have a good selectivity index (S.I). **MAS 587**, in which the salicylic moiety has been replaced by tetrazole, displayed an improvement in its activity and a reduction in the cytotoxic effect. Conversely, the introduction of two fluoride atoms resulted in an inactive compound (**MAS 602**).

MAS CPD	ZIKV EC ₅₀ (μ M)	Vero cells CC ₅₀ (μ M)	MAS CPD	ZIKV EC ₅₀ (μ M)	Vero cells CC ₅₀ (μ M)
575	23.06	>100	595	36.42	>100
582	>100	98.15	596	8.75	5.37
584	>100	22.41	597	19.71	>100
586	37.99	100	598	9.28	38.97
587	1.11	95.51	599	>100	52.17
588	4.37	2.55	600	9.02	>100
589	8.93	>100	602	86.60	9.02
590	9.68	>100	603	20.39	>100
591	9.65	7.94	604	2.10	>100
592	3.64	2.42	605	31.03	20.35
593	49.75	>100	607	Nd	Nd
594	22.42	26.11	608	Nd	Nd

Table 7

Antiviral activity of MAS compounds on ZIKV. Nd: not determined.

The introduction of polar groups, both in presence of the salicylic and tetrazole moiety, have led to a quite good activity profile and restored a good selectivity index, while the introduction of lipophilic groups resulted in toxic (**MAS 591, 592, 596**) or not active (**MAS 599**) compounds. The length of the chain between the thiobarbituric nitrogen and the phenyl

moiety influenced the selectivity index; the longer the chain the worse the selectivity index. The *N*-pyrrole methylation resulted in a better cytotoxicity profile for **MAS 603** and increased activity of **MAS 604**, while **MAS 605**, the adamantanyl derivative, confirmed the toxicity of parent **MAS 596**.

Double rounds of infection: ZIKV and DENV

As reported in Table 8, compounds with modification A, like **MAS 584** and **MAS 587**, showed high antiviral activity and an improved selectivity index.

MAS CPD	ZIKV IC ₅₀ 1 st round (μM)	DENV-2 IC ₅₀ (μM)	HUH-7 CC ₅₀ (μM)
575	18.7	13.2 (2 nd round)	87
584	0.25	1.4 (1 st round)	7.9
587	0.61	3.4 (1 st round)	70
596	0.6	0.3	5
604	Na	Na	75

Table 8

Antiviral activity of MAS compounds on ZIKV and DENV-2 assayed with ELISA test. Na: not active.

Data obtained for compounds with modification on part B of the scaffold confirmed what was seen in the CPE assay: the introduction of polar groups increased the selectivity index while lipophilic groups made compounds more toxic. The only exception was **MAS 596** which is proven to be both active and quite safe. Only the *N*-pyrrole methylated derivative **MAS 604** resulted inactive on both viruses.

In vitro ADME profiling

Solubility

Data obtained from prediction, are reported in Table 9.

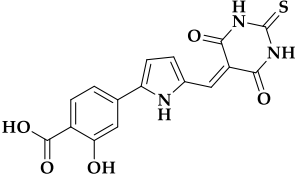
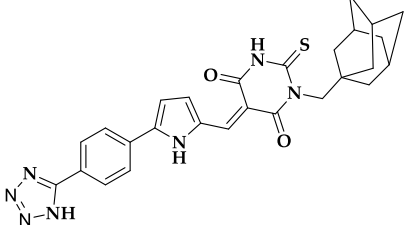
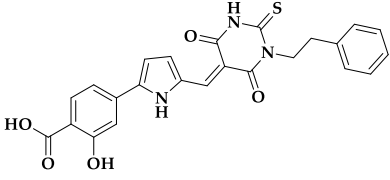
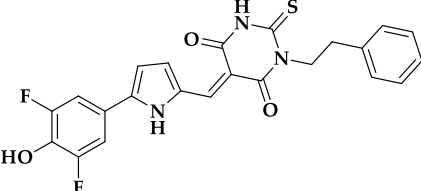
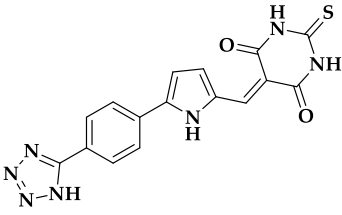
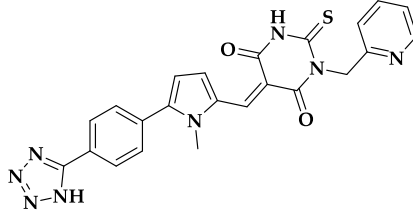
CPD	Structure	LogS	CPD	Structure	LogS
MAS 575		-4.66	MAS 596		-7.76
MAS 584		-6.86	MAS 602		-7.23
MAS 587		-7.22	MAS 604		-6.96

Table 9

Solubility values of MAS compounds expressed as LogS, predicted with QikProp software.

As expected MAS compounds presented the same trend seen for the 2nd generation of derivatives. Although the exception of MAS 575 with a LogS value of -4.66, the other derivatives were characterized by not encouraging values.

Permeability

Permeability values obtained with the PAMPA assay provide an overview of which molecules have the best ability to cross cell membranes through passive transport mechanisms. The determination of these values was carried out using the experimental conditions reported previously. Results obtained in terms of P_{app} expressed in cm/sec, and the percentage membrane retention values (MR %) obtained are shown in Table 10.

CPD	<i>P_{app}</i> (10 ⁻⁶ cm/sec)	MR %
MAS 575	0.06	45.1
MAS 584	0.07	12.5
MAS 587	0.06	30.2
MAS 596	0.04	47.6
MAS 602	0.01	0
MAS 604	0.03	54.1

Table 10

Permeability values of MAS compounds obtained from PAMPA assay expressed as P_{app}, and MR %.

The results obtained from the PAMPA assay showed a common tendency towards suboptimal permeability and the high MR % values also reflected the hydrophobic nature of these thiobarbituric compounds.

Metabolic stability

From the results of the metabolic stability assay carried out on selected MAS compounds, it has been possible to assess the metabolism rate of molecules and quantify the main metabolites formed. In Table 11 the % values obtained during the studies were reported.

CPD	<i>Metabolic Stability (%)</i>	<i>Metabolite M1 (%)</i>
MAS 575	>99	-
MAS 584	>99	-
MAS 587	>99	-
MAS 596	>99	-
MAS 602	>99	-
MAS 604	36.5	63.5

Table 11

Metabolic stability values of compounds expressed as % of parent compound and % of metabolite M1.

Data highlighted a common tendency of MAS compounds obtained from modification on parts A and B of the scaffold not to undergo metabolization by microsomal enzymes; in fact, the percentages of metabolic stability do not fall below 99%. The only exception was represented by the *N*-methylpyrrole derivative **MAS 604**.

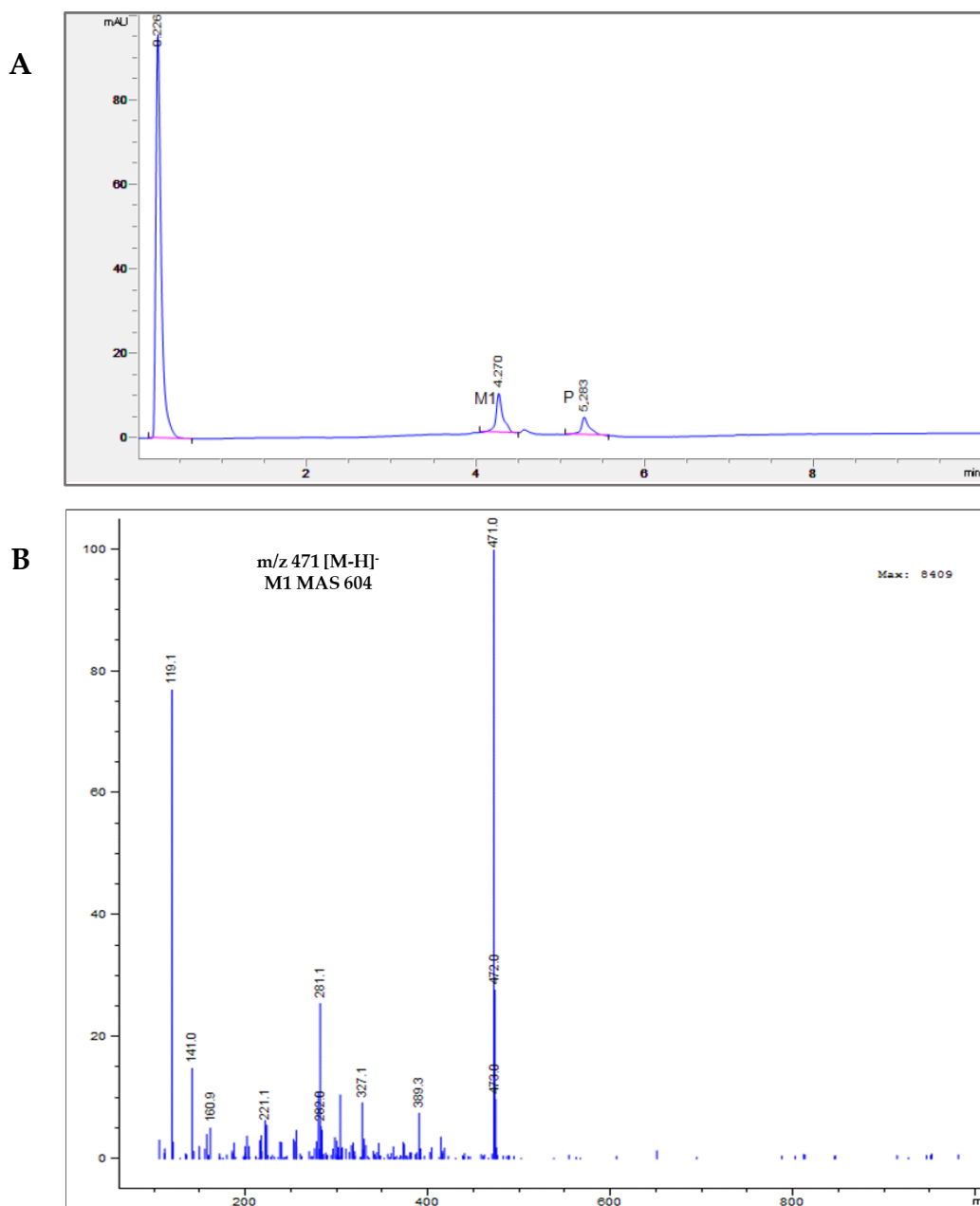


Figure 25

HPLC-UV (A) and MS (B) Chromatographic profile of MAS 604 after metabolization.

In this case, was observed a greater tendency to undergo the microsomal activity and the consequent formation of the main metabolite M1 (63.5%) obtained from the loss of the methyl group from the *N*-methylpyrrole and subsequential oxidation probably on the pyridine ring. As seen in the chromatographic profiles (Figure 25 A-B) obtained after the

metabolization step for compound MAS 604, M1 was characterized by an MS (ESI): $m/z = 471 [M-H]^-$.

Plasma stability

Plasma stability was determined on two of the most promising compounds **MAS 596** and **MAS 604**, reported in Figure 26.

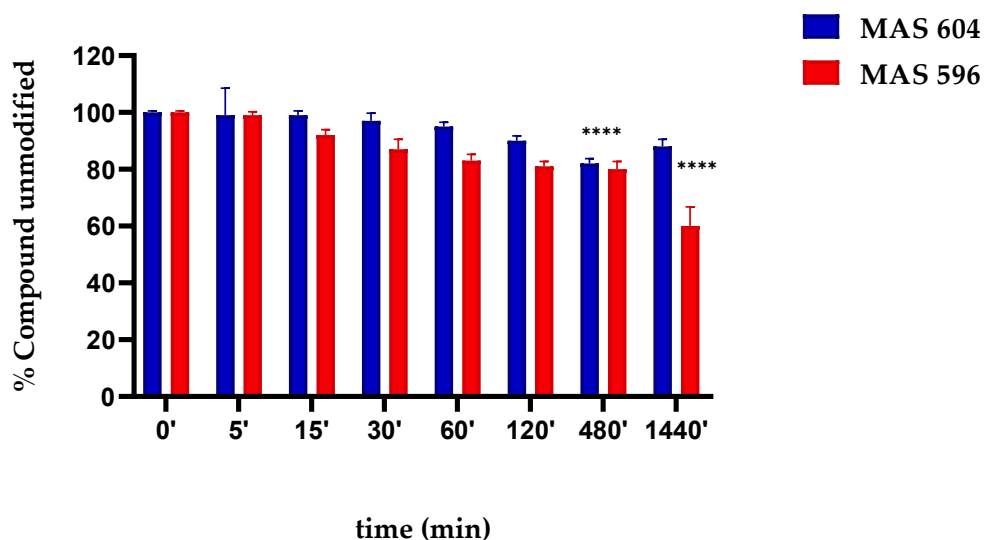


Figure 26

Plasma stability of MAS 596 and MAS 604 after different time points of incubation.

The results showed a significant decrease of stability in presence of plasma proteins of **MAS 596** close to 60% after 24 hrs of incubation, while **MAS 604** maintained a high percentage of the unmodified compound, never less than 80%.

Albumin binding

Albumin binding assays were performed by fluorescence spectroscopy; HSA (human serum albumin) was used as the interested protein from which the K_d values, representing the dissociation constant, were then obtained. From literature is well known the strong interaction between salicylic moiety and HSA.⁵⁷ Usually a higher binding between compounds and plasma proteins can be translated into a loss of activity because only the free drug fraction can reach the tissue target.

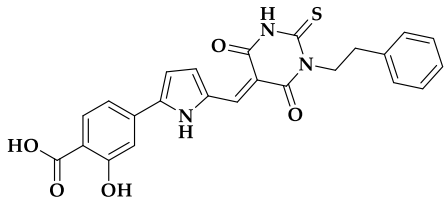
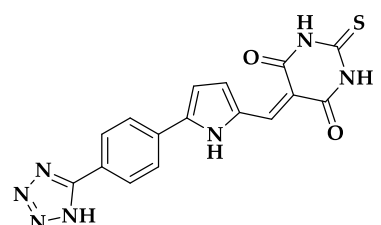
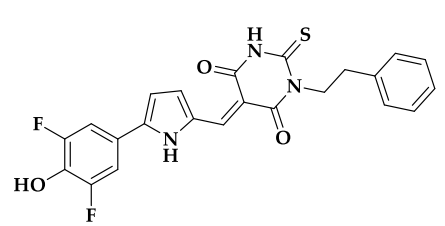
CPD	Structure	K_d (μM)
MAS 584		6.0
MAS 587		19.9
MAS 602		23.5

Table 12

Binding results of selected MAS compounds to HSA expressed as equilibrium dissociation constant (K_d).

For this reason, starting from a MAS derivative characterized by the presence of the salicylic moiety (**MAS 584**) was investigated how modification in part A of the scaffold with the introduction of a tetrazole (**MAS 587**) or difluorophenol (**MAS 602**) moiety, could modify the entity of interaction with HSA. As reported in Table 12, all K_d values obtained from assays did not demonstrate any significant improvements; even though the K_d values of **MAS 587** and **MAS 602** were higher than **MAS 584**, all K_d resulted lower than 100 μM suggesting a strong binding to HSA.

In conclusion, from the evaluation of ADME properties, poor solubility, and a limited passive permeability were observed for all MAS compounds assayed. Evaluating the metabolic stability in the presence of HLM, all MAS derivatives tested resulted in high stability, with the only exception of **MAS 604** which underwent a massive formation of metabolite M1 (63.5%). The well-known high affinity of salicylic moiety for the plasma proteins was confirmed by K_d values of three selected derivatives (**MAS 584**, **587**, **602**) The

compounds **MAS 596** and **MAS 604** resulted to have the highest antiviral activity against influenza virus strains, were tested for determining their plasma stability; while **MAS 604** resulted after 24 hrs to be stable at the degradative action of plasmatic esterases (~80%), **MAS 596** was characterized by the lowest stability close to 60%.

Although **MAS 604** resulted more stable than **MAS 596** in plasma at 24 hrs, it was discarded for the *in vivo* study because of its poor metabolic stability. Hence, **MAS 596**, due to its activity on influenza virus strains and, more importantly on the pandemic strain, with nanomolar activity, was chosen for the *in vivo* PK studies.

***In vivo* preliminary pharmacokinetic (PK) studies**

Considering all the data collected, from the antiviral activity to the preliminary solubility, permeability and metabolic stability, **MAS 596** was selected for further *in vivo* PK assays. **MAS 604** was initially chosen for its nanomolar efficacy on H1N1, its higher polarity, and good stability in plasma, but the poor metabolic stability forced us to exclude it. Moreover, **MAS 596** was found to have low nanomolar activity on the pandemic influenza strains, a sub-standard plasma stability profile, but high metabolic stability comparable to **MAS 604**. To overcome the poor solubility profile of **MAS 596** in common organic solvents, excipients, and aqueous solutions, various solubilization attempts were made. Various excipients (e.g., PEG, TWEEN and DMSO) with different solubilizing abilities and good biocompatibility were tested to obtain the best injectable formulation. However, no positive results were obtained. Finally, a literature protocol was chosen consisting of a 15 mM three amino acids (aspartic acid, glutamic acid, and histidine) solution solubilized in 10 mM TRIS buffer at pH 8.0.

Using this formulation, mice were divided into two groups and the compound was administered intravenously at doses of 25 mg/kg and 12.5 mg/kg.

After sacrifice, carried out at set times, the plasma was analysed according to the procedure described in the experimental part for the quantification of **MAS 596**.

The calibration curve used for **MAS 596** quantification, prepared both in organic solvent and in plasma, showed good linearity in the range of 0.5 µg/mL to 50 µg/mL (Figure 27).

The substantial overlap between the two lines ensures optimal recovery (>98%) from the biological matrix.

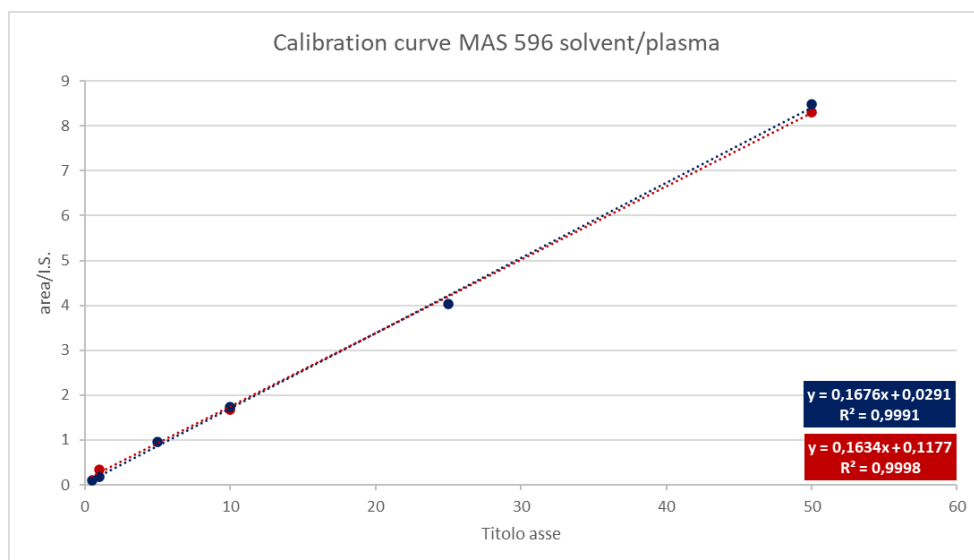


Figure 27

Calibration curve of MAS 596 both in solvent (blue) and plasma (red).

The determination of the pharmacokinetic parameters was conducted with the PK Solver software using a Non-Compartmental Analysis (NCA) approach (Table 13).

Results obtained after **MAS 596** *iv* administration underlined the same elimination profile for both doses; **MAS 596** followed a first-order kinetic, as can be appreciated from the logarithmic curve in Figure 28.

Parameters	Unit of measure	25 mg/kg	12.5 mg/kg
$t_{1/2}$	min	14.74	17.16
T_{max}	min	5	5
C_{max}	$\mu\text{g/ml}$	125.32	63.23
$AUC_{0 \rightarrow t}$	$\mu\text{g/ml} \cdot \text{min}$	3443.19	2201.14
$MRT_{0 \rightarrow \infty}$	min	28.63	29.41
V_z/F	$(\text{mg/kg})/(\mu\text{g/ml})$	0.15	0.28
Cl/F	$(\text{mg/kg})/(\mu\text{g/ml})/\text{min}$	0.01	0.11

Table 13

Pharmacokinetics parameters obtained after *iv* administration of MAS 596 at doses of 25 and 12.5 mg/kg.

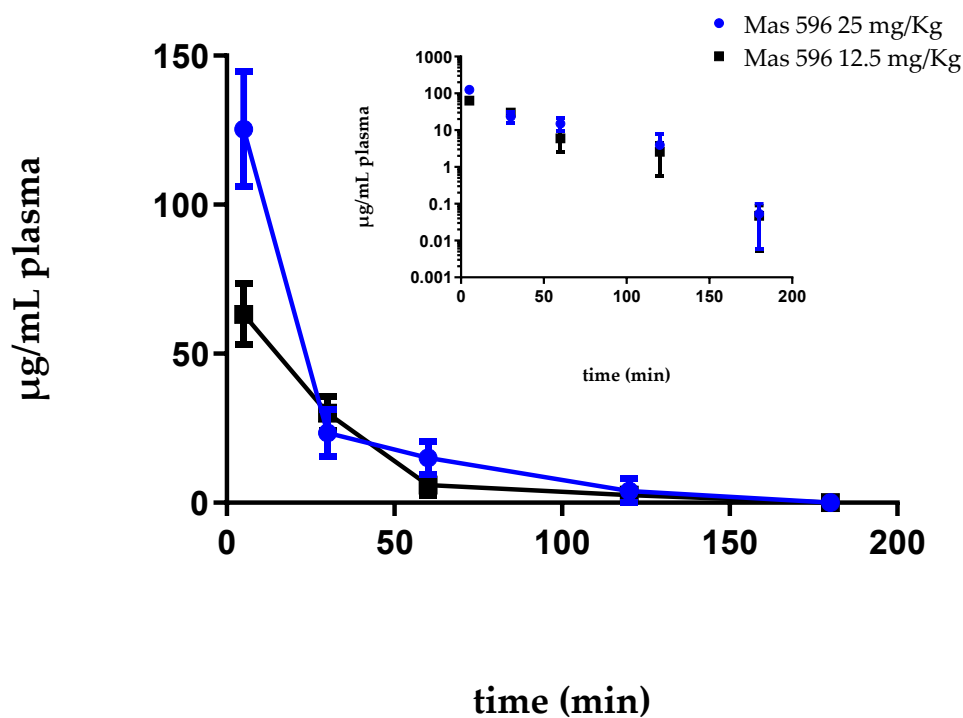


Figure 28

Plasmatic concentration of MAS 596 after *iv* administration at doses of 25 and 12.5 mg/kg.

Evaluating the half-life ($t_{1/2}$) and mean residence time (MRT) values, the rapid kinetic of **MAS 596** elimination was confirmed. Anyway, the pharmacokinetic parameters obtained were not satisfactory due to the very low T_{max} value (5') and the impossibility to achieve optimal therapeutical levels after an *iv* administration. These results also suggested the inadequacy of intravenous administration of **MAS 596**, due to the poor compliance of patients who would need to receive repeated doses over 24 hrs.

Due to the very low T_{max} and $t_{1/2}$ values, organs samples were collected from mice treated for 5' and 1 hour and immediately analyzed. Tissue distribution, reported in Figure 29, showed how **MAS 596**, at both dosages, tended to accumulate in lungs after 5 minutes, while in plasma, liver, and kidneys the concentrations of **MAS 596** were lower.

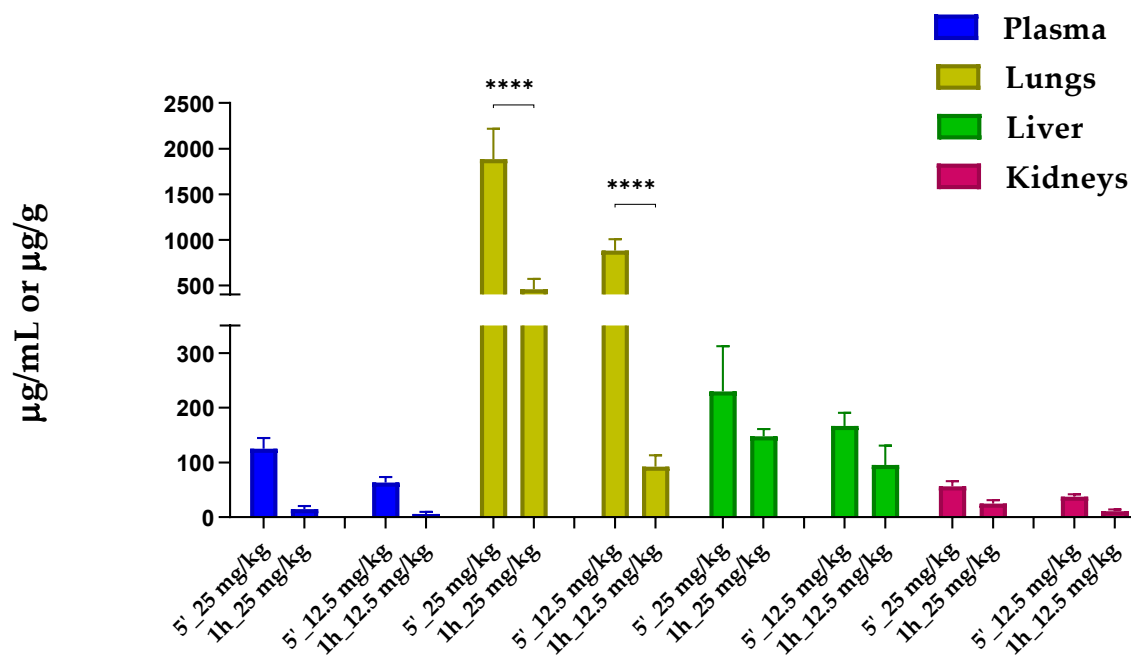


Figure 29

Tissue distribution of MAS 596 after 5' and 1 hour *iv* administration at doses of 25 and 12.5 mg/kg.

As expected from the PK values, low T_{max} , $t_{1/2}$ and MRT, plasmatic and tissue distribution after 1 hour drastically fell in both dosages, especially in the plasma and the lungs. The higher accumulation of **MAS 596** in the lungs can be explained by the first-passage filter role played by this organ for any drugs intravenously administrated, the short heart distance and the high rate of perfusion. Moreover, the high affinity of lipophilic compounds to lungs increased the retention of **MAS 596** in this tissue. ⁶⁴

Conclusions

During this Ph.D. project, I investigated the principal chemical-physics properties for the determination of the ADME profile of a new family of potent broad-spectrum antiviral thiobarbituric derivatives. MAS compounds were characterized by low solubility, limited passive permeability, reflecting their hydrophobic profile, and in general excellent metabolic stability. Regarding the metabolic stability, the only exception was represented by **MAS 604**, which has undergone a massive metabolic reaction, resulting in very low stability to the action of human pooled microsomes. Contrarily, **MAS 604** resulted stable to the metabolic action of plasma esterases (~80%) if compared to **MAS 596** which after 24 hrs almost ~40% has been metabolized. The investigation of binding affinity to HSA was performed only for selected molecules in order to evaluate if the replacement of the salicylic moiety (**MAS 575**) with a tetrazole (**MAS 587**) or difluorophenol (**MAS 602**) portion improved the K_d value, resulting in weaker binding to the plasma protein assayed. Although the modification in part A of the scaffold retained the antiviral activity and partially decreased the interactions, the K_d values remained low than 100 μM, synonymous with considerable interaction between compounds and HSA. From ADME *in vitro* results, **MAS 604** was initially selected for further *in vivo* studies, because of its excellent plasma stability after 24 hrs and nanomolar efficacy on H1N1 strain. This molecule was then discarded due to its poor metabolic stability, and **MAS 596** was chosen. **MAS 596** was administrated *iv* on healthy Balb/c male mice. Its poor aqueous solubility was efficiently overcome thanks to the use of the three amino acids solution as the optimal vehicle for its solubilization. The pharmacokinetic profile and tissue distribution were studied and it was found that **MAS 596**, due to its low half-life in plasma, should be administered several times over 24h in a therapeutic regimen to reach effective concentrations.

Taking together our results are compelling, even if the potent broad-spectrum antiviral **MAS 596** was not characterized by a good *iv* pharmacokinetic profile, its good pulmonary distribution, and the tropism of the influenza virus in the airways allowed us to think about future *in vivo* studies after inhalation administration.

Histone Deacetylases

The interaction between long eukaryotic DNA and histone proteins is a fundamental step in the gene-expression process. The ionic interaction between the positively charged histones and the negatively charged DNA backbone leads to a compact nucleosome that inhibits transcription restricting the access of the transcriptional machinery. Acetylation of the positive charge of the lysine residues on the histone surface by histone acetylase (HAT) allows the tight chromatin structure to open up and the binding of RNA polymerase II (RNA Pol II).

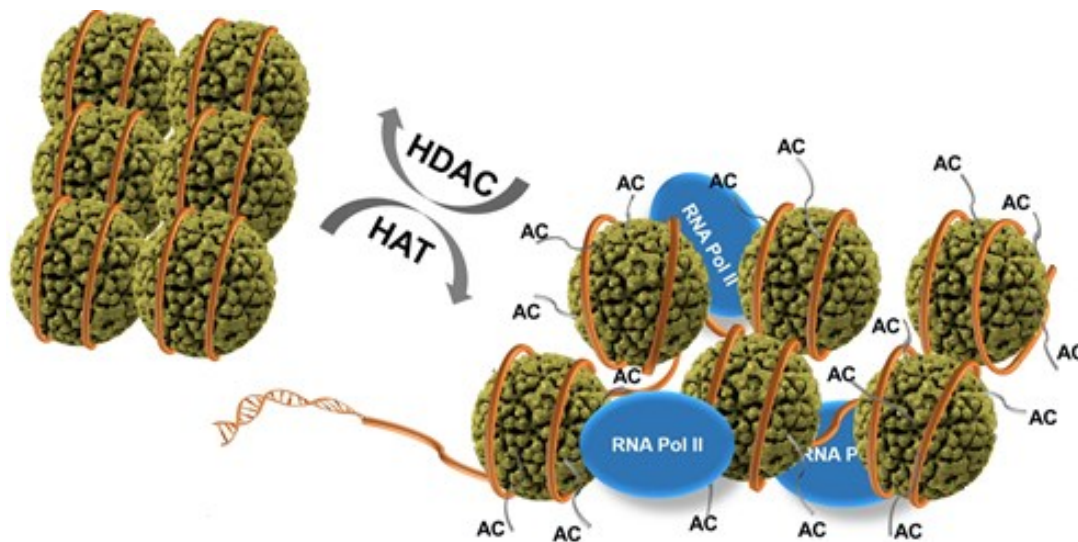


Figure 30

Regulation of gene expression by HAT and HDAC. Acetylation (AC) on histone lysine surface by HAT brings to a loose chromatin structure which allows binding of RNA Pol II, while HDAC deacetylates histone lysine residues regenerating a closer chromatin conformation and preventing RNA Pol II binding.

On the other hand, the deacetylation and the restoration of a positive charge on the histone lysine residues made by histone deacetylase (HDAC) leads to a stronger interaction between the positive-charged histones and the negative-charged DNA resulting in a tighter chromatin conformation that enable the binding of RNA Pol II inhibiting transcription (Figure 30).⁶⁵ Histone deacetylases (HDACs) are a group of epigenetics enzymes that

catalyze the removal of ϵ -N-acetyl lysine in H3 and H4 histone tails. To date, eighteen HDACs have been identified and catalogued into four major classes based on their primary homology to yeast HDACs:

- Class I (HDAC-1, HDAC-2, HDAC-3, HDAC-8);
- Class II
 - Class IIa (HDAC-4, HDAC-5, HDAC-7, HDAC-9)
 - Class IIb (HDAC-6, HDAC-10);
- Class III (Sirtuin-1, Sirtuin-2, Sirtuin-3, Sirtuin-5, Sirtuin-6, Sirtuin-7);
- Class IV (HDAC-11).^{66,67}

Class I, class II and class IV HDACs contain Zn^{2+} in their catalytic site that mediates the deacetylation of histone proteins by a metal-dependent mechanism, while class III HDACs require nicotinamide adenine dinucleotide (NAD^+) as cofactor for their catalytic activity.^{68,69}

Class I HDACs are expressed ubiquitously, predominantly localized within the nucleus, and play a crucial role in cell survival and proliferation. These HDACs are characterized by a relatively simple structure with the conserved deacetylases domain with amino- and carboxy-terminal extensions and a relevant enzymatic activity toward histone substrates. HDAC-1 and HDAC-2 are nearly equal and form usually repressive complexes with transcriptional regulatory protein Sin3, the nucleosome remodelling and deacetylase complex (NuRD), and the mitotic deacetylases complex (MiDAC). HDAC-3 is found in complexes such as the N-CoR-SMRT, whereas no complex has been described for HDAC-8 which functions alone. Although they are quite similarly expressed between malignant and non-malignant tissues, certain tumor types such as prostate and esophageal cancers, are characterized by an over-expression of class I HDACs.^{65,70,71}

Class II HDACs, mostly present in both the nucleus and the cytoplasm, shows a conserved deacetylase domain at their C-terminus and can be divided into two sub-families:

- Class IIa HDACs can be identified thanks to a large N-terminal extension with binding sites for the transcription factor myocyte enhancer factor 2 (MEF2) and the chaperone protein 14-3-3. These HDACs bind protein 14-3-3 and move from the nucleus to the cytoplasm after phosphorylation by calcium-calmodulin-dependent

protein kinase (CaMK) and protein kinase D (PKD). Class IIa HDACs display an important role in cell differentiation; their expression is regulated in a tissue-specific way and they are characterized by a very low enzymatic activity. While HDAC-5, HDAC-9, and HDAC-4 are highly expressed in skeletal muscle, heart, and brain respectively, HDAC-7 is mostly expressed in endothelial cells and thymocytes.

- Class IIb HDACs exhibit an extra tail domain at the C-terminus and are typically present in the cytoplasmic compartment. HDAC-6, the principal cytoplasmic deacetylase in mammalian cells, is constituted by two deacetylase domains and a C-terminal zinc ubiquitin-binding domain. Thanks to its second deacetylation domain, HDAC-6 can deacetylate α -tubulin stimulating cell mobility, cortactin and transmembrane proteins such as the interferon receptors (IFN α R) and chaperones. Conversely, very little is known about HDAC-10, the last of HDACs to be identified and characterized. To date, it has been found that HDAC-10 presents only one deacetylase domain and a leucine-rich repeat domain at its C-terminus and that can be used as a good indicator of poor prognosis in cancer patients due to its low-level expression in tumors.^{65,71,72}

The class III HDAC are enzymes involved in the repair of double-strand DNA breaks, control of recombination, cell cycle division and microtubule organization through a NAD-dependent mechanism. Their catalytic site consists of two domains that bind NAD and the acetyl-lysine substrate, respectively. Moreover, the presence of amino- and carboxy-terminal extensions lead Sirtuins to control their catalytic activity and subcellular localization. Class III has been found in a wide variety of subcellular compartments (Figure 31). Sirtuin-1 and Sirtuin-6 are localized in the nucleus, while Sirtuin-7 is found in the nucleolus. Sirtuin-2 and Sirtuin-3 are both present in the extra-nuclear compartment, in the cytosol and mitochondria, respectively. Even if Sirtuin-1 is generally present in the nucleus, it can also be localized in the cytoplasm in certain cell lines, where it probably is associated with apoptosis. Sirtuin1 forms a complex and deacetylates the histone acetyltransferase PCAF and the muscle transcription factor MyoD; its catalytic activity is involved in the repair of DNA thanks to its ability to deacetylate the tumor suppressor p53 leading to the

suppression of apoptotic mechanisms and prolongment of the cell cycle in response to DNA damage.^{73,74}

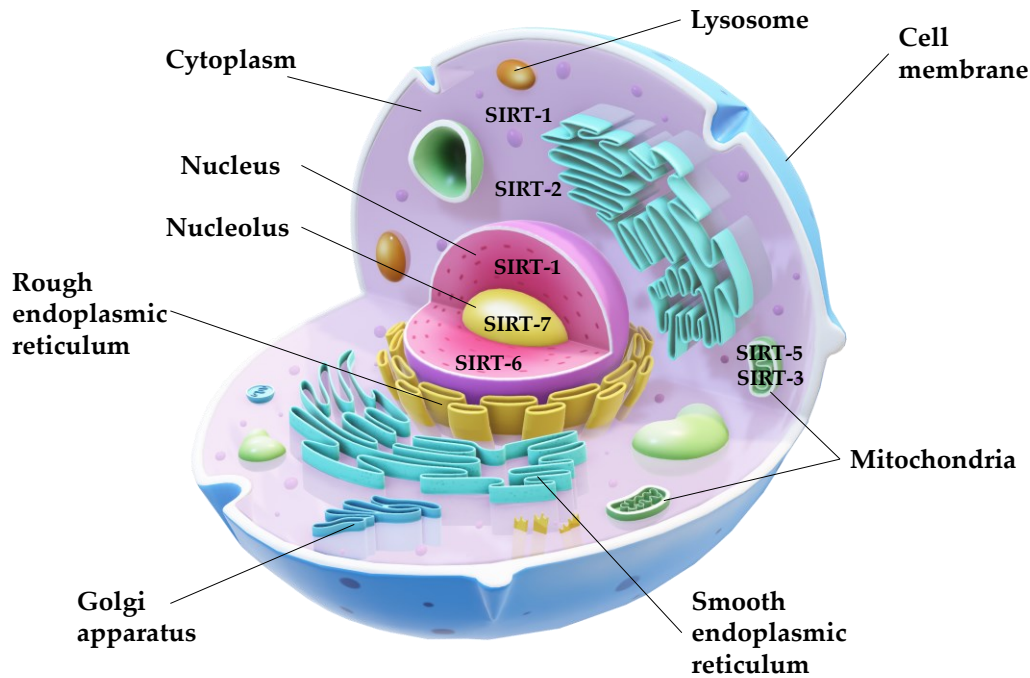


Figure 31

Localization of human Sirtuins in cells. Sirtuin-1 is mostly localized in the nucleus and a small percentage is also present in the cytoplasm. Sirtuin-2 is found in the cytoplasm, while Sirtuin-3 and Sirtuin-5 are typically present in mitochondria. Sirtuin-6 and Sirtuin-7 are localized in the nucleus and nucleolus, respectively.

Despite Sirtuin-2 predominantly being found in the cytoplasm where it was first identified as an α -tubulin deacetylase, it is continuously shuttled between the cytoplasmatic and the nuclear compartment. Sirtuin-2 tends to accumulate in the nucleus during different physiological conditions, such as mitosis and mediates the deacetylation of H4 Lys16. This enzyme has been demonstrated to play regulatory roles in the oxidative stress and inflammatory responses throughout the deacetylation of FOXO3 and NF- κ B.⁷⁵

Sirtuin-3 is the major mitochondrial deacetylase which shares a high degree of homology with the cytosolic Sirtuin-2. Though its primary enzymatic activity is deacetylation, Sirtuin-3 is fundamental for the regulation of many aspects of mitochondrial biology such as FAO, amino acid metabolism, TCA cycle, ETC, ATP production and ROS defence. Under genotoxic stress, protects against cell death in human embryonic kidney (HEK293) and fibrosarcoma cell lines, protects cardiomyocytes and HeLa cells from oxidative stress-

mediated cell death. Moreover, Sirtuin-3 has a protective effect on the heart, preventing cardiac hypertrophy by blocking ROS and regulating the mitochondrial permeability transition pore (mPTP).^{76,77}

Sirtuin-5 is predominantly localized in the mitochondria. Due to the presence of positively charged amino acid groups in its catalytic site, Sirtuin-5 shows a high affinity towards negatively charged substrates like succinyl, malonyl and glutaryl groups; in fact, displays demalonylation, deglutarylation and desuccinylation activity much higher than its deacetylation activity. Sirtuin-5 is also involved in glucose metabolism, the TCA cycle through desuccinylation and inactivation of the PDH and SDH complexes and in ROS defence through binding and desuccinylation of SOD1.⁷⁶

Sirtuin-6 is a protein involved in the regulation of chromatin, telomere maintenance, DNA repair and gene expression. Mostly localized to the nucleus, Sirt6 can be found in the nucleolus during the G₁ phase of the cell cycle, while in the S phase is completely absent. Sirtuin-6 defection compromises the base excision repair (BER) pathway involved in the repair of spontaneously occurring single-stranded DNA lesions. Moreover, Sirtuin-6 may have a role in double-stranded DNA break repair.^{78,79}

Sirtuin-7 is localized to the nucleolus and, in comparison to the other sirtuins, exhibits a low deacetylase activity due to the serine residue 111 (S111) and histidine residue 187 (H187) within the Sirtuin-7 catalytic domain. However, Sirtuin-7 is a highly selective histone H3 lysine 18 (H3K18) deacetylase and displays other enzymatic activities like NAD-dependent histone desuccinylase and defatty-acylase. Sirtuin-7 is mostly expressed in spleen, liver, and testis, while the lowest expression is found in the heart and brain. Usually, its presence in different organs or tissues can be used as a positive or negative indicator of cellular proliferation, differentiation and stress response.⁸⁰

The last class of HDAC is the fourth which consists of only one member, HDAC-11. From the structure point of view, this HDAC is strictly related to class I and class II HDACs, sharing amino acids residues in the regions of catalytic active sites. HDAC-11 is located in the nucleus and its higher expression can be found in brain, heart, and kidneys; this protein is involved in a regulation mechanism of interleukin 10 (IL-10) expression, by interacting at chromatin level with the distal region of the IL-10 promoter.^{81,82}

HDACs & Cancer

Over the last decades, has been cleared up how epigenetic abnormalities are primarily involved in malignant cellular transformation leading to cancer. Histone undergoes multiple posttranslational modifications, such as the reversible acetylation of the ϵ -amino lysine residues on its tails, that modulate chromatin structure and gene expression. All these abnormal variations can promote cancer development and progression. In physiological conditions, HDACs and HATs activities are perfectly balanced: HDACs deacetylate histone tails inducing chromatin compaction, while HATs transfer acetyl groups to lysine leading to a more relaxed chromatin structure. HDACs up-regulation and abnormal activity represent a common condition in different human diseases such as nervous system, cardiovascular, inflammatory diseases, and also cancer. Several alterations of HDACs functions have been associated with a large number of solid and hematological tumors where these enzymes are involved in several crucial steps of cancer development such as differentiation, proliferation, metastasis, angiogenesis, apoptosis, and aberrations of the cell cycle (Figure 32). The disrupted balance between histone acetylation and deacetylation alters the expression of genes involved in both cancer initiation and progression; in fact, HDACs induce a blockage of the mechanisms of cell cycle inhibition, cell differentiation and adhesion, and apoptosis. Furthermore, HDACs promote angiogenesis, cell invasion and migration.⁸³

Several studies have shown the important role of HDACs in DNA-damage repair (DDR) because these enzymes modulate chromatin structure and maintain dynamic acetylation-deacetylation equilibrium of DNA-damage-related proteins. Class I HDACs regulate the acetylation status of histones and alter other proteins involved in the DNA-damage response. For instance, HDAC-1 and HDAC-2 play a direct role during DNA replication and double-strand breaks repair deacetylating histone H3K56 and H4K16. Among the class II HDACs, several are involved in DNA-damage-repair mechanisms. These enzymes regulate proteins involved in the DNA mismatch repair system, which come in during the replication and recombination process correcting DNA mismatches in order to maintain genomic integrity.

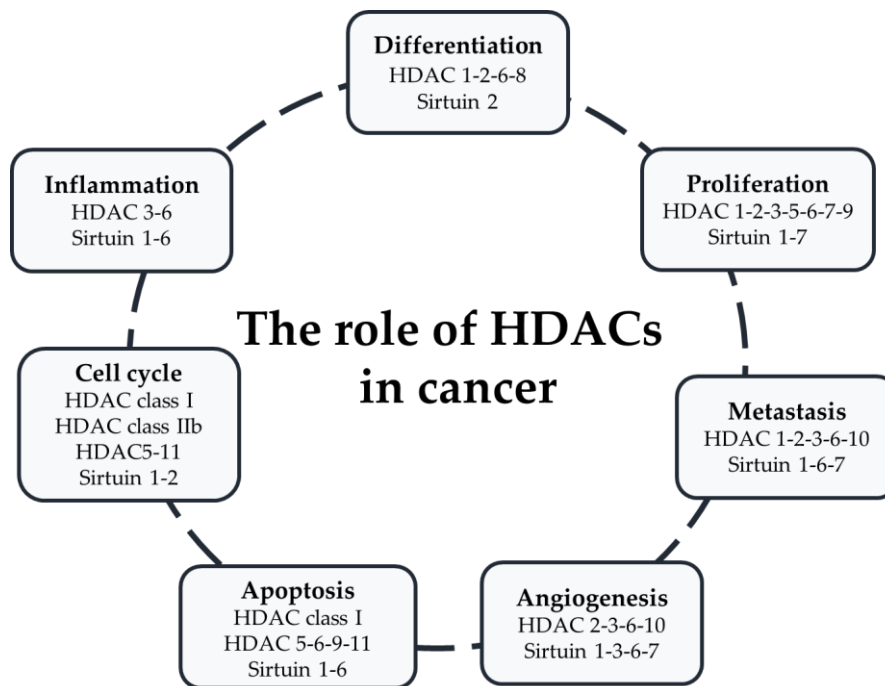


Figure 32

Histone deacetylases (HDACs) involved in cancer development. The exact mechanisms by which HDACs contribute to cancer are several; here is a schematic illustration of the multiple functions of HDACs regulating different key steps in tumor progression.

In particular, HDAC-6 deacetylates and ubiquitinates DDR proteins leading to a cellular tolerance to DNA damage and a blockage of cellular DNA mismatch repairs mechanisms. Class III HDACs are important components of the DNA repair pathways regulating several steps of DDR (e.g., signal transduction, DNA repair, apoptosis). Between Sirtuins, SIRT-1 seems to be the most involved in the DNA-damage repair system, interacting and deacetylating several DDR proteins. Although SIRT-1 plays a key role in maintaining genome integrity and stability, blocking p53 acetylation promotes cancer cells' survival after DNA damage.

Class I, class IIb and class III HDACs are recruited in the epithelial to mesenchymal transition (EMT) process, the principal in cancer cells invasion and metastasis, which leads to the loss of epithelial-cadherin (CDH1) cell markers and several transcriptional repressors. During the metastatic process, cells have lost their ability to interact with the micro-environment and other cells surrounding them. Class I HDACs can regulate extracellular matrix-related genes and repress cystatin, a peptidase inhibitor that puts down cancer

invasion. SIRT-1 also favours tumor cell migration and metastasis by making a complex with the transcriptional factor ZEB-1 that inhibits CDH1 expression.

Furthermore, almost all the HDACs are involved in the angiogenic process. Angiogenesis, an essential step for tumor growth and metastasis, is brought about by hypoxia and the cellular response to this event is guided by the transcriptional factor HIF-1 α . Even if the antiangiogenic activity of HDACs inhibitors (HDACi) has been shown by several studies, the influence of every enzyme on angiogenic gene expression is doubtful. For instance, HDAC-5 is a negative regulator of angiogenesis because of its repression mechanism of pro-angiogenic gene expression. Moreover, HDAC-6 displays a dual role in the angiogenic process; while inducing angiogenesis in endothelial cells by regulating migration, a high expression of HDAC-6 inhibits angiogenesis by a down-regulation of the expression of HIF-1 α . HDAC-7 is essential in maintaining the endothelial angiogenic functions, like tube formation, migration, and proliferation. HDAC-9 has a positive control on the endothelial cell and vascular growth by repression of a cluster which reduces the expression of proangiogenic proteins. In order to understand the development, maintenance, and progression of tumor cells, the role of autophagy has been often investigated. The mechanism of autophagy in response to oncogenic stresses is involved both positively and negatively in tumorigenesis. On one hand, autophagy removes damaged organelles and cellular components to prevent normal cells from transforming into tumor cells. It seems clear that, in physiological conditions, any alteration in the autophagy process might promote cancer development. On the other hand, when the tumorigenic mechanism has already started, autophagy built up cancer cells' survival and might also confer resistance to anticancer therapies. According to the dual role of autophagy in cancer development, many HDACs enzymes show both pro- and anti-autophagy activities. For instance, down-regulation or inhibition of HDAC-1 promotes accumulation of the autophagosomal marker LC3-II, leading to an induction of autophagy. HDAC-4 and HDAC-5 knockdown induces autophagy by enhancing LC3-II, Beclin-1, and ATG-7 cellular levels. HDAC-6 and HDAC-10 deacetylate some cytoplasmic proteins directly involved in the autophagy process because they modulate key autophagy proteins (e.g. LC3-II, Beclin-1). In neuroblastoma disease, downregulation, or inhibition of HDAC-10 interrupts autophagic flux shooting

down autophagosome/lysosome fusion, resulting in higher sensitization to treatments. Among the HDACs, class IIb (HDAC-6, HDAC-10) seem to mainly regulate autophagy via deacetylation of cytoplasmic proteins.⁸⁴⁻⁸⁶

The dual role of Sirtuins in cancer progression

Sirtuins family members play crucial roles in carcinogenesis by regulating cancer cell viability, apoptosis, metastasis, and tumorigenesis. Although they control several steps of cancer development, Sirtuins act as a dual character, as tumor promoters and suppressors. Sirtuin-1 has a contradictory role in cell viability; while managing genetic stability in normal cells slowing down proliferation, Sirtuin-1 promotes cellular growth and proliferation in different types of cancer (i.e., leukemia, colorectal cancer) and cell growth deacetylating FOXO3, RB1, KU70 and E2F1. When occurring DNA damages and oxidative stress, Sirtuin-1 acts as a regulator of apoptosis by deacetylating some apoptosis-related proteins and cell signaling molecules, such as p53, NF- κ B and FOXO3; on the other hand, downregulates the antiapoptotic gene. The cellular expression levels of Sirtuin-1 are directly correlated to tumor stage, invasion, metastasis, and usually, its expression is tightly connected to a poor prognosis. Moreover, Sirtuin-1 knockdown damps down cancer cells migration and invasion. Sirtuin-1 promotes epithelial to mesenchymal transition (EMT) in cancer and fibrosis by deacetylating Smad4 and cooperating with the EMT inducible transcription factor ZEB1. Conversely, acts as a positive regulator of EMT influencing the metastatic growth of tumor cells.

Regarding Sirtuin-2, it plays as a tumor suppressor by deacetylating histone H4K16, p53, p65, FOXO3, and CDK4; moreover, interacts with β -catenin in order to inhibit cell growth and can be identified as an oncogenic factor involved in the cell proliferation mechanism. Sirtuin-2 can induce apoptosis in response to DNA damage by catalysing P53 deacetylation. Sirtuin-3, the major deacetylating enzyme in mitochondria, has a key role in cancer cell growth regulation acting as a tumor promoter and suppressor. Several studies have demonstrated that Sirtuin-3 is involved in the regulation of a variety of substrates, such as p53, GSK-3 β , and enhances the degradation of the oncoprotein MYC and inhibits cancer cell progression both *in vitro* and *in vivo*. Its dual role can be well established by looking at how

Sirtuin-3 both induces apoptosis by affecting BAX and p53 and blocks apoptosis by deacetylating and downregulating AGFG1 in response to chemotherapeutic agents. Previous studies have demonstrated the capability of Sirtuin-3 to suppress cell migration and invasion through the activation of FOXO3A and the suppression of EMT. Furthermore, Sirtuin-3 has a controversial role in different types of tumors; in fact, it influences tumorigenesis by reducing reactive oxygen species (ROS), regulating metabolism and the apoptotic pathways. When overexpressed, Sirtuin-3 behaves as a tumor suppressor by decreasing tumorigenesis and glycolysis proliferation. While its knockdown induces the tumorigenic process and the enzyme acts as a promoter of cancer development throughout the deacetylation and activation of lactate dehydrogenase.

Sirtuin-5 has been considered a potential oncogene as well because it mediates lysine deglutarylation, desuccinylation, and demalonylation by blocking cell growth and activating glutamate dehydrogenase 1 (GLUD1). Displaying apoptotic and antioxidative role in cancer development and contributing to cell invasion and metastasis, Sirtuin-5 acts as a tumor-promoter in multiple types of cancer (i.e., colon cancer, human osteosarcoma, breast cancer). Similar to other sirtuins, Sirtuin-6 also displays a dual role, being involved in both tumor suppression and progression; in fact, it has been demonstrated that Sirtuin-6 can deacetylate PKM2, NF- κ B, HIF1 α and several other genes, leading to a cell proliferation reduction. If its low expression has been reported in pancreatic and colorectal cancer, Sirtuin-6 is overexpressed in acute myeloid leukemia (ALM) and skin squamous cell carcinoma where inhibits AMPK signaling promoting COX-2 expression, thereby cell proliferation and survival are increased.

An overexpression of Sirtuin-6 deacetylates fundamental cell signaling molecules (e.g. KU70, Bax, P53) in response to DNA damage and oxidative stress, provoking huge cell apoptosis in cancer cells but not in the normal ones. Moreover, promotes the migration and invasion of cancer cells. For example, in glioblastoma, Sirtuin-6 deacetylates and inhibits the JAK2/STAT3 pathway promoting cell apoptosis. In contrast, a Sirtuin-6 deletion provides to metastasis and cancer development. However, it acts also as a tumor inhibitor, preventing genomic instability, maintaining telomere integrity, and regulating metabolic homeostasis.

The last member of the Sirtuin family, Sirtuin-7, acts as a tumor suppressor for cell growth, deacetylating P53, H3K18 and other critical substrates involved in several cellular activities. It can regulate apoptosis progression after DNA damage and oxidative stress. Recent studies have reported that Sirtuin-7 may help along tumorigenesis in human cancer, playing a role as a tumor promoter in gastric, hepatic, ovarian, and breast cancer. This is considered a secondary effect probably due to its impact on ribosome biogenesis, in fact, Sirtuin-7 itself is not able to induce the oncogenic transformation of normal fibroblasts.⁸⁷

HDACs inhibitors

Histone acetylation is an important regulatory mechanism in controlling genetic transcription, while histone deacetylation leads to chromatin condensation preventing transcription. Any alterations in the balanced activity of HAT/HDAC can alter gene expression changing some signaling pathways, leading to proteasomal degradation, influencing protein kinase C activity, or changing DNA methylation status. Recent studies have demonstrated how the inhibition of HDAC promotes cancer cell cycle arrest, differentiation, and cell death, reduces angiogenesis, and modulates the immune response. HDACi can prevent the aberrant protein acetylation and up-regulate the tumor suppressor mechanisms, leading to a cell-cycle arrest, apoptosis, and inhibition of angiogenesis and metastasis. To date, a large number of synthetic and natural molecules identified as HDAC inhibitors have been studied, developed, and characterized. They may act in a selective way against a specific HDAC isoform (HDAC isoform-selective inhibitors) or against all types of HDACs (pan-inhibitors).^{85,88}

As shown in Table 14, HDAC inhibitors can be distinguished into five classes of molecules:

1. Hydroxamic acids (Hydroxamates)
2. Short-chain fatty acids
3. Benzamides
4. Cyclic tetrapeptides
5. Sirtuin inhibitors

Class	Inhibitor	Target
Hydroxamic acids	SAHA	Pan-HDAC
	Panobinostat	Pan-HDAC
	Givinostat	Pan-HDAC
	Rocilinostat	HDAC II
	Practinostat	HDAC I, II, IV
Short-chain fatty acids	Valproic acid	HDAC I, IIa
	Butyric acid	HDAC I, II
Benzamides	Entinostat (MS-275)	HDAC I
	Tacedinaline	HDAC I
	Mocetinostat	HDAC I, IV
Cyclic tetrapeptides	Romidepsin	HDAC I
Sirtuin inhibitors	Nicotinamide	HDAC III
	Sirtinol	Sirtuin-1
	Cambinol	Sirtuin-2

Table 14

Overview of HDACi. Different compounds identified as HDAC inhibitors and classified according to their chemical family and target.

Belonging to the Hydroxamic acids class, the pan-HDAC inhibitor SAHA (suberoylanilide hydroxamic acid, Vorinostat, Zolinza) was the first HDACi to be approved by FDA for the treatment of the refractory primary cutaneous T-cell lymphoma (CTCL). Preclinical studies have shown that SAHA can induce apoptosis and cell-cycle arrest, reducing proliferation and metastasis in cancer cells. Panobinostat, another pan-HDAC, has been approved for therapy of multiple myeloma, while Givinostat has been recently tested in phase II clinical trials for leukemia and multiple myeloma. Selective HDACs inhibitors, like Rocilinostat (HDAC II) and Practinostat (HDACs I, II, IV) are compounds tested in clinical studies against multiple myeloma and prostate cancer, respectively. Among the short-chain fatty acids, Butyric acid inhibits HDAC I and II, while Valproic acid (VPA) is a weak

inhibitor of HDAC I and IIa; it has been approved for the treatment of epilepsy, bipolar disorders, and is under investigation for its anticancer activity. The benzamides, Entinostat (MS-275) and Tacedinaline inhibit class I HDACs, instead, Mocetinostat is a selective inhibitor of HDAC I and IV. Romidepsin, a cyclic tetrapeptide, has been approved by FDA and EMA for the treatment of CTCL. Acting as a prodrug, it is reduced to a metabolite whose thiol group chelates Zn^{2+} ions in the catalytic site of class I HDACs.⁸⁸

Among the Sirtuin inhibitors, Nicotinamide was the earliest discovered; it is a pan-inhibitor of the Sirtuin class, with IC_{50} values of between 50 and 184 μM . Nicotinamide blocks cellular proliferation and promotes apoptotic mechanisms in leukemic cells, induces growth suppression and inhibits human prostate cancer cells viability. Sirtinol is a β -naphthol-containing Sirtuin-1 selective inhibitor with anticancer activity; it induces senescence-like growth arrest and cell apoptosis. Sirtinol, combined with cisplatin displays a synergistic effect, inhibiting HeLa cell proliferation. Cambinol is another β -naphthol compound that inhibits Sirtuin-2; it shows also a weak inhibition against Sirtuin-5 and no one against Sirtuin-3.⁸⁹

Naturally occurring HDAC inhibitors

Over the last few decades, a multitude of new Histone Deacetylase inhibitors has been discovered from natural sources. They can be distinguished in several classes thanks to the wide variety of their structural features. Trichostatin A (TSA), Psammaplin A, and Depudecin are identified as linear inhibitors. TSA (Figure 33. a), isolated from *Streptomyces hygroscopicus* bacteria, was firstly studied for its antifungal activity, and only later was found to be an HDAC inhibitor. From its crystal structure in the active site of the *A. aeolicus* can be seen that TSA binds the active site of HDACs in a non-covalent way; in fact, the terminal hydroxamic acid group chelates the Zn^{2+} in a bidentate mode. Psammaplin A, isolated from the marine sponge *Psammaphysilla sp.*, is a potent HDAC-1 selective inhibitor against human colon, lung, and ovarian carcinomas. Depudecin, instead, is a fungal product characterized by the presence of six asymmetric centers and a bis-*trans*-epoxide moiety; it acts like an HDACi showing anti-angiogenic activity both *in vitro* and *in vivo*.

Within the class of cyclic tetrapeptides, natural compounds can be identified such as HC toxin and Cyl-1/2, Chlamydocin, Trapoxins, Apicidins, and Microsporin. HC toxin has been the first cyclic tetrapeptide isolated from a fungal plant pathogen, classified as an HDAC inhibitor; it consists of D-proline, D-alanine, L-alanine, and (2S)-amino-8-oxo-9,10-epoxydecanoic acid (Aoe), but its potency is weaker than TSA one. Isolated from the fungus *Cylindrocladium scoparium*, Cyl-1 and Cyl-2 are structurally correlated to HC toxin being characterized by the presence of the Aoe residue that is fundamental for the inhibitory function, because it acts as an acetylated lysine residue; Cyl-2 shows an HDAC class I selectivity with a prominent HDAC-1 inhibitory activity and a lack of inhibition for HDACs 4 and 6 (class IIa and IIb, respectively). Chlamydocin (Figure 33. b), isolated from the fungus *Diheterospora chlamydosporia*, is composed of L-phenylalanine, D-proline, 2-aminoisobutyric acid (Aib) and the Aoe group. It displays an extremely potent HDACs inhibition activity increasing the levels of H3 and H4 acetylation in a dose-dependent manner; on ovarian (A2780), colon (HT29), cervix (HeLa), and lung (H1299) cancer cell lines, chlamydocin shows IC₅₀ values in the nanomolar ranges. Trapoxins are fungal products characterized by two L-phenylalanine, D-proline or D-pipecoline acid, and the Aoe moiety; they inhibit class I and IIa HDACs resulting in a hyperacetylation of histones.

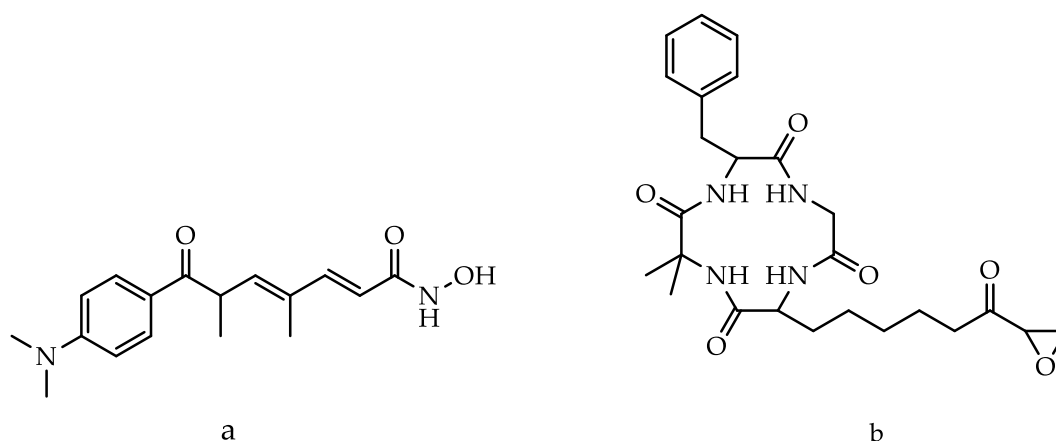


Figure 33

Chemical structures of natural HDAC inhibitors. (a) The linear HDAC inhibitor Trichostatin A (TSA). (b) The cyclic tetrapeptide HDAC inhibitor Chlamydocin.

Apicidins are also fungal natural extracts containing (2S)-amino-8-oxo-decanoic acid (Aoda) that differ in the presence of different amino acids. Inducting the cyclic-dependent kinase

(CDK) inhibitors p21, Apicidins show an antiproliferative action in various cancer cell lines, probably due to the dose-dependent increase of H4 acetylation. Their potent HDAC inhibition depends on the insertion of the acetylated lysine mimic into the active site and the carbonyl group that binds and chelates to the Zn^{2+} , allowing the entry of the natural substrates. Lastly, Microsporins have been isolated from a marine fungus and act as HDACs inhibitors probably inserting their Aoda residue into the enzyme active site.⁹⁰

Largazole

Largazole is a potent and selective HDAC inhibitor isolated from a marine cyanobacterium of the genus *Symploca*, that is characterized by a nanomolar selective potency for Class-I HDAC (HDAC-1 IC_{50} 25 nM, HDAC-2 IC_{50} 21 nM and HDAC-3 IC_{50} 48 nM).⁹⁰

From a structural point of view, largazole is an intriguing planar 16-membered depsipeptide macrocycle with a 4-methylated thiazoline unit fused to thiazole, a 3-hydroxy-7-mercapt-4-enoic acid group, and a metabolically labile thioester moiety, which undergoes a hydrolytic cleavage and liberates the bioactive largazole-thiol (Figure 34), able to coordinate to the Zn^{2+} inside the HDAC active site.^{66,91}

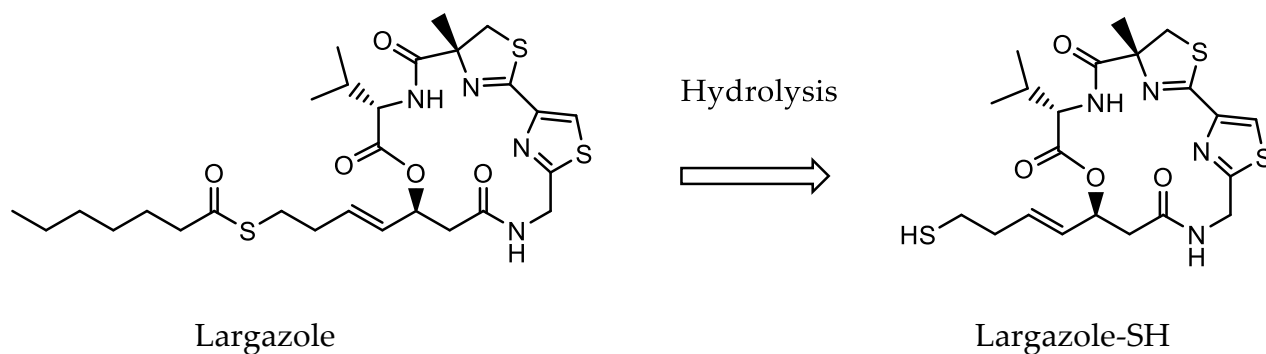


Figure 34

Chemical structure of the cyclic depsipeptide largazole and the thiol bioactive specie. Largazole acts as a prodrug which after hydrolysis releases largazole-SH.

After hydrolysis conducted by cellular and plasmatic proteins, largazole thiol is rapidly released and can interact with its catalytic site; this activation process is induced by a protein-mediated mechanism that can explain why largazole itself shows an *in vitro* potency 10-fold lower than thiol specie. SAHA (Vorinostat) and romidepsin represent the first- and second-generation of HDACi, and they show an *in vitro* profile very similar to largazole one;

they are also prodrugs that liberate the bioactive thiol after by thioester hydrolysis (SAHA) or by disulfide reduction (romidepsin). Although these peculiar similarities, largazole shows a higher inhibitory potency than these two HDACi.⁹¹ This potent HDAC inhibitor is characterized by a peculiar anticancer activity letting to discriminate between tumor cells and normal cells. In fact, it inhibits the growth of epithelial and fibroblastic cancer cell lines (i.e., colorectal carcinoma, neuroblastoma, glioblastoma, breast cancer, and osteosarcoma)^{92,93} at nanomolar concentrations, while for what regards non-transformed epithelial cells and fibroblasts, their cellular growth is inhibited at the much higher micromolar concentration. In colon cancer cells (HCT116), largazole induces p21 expression and G1 cell cycle arrest at low nanomolar concentration (3 nM), while in NB4 leukemia cells largazole also induces p21 expression; other CDKs (cyclin-dependent kinases), which plays a key role in cell cycle progression (e.g., p19, p57, p15), are overexpressed upon largazole treatment, while CDKs-6 and cyclin-D1 are downregulated. All these opposite effects probably potentiate and enhance the antiproliferative action of largazole. At higher concentrations this potent HDACi causes a cell cycle arrest in G2/M phase, instead at concentrations greater than 30 nM, largazole induces apoptosis that can be assessed by the activation of caspases 3/7. Moreover, as demonstrated by Luesch and co-workers, the antiproliferative activity of largazole, is mainly due to the inhibition of HDACs that use Ac-H3 (Lys9/14) as substrate.⁹⁴

More recently, largazole has been studied for its relevant role in osteogenesis; in fact, HDACs, thanks to their capability to modify chromatin structure and regulate gene transcription, are involved in osteogenesis, and thus considered important targets for bone disease, such as osteoporosis. Although several HDACi (e.g., Trichostatin A and Valproic acid) have been tested for their osteogenic activity, none have been shown relevant results; on the contrary, long-term treatment with Valproic acid seems to increase the incidence of osteoporosis. Largazole shows *in vitro* and *in vivo* osteogenic activity, inducing the expression levels of alkaline phosphatase (ALP) and osteopontin (ONP). So it has been suggested that the osteogenic activity of largazole would be mediated by the increased expression of Runx2 and BMPs.⁹⁵

Furthermore, Liu Y. and co-workers have studied the largazole effect in liver fibrosis. The natural HDACi potentially mitigated the development of the disease through the inhibition of the mechanism of fibrosis and angiogenesis, without affecting the proliferation of normal human hepatocytes. From these studies, has been demonstrated that largazole induced the acetylation of histone H3 and histone H4, and apoptosis in hepatic stellate cells (HSCs), inhibited the TGF β R2 and the vascular endothelial factor (VEGF) expression, reduced phosphorylation of Smad2 and Akt, and suppressed VEGF-induced proliferation of HSCs and activation of Akt and p38MAPK.⁹⁶

In terms of structure-activity relationship (SAR), initially, Luesch and co-workers, have studied and defined the pharmacophore of largazole, testing an acetyl analogue that showed the same antiproliferative activity and potency, but only a transient protective role played by the carboxylic acid group linked to the thiol moiety. To further investigate the pharmacophore, they also tested other hydroxyl analogues and a macrocycle devoid of the sulfur-containing aliphatic chain; both of them showed a lack of inhibitory function on HDACs. Subsequently, has been reported the X-ray crystal structure of the complex of HDAC-8 and largazole (Figure 35), demonstrating that the 16-membered depsipeptide core interacted as capping moiety with the enzyme, which undergoes conformational changes to accommodate the inhibitor, and that the terminal thiol moiety reached the catalytic site where chelated the Zn²⁺ ion.

Moreover, with the X-ray analysis, it has been possible to reveal the ideal geometry of thiolate-Zn²⁺ coordination and that any attempt to develop largazole analogues with structural changes in the thioester moiety, the L-valine subunit, and the 4-methylthiasoline-thiazole portion, could result in a loss of potency. Modifications such as the shortening and the lengthening of the thiol side chain, the olefin geometry changed from *trans* to *cis* and the C17 conformation inverted from (*S*) to (*R*) prejudice the ideal thiolate-Zn²⁺ interaction leading to analogues less potent than largazole. On the contrary, the L-valine subunit can be easily replaced with other L-amino acids (i.e., L-tyrosine, L-alanine, glycine) that are well tolerated; this is because the isopropyl group of L-valine is exposed to the solvent and does not alter the thiolate-Zn²⁺ coordination. Also, the 4-methylthiasoline portion does not represent an essential moiety for the potency of the largazole; in fact, structural modification

such as the replacement with a hydrogen atom, ethyl, or a benzyl group, does not modify the biological activity.

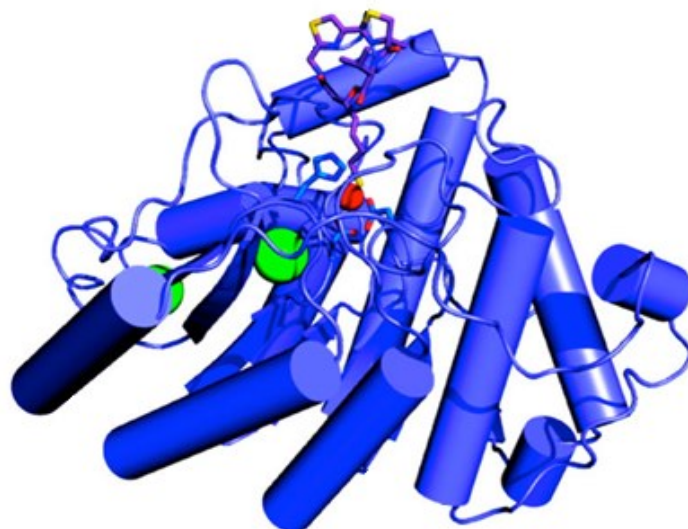


Figure 35

X-ray crystal structure of the complex of HDAC-8 and largazole-thiol. The catalytic Zn²⁺ ion is represented with a red sphere, the inhibitor is shown as a stick figure (C in magenta, N in blue, O in red, and S in yellow).

Probably, the introduction of larger and/or longer substituents in this position would increase the affinity interaction on the surface of the protein. Looking at the structure of the HDAC-8-largazole complex, the thiazole ring faces the solvent and is oriented away from the protein; this suggests that this position could tolerate substitution without reducing potency. In fact, replacing the thiazole ring with a pyridine one has been obtained a 3-4 fold activity enhancement.⁹⁷

Nitric Oxide

Nitric oxide (NO) is an endogenous, chemically reactive, water-soluble, free radical gas identified as the smallest signaling molecule in living organisms. It plays a key regulatory role in functions such as neurotransmission, vascular tone, gene transcription and mRNA translation. Due to its chemical instability, NO reacts with superoxide anion leading to the formation of peroxynitrite (ONOO⁻), a potent oxidant specie that can cause oxidative damages to biological molecules such as proteins, lipids and also DNA. NO is synthesized in mammals starting from three co-substrates molecular oxygen, amino-acid L-arginine,

and reduced nicotinamide-adenine-dinucleotide phosphate (NADPH), by three different homodimeric isoforms of the enzyme NO synthase: neuronal NOS (nNOS), endothelial NOS (eNOS), and inducible NOS (iNOS). Neuronal NO synthases (nNOS) are primarily expressed in the central nervous system (CNS) and can be identified in soluble and particulate forms; they show a Ca^{2+} /calmodulin-dependent enzymatic activity and are involved in physiological functions such as memory, learning and neurogenesis. Although iNOS have been primarily identified in macrophages, their tissue expression can be stimulated by endogenous and/or exogenous agents (i.e., cytokines, bacterial lipopolysaccharide); once activated, iNOS release a large amount of NO that may not be toxic only for exogenous (i.e., microbes, parasites) or endogenous (e.g., tumour cells) agents, but also for healthy tissues due to the NO radical nature or to the formation of peroxynitrite (ONOO⁻). Conversely, iNOS once expressed and activated are controlled and regulated by intracellular Ca^{2+} levels. For what regards eNOS, these enzymes are mostly expressed in endothelial cells, but can also be found in platelets, cardiac myocytes, human placenta, and kidney tubular epithelial cells. Similar to nNOS, also their enzymatic activity is Ca^{2+} /calmodulin regulated; in fact, NO is produced in an intermittent way depending on the increasing intracellular Ca^{2+} levels. Moreover, eNOS can be activated by stimuli inducing a long-lasting NO release without inducing relevant increases in intracellular Ca^{2+} levels. All the isoforms use flavine adenine dinucleotide (FAD), flavin mononucleotide (FMN), and (6R-)5,6,7,8-tetrahydro-L-biopterin (BH_4) as cofactors. To produce NO, these enzymes catalyze the electron transport from NADPH to the haem in the amino-terminal oxygenase domain, throughout FAD and FMN in the carboxy-terminal reductase domain.

The essential cofactor BH_4 , molecular oxygen and L-arginine interact in the oxygenase domain, while at the haem site O_2 is reduced and activated, and L-arginine is oxidated to L-citrulline and NO thanks to the electrons given by NADPH.³⁴⁻³⁶

NO & Cancer: a bimodal effect

It seems clear how NO is involved in the regulation of several physiological pathways displaying a crucial role as a neurotransmitter in CNS implicated in learning and sleep mechanisms, regulating gene transcription and mRNA translation, controlling vascular

tone, and inhibiting platelet aggregation and leukocyte adhesion to endothelium. Furthermore, NO shows a dual role in cancer development (Figure 36); if at lower levels NO facilitates cancer events, such as cell growth, anti-apoptotic responses, metastasis cascade initiation, and formation of neoplastic lesions, at higher concentrations (>200 nM) NO can induce cell cycle arrest and apoptosis acting as a potent anticancer agent.^{66,100}

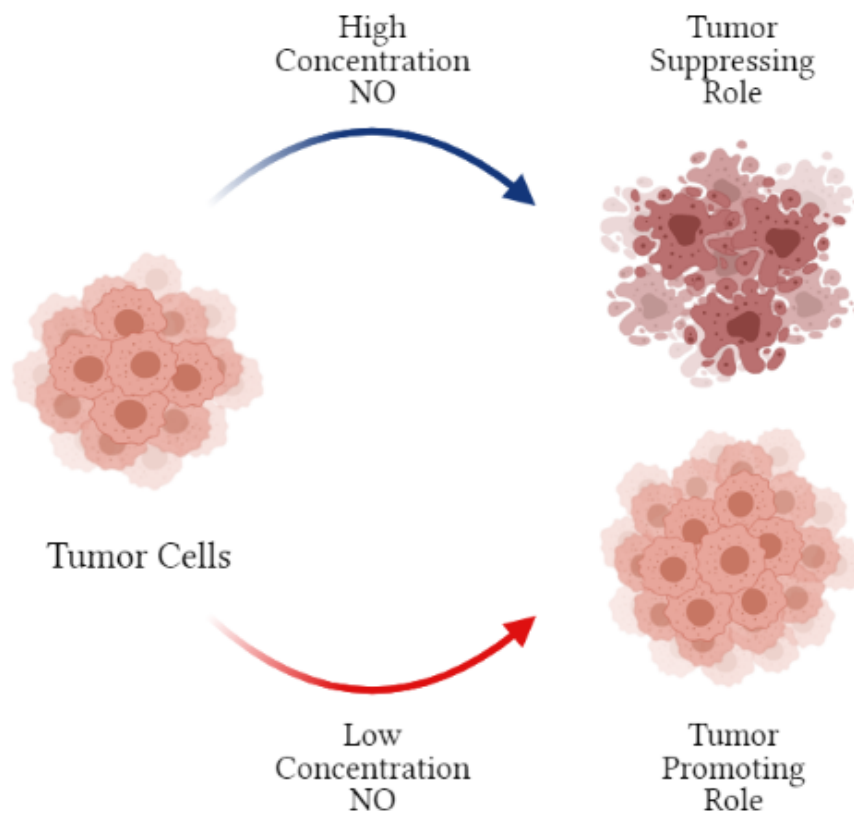


Figure 36

The dual role of NO in cancer. NO shows a dichotomous effect-concentration dependent in cancer, either inducing cancer development or promoting cancer suppression.

Several experiments have been conducted to demonstrate that particular signaling pathways are activated/inhibited by different NO concentrations. Lower levels of NO can activate the cyclic guanosine monophosphate (cGMP) pathway enhancing endothelial cells cancer proliferation. As NO concentration increases, PI3 kinase-Akt signaling is directly activated and promotes migration and angiogenesis.^{101,102}

The involvement of low levels of NO in tumorigenesis is broad and participates in the most crucial phase of cancer development:

- **Genotoxic events:** it has been demonstrated that NO can cause DNA damage due to the generation of two reactive species, peroxynitrite (ONOO⁻) that can oxidize and nitrate DNA potentially causing single-strand DNA breaks by attacking the backbone made of sugar-phosphate, and N₂O₃ that can alkylate DNA after N-nitrosamines formation. Moreover, this reactive specie can form diazonium ions by nitrosation of primary amines (e.g., DNA bases) which lead to deamination and DNA-crosslinks;
- **Angiogenesis:** endogenous NO activates COX-2 leading to increased production of prostaglandins and proangiogenic factors, stimulates the production of PGE₂ resulting in increased tumor vascular permeability, enhances cancer blood flow dilating arterioles vessels;
- **Antiapoptotic effects:** NO directly blocks the activity of caspase through s-nitrosylation of thiol-cysteine, increases Bcl-2 expression involved in the mitochondrial permeability transition pore control, activates cyclooxygenase, and inhibits cytochrome C release;
- **Metastasis:** NO shows also an invasion stimulating effects by inducing the expression of MMP-2 (matrix metalloproteinases) and MMP9, downregulating TIMP-2 (tissue inhibitors of MMP) and TIMP-3, and stimulating lymphangiogenesis;
- **Host immune response inhibition:** NO can suppress leukocytes proliferation and infiltration reducing their interaction with endothelial. ^{100,103}

As shown in Table 15, NO and NOS play various and diverse roles in several human tumors, providing innovative potential strategies for cancer prevention and therapy.

Tumor Type	Tumor Effects
Breast Cancer	NO modifies redox state of cells, provokes DNA, lipid, and protein modifications, induces angiogenesis, and enhances tumor blood flow. High NOS activity and a large amount of NO have been found in breast cancer tissues. The NO biomarker nitrotyrosine seems to be correlated with VEGF-C expression and lymph node metastasis.

Lung Cancer	<p>High levels of exhalate NO, its metabolites nitrite and nitrotyrosine and serum nitrite/nitrate are synonymous with an advanced stage of the disease.</p> <p>NO and its metabolites interact with ROS generating potent nitrating agents that form 3-nitrotyrosine in proteins and modifications during oxidative/nitrification stress. Large amount of NO can downregulate p53 activity by nitration leading to an enhanced contribution to carcinogenesis.</p> <p>NO with a broad effect on angiogenesis, extensive glycolysis, alteration of cell growth pathways and antioxidant capacity in the tissue, promote tumor heterogeneity and metastasis.</p>
Colorectal Cancer	<p>VEGF, p53 and NOS are overexpressed in human colon cancer (HCC).</p> <p>The high expression level of iNOS and eNOS characterize the early stage of human colon cancer progression, along with APC loss. iNOS provokes DNA deamination and induces mutations in tumor suppressor genes, is involved in the NF-κB pathway suggesting a role as an indicator of HCC and inflammation at the very early stages. COX-2 is also highly expressed in HCC and correlated with poor prognosis and huge aggressiveness of tumor.</p> <p>Large amount of NO induces cell cycle arrest due to the accumulation and phosphorylation of p53.</p>
Cervical Cancer	<p>Elevated levels of NO are detected in the serum of cervical cancer patients and markers of NO-mediated mutagenesis are found in the cervixes of women affected by this neoplasia, suggesting the potential mutagenic and carcinogenic role played by NO in cervical tumor.</p> <p>Human papilloma virus (HPV) infection is associated with an increased amount of NO in the human uterine cervix that causes mRNA expression, downregulation of p53 and pRb, and apoptotic indices in HPV-infected cells, resulting in carcinogenesis due to the increased survival of mutant cells.</p>
Ovarian Cancer	<p>NO is involved in several aspects of ovarian cancer, such as growth, apoptosis, angiogenesis, response to treatments, and cancer-stromal cell interaction. iNOS and NO display a bimodal role in tumor progression through the EGF receptors/extracellular kinase 2 (ERK-2)/pyruvate kinase isozyme 2 pathway and interfere with tumor glycolysis opening up the possibility of a new therapeutic approach for the treatment of ovarian cancer.</p>

**Brain
Cancer**

High expression of NOS is typically observed in cancer of the central nervous system so their expression may be a useful marker of brain tumor differentiation and malignancy. Large amount of NO in brain tumor tissue creates a favourable environment for tumor cell growth, stimulating cell proliferation and neovascularization.^{100,101,104}

Table 15

NO involved in cancer. Moving through different severe human tumors, it is possible to identify overexpression of NOS and high levels of NO as common denominators.

However, NO displays also a cytostatic/cytotoxic effect on tumor cells. Higher concentrations of NO (>1 μM) seem to regulate the hypoxia-inducible factors (HIF-1 α), whose overexpression is heavily involved in tumor-promoting and angiogenesis, leading to cell proliferation suppression and a wound repair delay. Moreover, when exposed to a higher amount of NO, the cell growth results hindered due to p53 overexpression that induces apoptosis and downregulates VEGF and iNOS, suppressing angiogenesis. Higher NO local concentrations activate caspase family proteases leading to a proapoptotic effect, altering the expression of several proteins involved in the apoptotic process, such as Bcl-2 family, suppressing cellular respiration, and shifting iron metabolism.^{100,101,103}

NO donor-based therapy represents an innovative strategy for cancer treatment; these new promising anticancer therapeutics act by increasing NO concentration within tumor tissues, without needing the endogenous production, bringing about more potent antitumoral effects, overcoming chemoresistance, reducing gastrointestinal side effects due to an enhanced specificity. NO donor compounds have been studied to be co-administrated with other chemo-/radio-/immune-therapeutics compounds; to amplify the antitumoral effect of the traditional therapies, hybridize drugs with NO but also other gaseous transmitters, such as hydrogen sulphide (H₂S) and carbon monoxide (CO), to obtain a synergic anticancer effect, combine with COX inhibitors, or encapsulate the inside drug delivery systems (e.g., liposomes and other nanoparticles) are successful strategies to deliver higher NO concentration to the tumor sites¹⁰¹

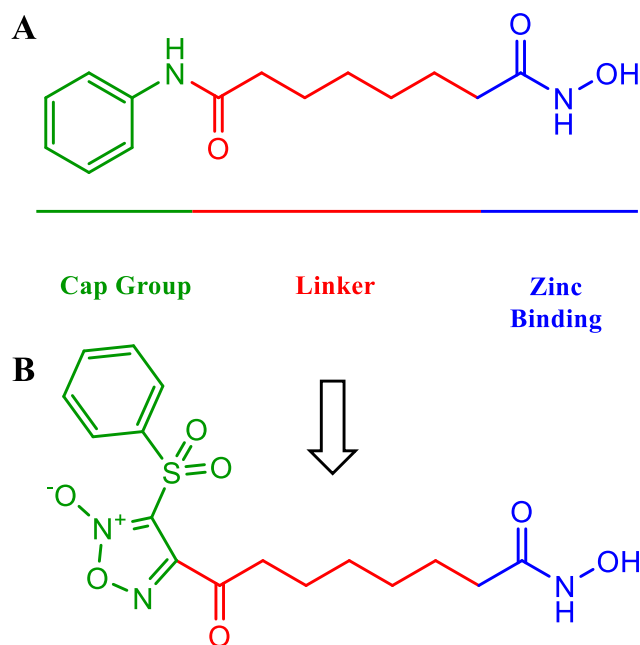
In advanced cancer states, NO donors-therapy represents a useful tool for overcoming hypoxia, which stimulates the hypoxia-inducible factor 1 α (HIF-1 α) pathway bringing

about cancer cells' survival against the common cellular death mechanisms (i.e., autophagy, apoptosis, DNA damage) inducted by chemo-/radiotherapy. In this scenario, NO donors increase tumor perfusion and enhance the antitumoral effect of the therapy attempting to reverse this effect. HIF-1 α mediated resistance has a central role in tumor resistance to treatments; NO donors therapy may be useful in the treatment of several cancer types by targeting the HIF-1 α mediated chemotherapeutic resistance. Even if the actual effectiveness of NO donors-therapy may be variable by the type of cancer, an enormous number of preclinical *in vitro* and *in vivo* studies have demonstrated the efficacy of using NO donors for the treatment of a wide type of tumors. Between the large amount of NO donors used in clinical trials, the diazeniumdiolates are the most promising scaffold; for instance, DETA/NO (Diethylenetriamine NO-adduct) seems to reverse the chemotherapeutic resistance for 5-fluorouracil (5-FU), doxorubicin and cisplatin, and when combined with farnesyltransferase inhibitors induce apoptosis in breast cancer cells. The diazeniumdiolate DETA-NONOate (Diethylenetriamine NONOate, a NO donor that spontaneously dissociates at pH 7.4 liberating two moles of NO per mole of parent compound)¹⁰⁵ inhibits the mesenchymal-epithelial transition and turns backward the metastatic effect of the tumor, while a synthetic ruthenium nitrosyl complex-NO donor, demonstrates a relevant capability of mitochondrial inhibition and ROS levels increment within the tumor, promoting caspase-mediated cell death in hepatocarcinoma. Arora et al. discovered how the treatment of castrate-resistant prostate cancer (CRPC) with the S-nitroso thiol GSNO (S-Nitrosoglutathione) reduces the expression of several markers of cancer progression and resistance such as M2 macrophage, VEGF, the androgen receptor and Androgen Receptor Splice Variant 7.¹⁰⁶

Dual NO donors/HDAC inhibitors

In light of the great broad anticancer capability of nitric oxide, dual NO donors/HDAC inhibitors have been developed as novel antitumoral chemical entities, potentially even more efficacious than single HDAC inhibitors; this incredible increase of potency is due to the capability of NO to specifically modulate the function of some HDAC isoforms.⁶⁶ In fact, several studies have demonstrated the direct and indirect action of NO on HDACs, showing

that NO can directly modify the Class I enzyme HDAC-2 that undergoes either Tyr-nitration or S-nitrosylation. HDACs enzymes belonging to class IIa might be indirectly activated by NO: due to the activation of protein phosphatase 2A (PP2A) through the sGC/cGMP signaling pathway, NO induces Class IIa HDAC nuclear shuttling. Moreover, has been demonstrated that Class I and III HDACs, crucial enzymes for skin repair processes, undergo functional crosstalk. Before the use in cancer treatment, clear examples of how the effect of HDACi and NO could be synergistic in controlling cardiac hypertrophy; in this disease, Class I HDACs have a pro-hypertrophic effect (HDAC-2 especially), whereas Class II downregulates it. Thus, it would be interesting the combination between a selective HDAC-2 and a moiety NO-releasing able to induce nuclear shuttling of Class IIa enzymes. NO and HDACi might have a relevant role in the repair process of wound healing; it is well known the key role of NO during wound healing and recently has been demonstrated that also Class I HDACs accelerate the skin repair process, promoting the release of Fibroblast Growth Factor 10 (FGF10), Epidermal Growth Factor (EGF) and Insulin Growth Factor I (IGF-I) from activated keratinocytes.¹⁰⁷ In 2013 was reported the creation for the first time of a new hybrid compound obtained from the well-known HDACi Entinostat (MS275) by the introduction of a NO-donor furoxan moiety, characterized by an analogous HDAC inhibitory profile with an additive myogenic differentiation activity due to the NO-donor moiety. Since then, the strategy of the dual synergistic effect con NO-donors and HDACi has been applied for the development of new anticancer agents; in particular, NO-/Doxorubicin derivatives resulted active against Doxorubicin-resistant human colon cancer (HT-29-dx).⁶⁶ In addition, a novel series of phenylsulfonylfuroxan-based hydroxamates have been developed combining the inhibitory activity of the HDACi SAHA and the NO-donating capability of phenylsulfonylfuroxan moiety. Within the new library of compounds, compound B shown in Scheme 1, displayed the greatest *in vitro* antiproliferative activity against human erythroleukemia (HEL) cell line, even greater than that of SAHA, strongly inducing G1 phase arrest and apoptosis in HEL cell line.¹⁰⁸



Scheme 1

Design strategy of the hybrid NO-donor/HDACi compound. Starting from SAHA (A), a hydroxamic acid pan-HDAC inhibitor has been modified the “cap group” introducing a phenylsulfonylfurazan moiety whereas, the Zn²⁺-binding hydroxamic moiety has been maintained.

In the light of the superior antiproliferative activity of these dual compounds, several hybrids of HDAC inhibitor Entinostat (MS275) and NO donors have been developed with the main purpose of improving the HDAC selectivity; all the efforts lead to a series of hybrids of N-acyl-*o*-phenylenediamine and phenylsulfonylfuroxan of which three analogues showed a remarkable *in vitro* antitumoral potency due to the strong HDAC-1, -2, -3 inhibitory activity and the relevant NO-releasing capability.¹⁰⁹

Aim of the work

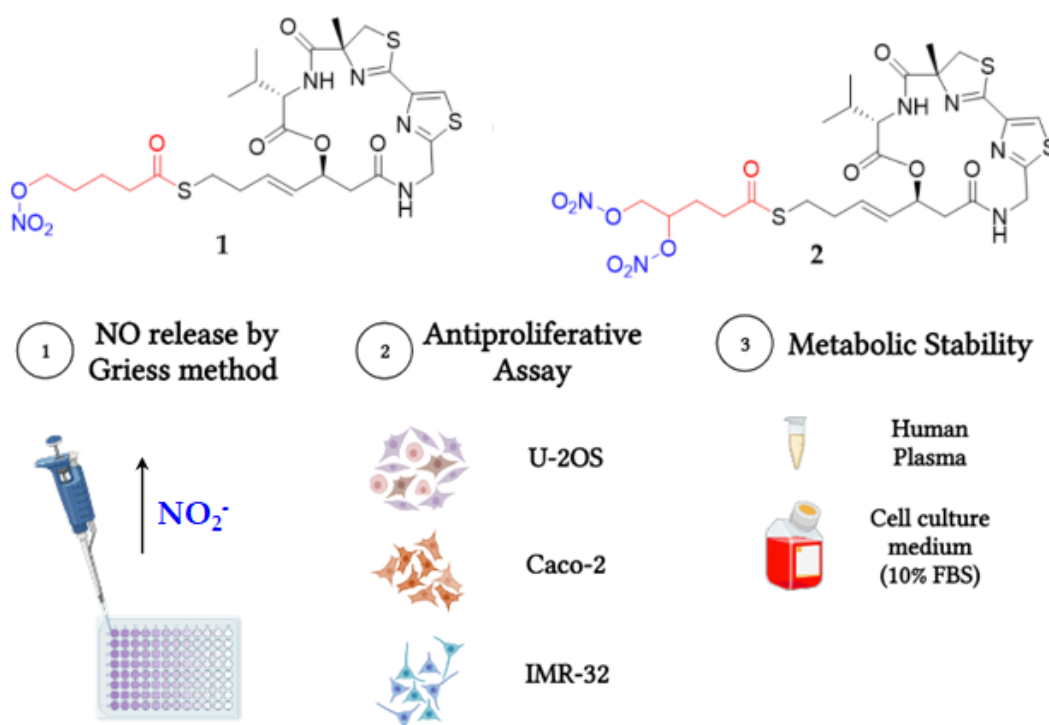


Figure 37

Graphical abstract of the project.

This Ph.D. project aimed to investigate the antiproliferative properties of new nitric oxide-donor largazole derivatives **1** and **2** on different tumor cell lines to evaluate the dual antitumoral effect due to the HDAC inhibition and the tumor-suppressing role of high concentration of NO (Figure 37).

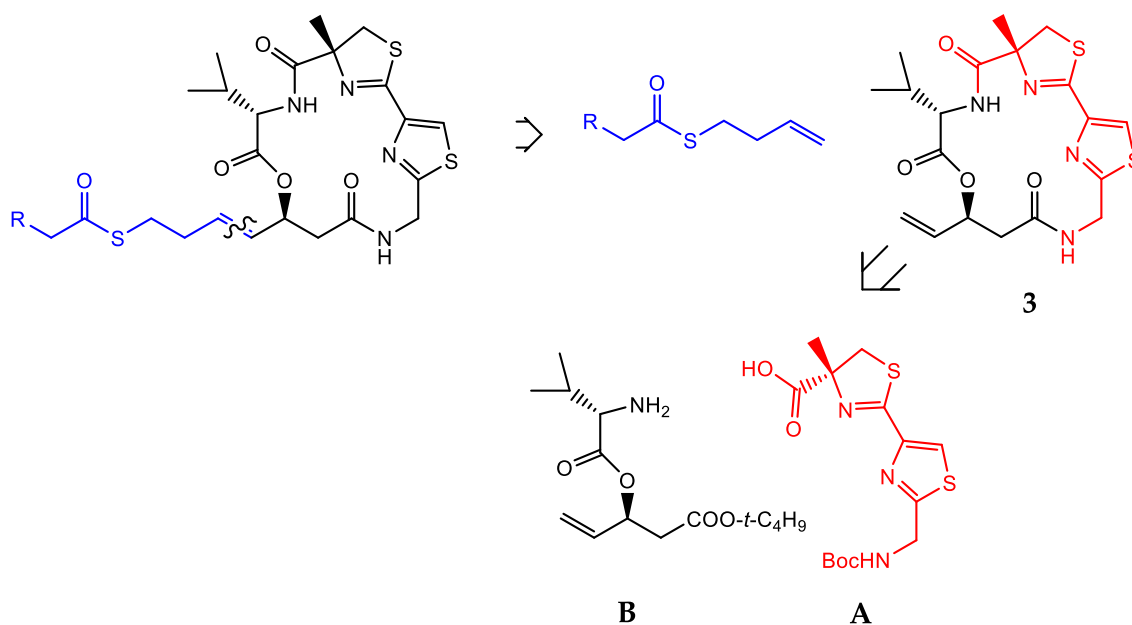
Thanks to Professor Maria Frosini, who performed the *in vitro* NO released assay, it has been possible to certify the effective release of nitric oxide, letting us conduct further experiments to evaluate the additive antiproliferative effect of NO in molecules **1** and **2** in comparison to largazole.

As described previously, largazole required to be hydrolysed in the bioactive compound in order to coordinate with the Zn²⁺ inside the HDAC active site; thus the metabolic stability of derivatives **1** and **2** has been studied in solvent, human plasma, and cell culture medium to determine the kinetics of hydrolysis of compounds.

Experimental Section

Synthesis of NO-donors/largazole hybrids

The retrosynthetic analysis of compounds **1** and **2**, as depicted in Scheme 2, suggested the disconnection of the olefin moiety and the obtainment of compound **3** by condensation of fragments **A** and **B**.



Scheme 2

*Retrosynthetic approach for the synthesis of NO-donor largazole derivatives **1** and **2**. The olefine moiety (blue) undergoes a disconnection from compound **3**, which is obtained from the condensation of fragments **A** (red) and **B** (black).*

The retrosynthetic approach and all the synthetic procedures used are detailed at the end of this Ph.D. thesis in the paper n°4 (Borgini M. et al., ACS Med. Chem. Lett., 2020, 10.1021/acsmchemlett.9b00643).

Biological Evaluation

In vitro determination of NO release by Griess method

To investigate the capability to release NO, compound **1** was incubated at 37°C in phosphate buffer (PBS; Sigma, Milano Italy) (1%DMSO; Carlo Erba Chemicals, Milan, Italy) at 0.1 mM concentration in the absence and the presence of L-cysteine (Sigma) 0.5 mM (5X) and 5 mM

(50X); because of its poor solubility in PBS at 0.1 mM, compound **2** required incubation with MeOH as cosolvent (PBS/MeOH 1:1_{v/v}). At fixed time, NO₂⁻ was evaluated in the reaction mixture by Griess (sulphanilamide, N-naphthylethylenediamine dihydrochloride, and 85% phosphoric acid in distilled water; Sigma, Milano Italy). After 10 minutes of incubation at room temperature, the absorbance was measured at 540 nm. More detailed information can be found in the specific paper (Borgini M. et al., ACS Med. Chem. Lett., **2020**, 10.1021/acsmchemlett.9b00643)

Cytotoxicity Assay

The *in vitro* cytotoxicity experiments were carried out using osteosarcoma U-2OS (ATCC®HTB-96TM), neuroblastoma IMR-32 (ATCC®CCL-127) and colorectal adenocarcinoma Caco-2 (ATCC®HTB-37TM) cell lines. Cells were cultured in Dulbecco's Modified Eagle's Medium (DMEM, Sigma, Milano Italy) supplemented with 20% FBS (Sigma), 2 mM L-glutamine and 10000 units/mL Penicillin/Streptomycin (Sigma) at 37 °C in 5% CO₂ atmosphere.

Briefly, 0.5 × 10⁴ cells were seeded in 96-well plates in triplicate, the day after seeding, compounds dissolved in DMSO were added at increasing concentrations (0.1 nM to 10 μM) and incubated for 24, 48 and 72 hrs at 37 °C in 5% CO₂ atmosphere.

At fixed time points, the working solutions were removed and cells were washed twice with 100 μL of PBS; the evaluation of the anticancer activity of compounds **1**, **2**, and largazole as internal control, was performed with the MTT (3-(4,5-dimethylthiazol-2-yl)-2,5-diphenyltetrazolium bromide; Sigma, Milano Italy) assay. The MTT reaction solution was prepared at the final concentration of 5 mg/ml in Minimum Essential Medium (MEM, Sigma, Milano Italy). Cells were treated with 150 μL of MTT solution and plates were incubated for 3-4 hrs in 5% CO₂ atmosphere at 37°C. After incubation, the exhausted MTT solution was removed and 150 μL of isopropanol (Carlo Erba Chemicals) was added to each well and plates were shaken for 30 minutes in an orbital shaker at room temperature. The absorbance function of a SpectraMax M5 Multi-Mode Microplate Reader (MolecularDevices) was used to quantify the light intensity produced of the blue formazan formation over time. Before sample testing, the instrument was internally calibrated, and a

blank 96-well clear bottom sample plate was run to control for any background light absorption. The absorbance value was read at 595 nm. EC₅₀ (drug concentration that determined the 50% of growth inhibition) was calculated by GraphPad Prism 6.0 software using the best fitting sigmoid curve.

Chemical and Metabolic Stability Assay

To understand the chemical stability in different solvents (i.e., HEPES buffer 25 mM pH 7.4, DMSO; Sigma), prodrugs-largazole (compounds **1** and **2**) stock solutions were prepared by dissolving compounds in DMSO at the final concentration of 1 mg/mL. The assays were performed by incubating 100 µL of compounds stock solution in 1900 µL DMSO and HEPES-buffer 25 mM (added with 140 mM NaCl, pH 7.4), respectively, at room temperature for 24 hrs. The experiments were conducted in triplicate and largazole was used as an internal reference compound. At fixed time points, aliquots were collected and were collected (10 µL), diluted 1:10_{v/v} in Acetonitrile (ACN; Sigma) and analysed by the following HPLC/UV-MS method.

The enzymatic stability was determined in the presence of pooled human plasma and in Dulbecco's Modified Eagle's Medium (DMEM) supplemented with 20% FBS, 2 mM L-glutamine and 10000 units/mL Penicillin/Streptomycin. Aliquots of plasma or medium (1000 µL), pH 7.4 HEPES-buffer (900 µL), and 100 µL of 1 mg/mL stock solution of prodrugs in DMSO were mixed in a test tube. After incubation at room temperature, 50 µL aliquots were removed at specific time points, mixed with 450 µL of ANC and centrifuged at 5000 rpm for 15 min. The hydrolysis of the compounds was followed by HPLC with UV-MS detection methods below reported. The percentage of hydrolysis of prodrug was achieved by a control DMSO solutions. The experiments were conducted in triplicate, on different days.

HPLC/UV-MS Method

LC analyses were performed by Agilent 1260 Infinity II LC/DAD/MSD system (Agilent Technologies, Santa Clara, CA) constituted by a vacuum solvent degassing unit, a binary high-pressure gradient pump, vial sampler, multicolumn thermostat, and UV diode array

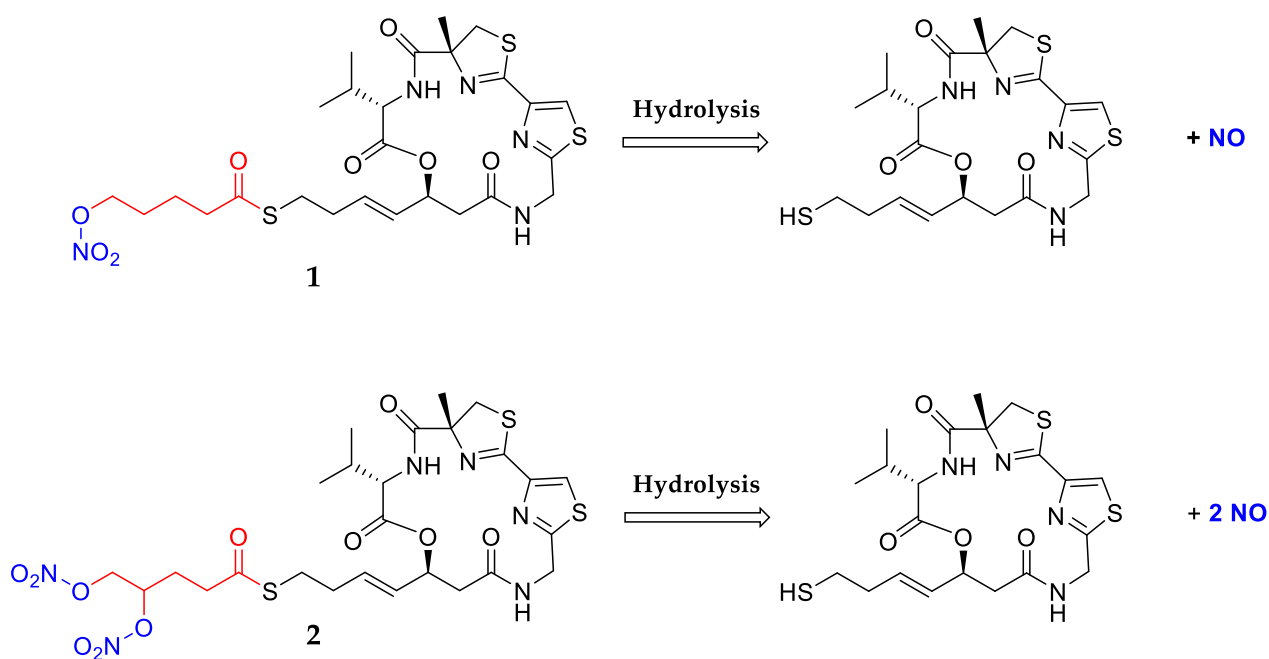
detector. An Agilent 1260/6310 ESI-single-quadrupole mass spectrometer was used. The mass spectra detection (MSD) instrument was equipped with the orthogonal spray APCI-ESI (Agilent Technologies, Santa Clara, CA). Nitrogen was used as nebulizing and drying gas. The pressure of the nebulizing gas, the flow of the drying gas, the capillary voltage, the fragmentor voltage, and the vaporization temperature were set at 40 psi, 5 L/min, 3000 V, 70 V and 350°C, respectively. UV detection was monitored at 240 nm. The LC-ESI-MS determination was performed by operating the MSD in the positive ion mode. Spectra were acquired over the scan range m/z 50-1500 using a step size of 0.1 u. Chromatographic analysis was performed using a column Phenomenex Gemini C18 110A (150x4.6 mm, 3 μ m particle size) at room temperature. Analysis were carried out using a gradient elution of methanol (MeOH) and water (H₂O): t = 0 min MeOH 0%, t = 3 min MeOH 0%, t = 12 min MeOH 98%, t = 18 min MeOH 98%. The analysis was performed at a flow rate of 0.6 mL/min and an injection volume was 20 μ L.

Results and Discussion

(Borgini M. et al., ACS Med. Chem. Lett., 2020)

Synthesis of NO-donors/largazole hybrids

Owing to the exceptional improvement of the antiproliferative activity of HDAC inhibitors on different cancer cell lines due to the NO-donor moiety, Professor Maurizio Botta's research group has been involved in the development of novel largazole derivatives bearing one or two NO-donor functions.



Scheme 3

Chemical structure of largazole derivatives 1 and 2. The largazole-SH, pharmacologically active after hydrolysis, is represented in black, the aliphatic chain in red, and the NO-donor moieties in blue.

Exploiting the enzymatically labile thioester chain of largazole, would be released the pharmacologically active specie as HDAC inhibitor (largazole-SH) and, depending on the functionalization of the aliphatic thioester chain, one or two equivalents of NO. To this aim, compounds **1** and **2** have been synthesized (Scheme 3).⁶⁶

NO release by Griess method

largazole derivatives **1** and **2** were studied in terms of capability to release NO using the Griess method. As shown in Figure 38, in the assay condition, both compounds spontaneously released NO; as expected, the amount of NO release was more abundant for compound **2** than compound **1**, due to the presence of two NO-donor groups.

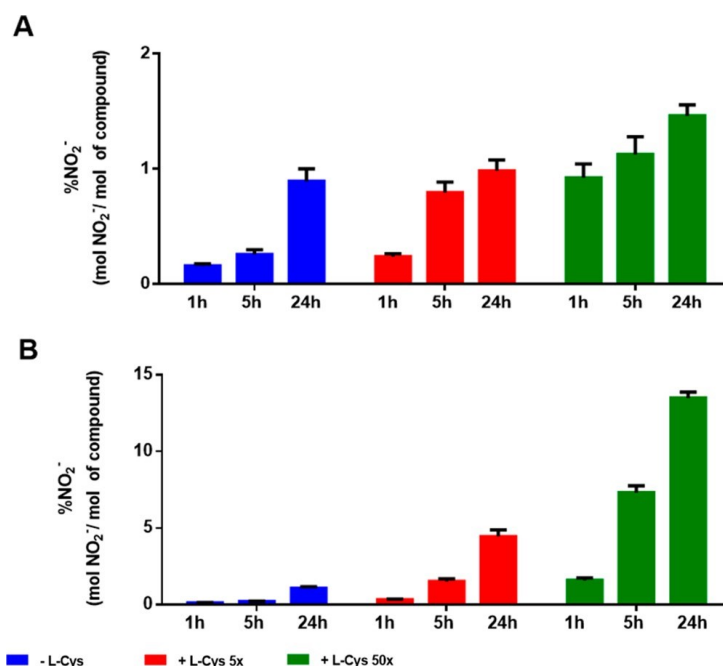


Figure 38

NO release assay. Compounds **1** (A) and **2** (B) were incubated at 0.1 mM in 50 mM PBS (pH 7.4) at 37°C, both in the absence (Blue) and in the presence of L-cysteine 5x (Red) and 50x (Green). The yield of NO₂⁻ is expressed as a percentage of compounds **1** and **2** at 1h, 5h and 24h, with respect to the initial concentrations. The reported values are the average of three independent experiments.

As expected, the NO production was amplified in the presence of an increasing concentration of L-cysteine. The NO release was more abundant for compound **2** than compound **1**, due to the presence of two NO-donor groups.

Antiproliferative Activity

Once established the capability of both compounds to efficiently release NO, their antiproliferative activity was evaluated against U-2OS (human osteosarcoma), Caco-2 (human colorectal adenocarcinoma), and IMR-32 (human neuroblastoma) cell lines, using the parent compound largazole as the internal control. As shown in Table 16, compounds **1**

and **2** showed a concentration and time-dependent inhibitory activity against tumor cell growth. In particular, as for the antiproliferative activity in the U-2OS cell lines, both compounds showed a relevant additive effect at 24 hrs concerning the antiproliferative activity of largazole, whereas, at 48 and 72 hrs, the antiproliferative effect was similar to that of largazole. The greater antiproliferative activity of compound **2** vs compound **1** at 24 hrs ($pEC_{50} = 6.33$ vs 5.71 , respectively) was most likely due to the higher production of NO by compound **2** with respect to compound **1**.

Cell line	Time (hrs)	pEC_{50}		
		Largazole	1	2
U-2OS	24	4.69 ± 0.12	5.71 ± 0.15	6.33 ± 0.10
	48	6.43 ± 0.15	6.51 ± 0.15	6.13 ± 0.20
	72	6.48 ± 0.10	6.77 ± 0.09	6.00 ± 0.70
Caco-2	24	>2.0	4.95 ± 0.19	5.04 ± 0.24
	48	6.12 ± 0.21	7.42 ± 0.14	8.25 ± 0.22
	72	7.84 ± 0.09	8.09 ± 0.16	8.35 ± 0.16
IMR-32	24	7.46 ± 0.16	7.82 ± 0.17	7.53 ± 0.12
	48	7.52 ± 0.14	7.71 ± 0.17	7.21 ± 0.18
	72	7.91 ± 0.08	7.92 ± 0.06	7.30 ± 0.14

Table 16

Antiproliferative activity. Cytotoxicity of largazole, compounds **1** and **2** against U-2OS, Caco-2 and IMR-32 cell line. The reported values are the average of $n=3$ independent experiments \pm SEM.

This general trend was even more evident in the Caco-2 cell line, in which the improved antiproliferative activity of both compounds was more pronounced than that shown by largazole at 24 and 48 hrs and, in part, at 72 hrs. As anticipated, compound **2** was more potent than compound **1** at all-time points. Conversely, in the IMR-32 cell line, the antiproliferative activity was already evident at 24 hrs, whereas the additive effect of compounds **1** and **2** concerning the parent compound largazole was minimal or even absent.

Chemical and Metabolic Stability

To further explain the additive antiproliferative effect of compounds **1** and **2** vs largazole, their metabolic stability was assessed with respect to largazole in solvents, cellular assay medium and human plasma. Firstly, the chemical stability of these compounds was evaluated in HEPES buffer 25 mM pH 7.4 and DMSO, without observing any chemical degradation, hence confirming the potential use of these compounds as prodrugs.

	Time (min)	Largazole	1	2
A	0	100.0 ± 7.2	100.0 ± 9.9	100.0 ± 7.4
	5	21.7 ± 5.6	21.2 ± 6.7	20.4 ± 4.3
	10	21.6 ± 4.3	20.9 ± 3.8	20.3 ± 5.5
	30	20.9 ± 3.9	20.3 ± 2.9	20.2 ± 5.0
	60	17.6 ± 5.7	19.9 ± 4.3	18.9 ± 3.9
	120	15.1 ± 4.9	18.6 ± 4.2	18.7 ± 5.0
	1440	3.6 ± 4.1	10.9 ± 2.4	8.9 ± 3.2
	B	0	100.0 ± 1.5	100.0 ± 2.1
5		19.4 ± 3.1	18.8 ± 2.9	19.4 ± 7.4
10		18.7 ± 0.7	19.1 ± 2.1	18.8 ± 8.0
30		17.4 ± 2.9	16.7 ± 2.8	18.9 ± 7.9
60		17.1 ± 2.0	17.2 ± 3.2	16.5 ± 1.4
120		17.1 ± 1.4	18.9 ± 3.8	17.9 ± 1.4
1440		16.4 ± 3.2	18.0 ± 2.9	18.3 ± 3.2

Table 17

Metabolic stability. Expressed as % of remaining largazole, compound **1** and **2** when incubated in human plasma (A) and in the assay cell medium (B), respectively.

Finally, the stability in cellular assay medium (A) and human plasma (B) profile were evaluated (Table 17), detecting the same rapid hydrolysis of the metabolically labile thioester side-chain reported in the literature for largazole. As expected, just after 5 minutes incubation, both in human plasma and in assay cell medium, about 80% of largazole,

compounds **1** and **2** underwent a hydrolytic process releasing the SH-largazole bioactive specie and the aliphatic chain with one or two NO-donor groups. Moving through the different time-points analysed, after the initial massive degradation of the thioester chain in both experiments, the percentage of remaining compounds remains almost constant, probably due to saturation of the active sites of esterase enzymes mainly involved in the hydrolysis of the thioester chain.

The general trend of an additive antiproliferative activity against tumoral cell lines has been confirmed from these metabolic stability experiments; in fact, the rapid thioester chain hydrolysis led the aliphatic chain, with one or two NO-donor groups, to reach the cellular target improving the natural antiproliferative activity of largazole.

Conclusions

A new class of largazole derivatives bearing one and two nitrate groups at the metabolically labile thioester side chain were efficiently synthesized and biologically characterized. These compounds were designed starting from the natural compound largazole endowed with a nanomolar selective potency for Class-I HDAC, and the peculiar capability to discriminate between tumor cells and normal cells. Starting from this natural HDAC inhibitor and from the anticancer property of nitric oxide and its capability to overcome tumor cell resistance, compound **1** and **2**, have been successfully synthesized.

Afterthought, the novel derivatives bearing one or two NO-donor functions at the metabolically labile thioester chain, have been characterized in terms of capability to release NO, antiproliferative activity in tumor cell lines and metabolic stability with largazole as reference compound.

Using the Griess method it has been possible to determine the amount of NO effectively released by compounds **1** and **2**; the abundance of NO released by the two novel derivatives was directly proportional to the number of NO donor groups and, as expected, was more abundant for compound **2** than compound **1**.

A dual antiproliferative profile of the novel derivatives **1** and **2**, was the consequence of the rapid liberation in cell medium of the HDAC inhibitor largazole-thiol and the efficient production of NO. The additive antiproliferative activity of derivatives **1** and **2** compared to the parent compound largazole, was determined in terms of cytotoxicity in three different types of tumor cell lines: U-2OS, Caco-2, and IRM-32. The efficacy of new derivatives was more pronounced in U-2OS and Caco-2 cells than in IMR-32.

Finally compounds **1** and **2** were also characterized in terms of metabolic stability in human plasma and cellular medium to further explain their additive antiproliferative action. Due to the hydrolysis of the thioester chain, the SH-largazole specie, the bioactive one, and the aliphatic chains with one or two NO-donor functions were rapidly released.

In conclusion, we have successfully developed a novel class of largazole derivatives compounds, characterized by the presence of one or more nitric oxide donor functions at

the thioester side chain, that showed promising antitumoral activity against Osteosarcoma (U-2OS), Adenocarcinoma colorectal (Caco-2) and Neuroblastoma (IMR-32) cell lines. Both novel compounds showed an intrinsic capability to release NO and, in comparison to largazole, the same metabolic stability profile.

Chapter 3

Introduction

RNA-target therapy

Advantages in the development of biomedical research have been made since the Human Genome Project (HGP) disclosed fundamental information regarding the human genome, allowing worldwide researchers to investigate and find out how much genetic factors could play a relevant role in several diseases. Among these genetic factors, several coding and non-coding RNAs (ncRNAs) such as microRNA (miRNA), long ncRNA (lncRNA), circulating RNA (circRNA), and small interfering RNA (siRNA), have been deeply involved in various diseases like cancer, autoimmune disorders (rheumatoid arthritis) and neurodegenerative diseases (Parkinson and Alzheimer).^{110,111}

The knowledge of these potential targets encouraged the development of pharmacological treatments able to vehicle nucleic acids inside cells, reach the target site and regulate the altered gene expression transiently or permanently. Thus, several RNA-targeted therapeutics have been studied as potential strategies for various diseases, from heart or neurological diseases to cancer.

Coding as well as non-coding RNAs, and synthetic DNA oligomers have been used as therapeutic strategies and can be distinguished into four types (Figure 39): 1) siRNAs and antisense oligonucleotides (ASOs), able to inhibit RNA target activity, 2) aptamers able to target proteins, 3) trans-splicing ribozyme and 4) mRNAs that encode therapeutic proteins.

1. *siRNAs* are long double-stranded molecules with a sense and antisense strand, and a typical 3' overhang. siRNAs are generated through an endonucleolytic process by a ribonuclease belonging to the RNase III family and explicate their functions by Watson-Crick base pairing with mRNA. The pharmacologically active moiety is represented by the antisense strand, while the sense strand acts as a drug delivery system allowing the transport of the active strand to the RNA endonuclease AGO2, intracellularly located. A second role function of the sense strand is that it protects

the active antisense strand from degradation by exo- and endo-nucleases. It must therefore be removed before the active moiety explicates its antisense effect. The presence of the double-strand makes siRNAs hydrophilic compounds with poly-anions not allowing the binding to serum proteins and leading to a rapid excretion. Thus, siRNAs are characterized by an unsatisfactory pharmacokinetic profile and low stability that prevent the accumulation of the unmodified siRNA in the intended tissue. For this reason, siRNAs require to be formulated with lipids or nanocarriers, or chemically modified to better interact with plasma proteins and reach an effective tissue distribution. In the early clinical phases, several siRNAs have been used to contrast metastasis and invasion, two of the major processes involved in cancer progression.^{112,113} Recently, the FDA has approved the use of ONPATRO® (Patisiran, ALN-TTR02) and GIVLAARI® (Givosiran, ALN-AS1) for the treatment of hereditary amyloidogenic transthyretin (hATTR) amyloidosis with polyneuropathy in adults, and acute hepatic porphyria (AHP), respectively.¹¹⁴

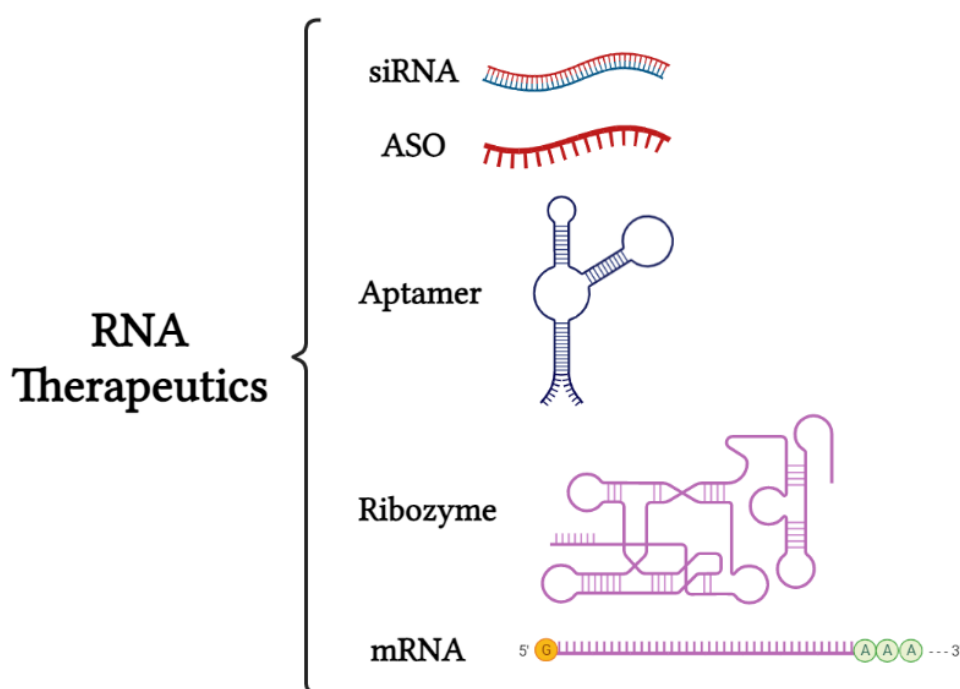


Figure 39

Schematic illustration of RNA therapeutics. siRNAs and ASOs inhibiting RNA target activity, aptamers binding target proteins, trans-splicing ribozyme, and mRNAs encoding therapeutic proteins

ASOs are synthetic DNA oligomers, small-sized single-stranded nucleic acids able to specifically knock down target genes or modify protein expression by hybridization via Watson-Crick base pair interactions. Steric hindrance, destabilization of pre-mRNA, and miRNAs cleavage to regulate gene expression are other mechanisms of action used by ASOs. ASOs are characterized by the natural tendency to accumulate in the liver, spleen, and kidneys, making it difficult to direct them to different target sites.¹¹² However, the insufficient stability due to nucleases degradation activity, and the poor intracellular delivery due to the difficult biological membrane crossing limit the antisense pharmacology.¹¹⁵

A more detailed review of ASOs is provided below.

2. **Aptamers** are single-stranded DNA or RNA with a high affinity towards specific target proteins that bind and inhibit. Their mechanism of action is quite similar to antibodies, thus for their synthetic origin, aptamers are identified as chemical antibodies. Aptamers are synthetically produced using the method of systemic evolution of ligands by exponential enrichment (SELEX). Several aptamers can be found in clinical trials for inflammatory diseases, macular degeneration, and diabetic macular edema. Recently, has been elucidated the significant role of the vascular endothelial growth factor (VEGF) in the progression of ocular degenerative conditions; EYE001, a pegylated aptamer against VEGF, has reported good results alone or with photodynamic therapy in terms of improving vision by the inhibition in retinal neovascularization. ARC1779 is an aptamer synthetically conjugated to a polyethylene glycol used in clinical trials in patients with thrombotic thrombocytopenic purpura and has been developed as an antagonist for the vWF A1 domain involved in the primary homeostasis regulation acting as a coagulation factor VIII carrier.^{112,116}
3. **Ribozymes** are catalytic RNA molecules usually involved in self-cleavage, splicing, ligation, and polymerization able also to hit, hybridize and degrade specific RNA sequences. Damaged RNA cannot be part of the translational process thus with this MoA ribozymes inhibit specific protein production. Their therapeutic application in silencing gene expression both *in vitro* and *in vivo* was investigated in clinical trials

for solid tumors and HIV infection. An anti-VEGFR-1 ribozyme conjugated with carboplatin and paclitaxel was demonstrated to be safe and efficient in advanced solid tumors but not in metastatic breast cancer. The anti-HIV ribozyme induced an increase in CD4⁺ lymphocytes after delivery with CD34⁺ cells, allowing higher safety and activeness of the ribozyme.^{112,117}

4. *mRNA* is a fundamental molecule involved in all aspects of cell biology. The use of messenger RNA as a therapeutic compound was firstly conceived over twenty years ago, when it has been demonstrated that the injection of *in vitro* transcribed (IVT) mRNA or plasmid DNA (pDNA) into mice could induce the expression of encoded proteins in the site of injection. The first decade was used by scientists to understand all the structural and functional characteristics of mRNA and its pharmacokinetic behaviour. Consequently, the attempts focused on overcoming the short half-life and unfavourable immunogenicity. mRNA therapeutics can be distinguished into protein replacement therapies and vaccines both for cancer and viral diseases. For almost two years, the COVID-19 pandemic focused the attention on the urgent need to develop drugs and vaccines able to fight SARS-CoV-2 infection. mRNAs are representing an example of the efficacy of this kind of vaccine that rapidly and safely can prevent serious infectious diseases. The mechanism of action is easy: the vaccine delivers mRNA into immune cells which receive the information and use the mRNA as a mould to produce foreign proteins that usually would be produced by the virus or other pathogens. These proteins synthesized can induce an adaptive immune response that is fundamental for the body to identify and destroy in the future, the corresponding pathogen.¹¹⁸ Due to the large dimension and the presence of negative charges, mRNA cannot pass the lipid bilayer of cell membranes. To overcome this limit and to prolong the short half-life escaping from the degradative action of nucleases, mRNA vaccines have been formulated in lipid-based nanoparticles (all SARS-CoV-2 mRNA vaccines use this strategy), polyplexes and polymeric nanoparticles, or using peptides whose cationic or amphipathic amine groups can help transfer mRNA into cells by binding it and forming nano complexes.¹¹⁹ Beyond vaccines application, mRNAs are employed as drugs in protein replacement

therapies. Studies have revealed the important role of modified mRNA in cardiac therapies, most of all after myocardial infarction, underlying the ability of this safe, non-immunogenic, and controlled nucleic acid delivery system to induce cardioprotection and vascular/cardiac regeneration.¹²⁰ Other mRNAs have been developed for the treatment of cystic fibrosis, as immunomodulators for solid tumors, lymphoma, and advanced ovarian carcinoma to enhance the expansion, activity, and survival of T cells. mRNA therapeutics have been proposed also for genetic disorders like α -1 antitrypsin and citrin deficiency.¹²¹

Antisense Oligonucleotides

Antisense oligonucleotides (ASOs) are nucleic acid analogues synthetically created to hit a target gene expression and silence it by hybridization via Watson-Crick base pair interactions. Generally, ASOs are 16-21 nucleotides long and single-stranded. The first attempt to use ASOs for modulating protein expression was in 1978, when Zamecnik and Stephenson showed the *in vitro* inhibition of viral replication, probably due to a translational arrest. Only later was found out the real mechanism of action: an ASO-mediated cleavage and followed degradation of the mRNA made by the RNase H.¹²² Since then, great improvements have been made and over 20 years later US Food and Drugs Administration (FDA) approved the first ASO for the treatment of the cytomegalovirus (CMV)-induced chorioretinitis. This triggered the development of new ASO derivatives classified into three ASOs generations:

- The 1st was made of short (8-50 nucleotides in length) oligodeoxynucleotides able to bind the target mRNA by complementary base pairing and silence gene expression through an endonuclease-mediated transcript mechanism. Unfortunately, the 1st ASOs generation failed in the clinical trials for the incapability to have sufficient intracellular bioavailability to suppress target genes and for the fast turnover they underwent.
- The 2nd and 3rd generations have been developed in the 90s and have been characterized by improved pharmacological properties obtained with backbones modifications. The new ASOs derivatives were improved also in terms of mechanism

of action (MoA); in fact, they were able to modify the pre-mRNA splicing by sterically blocking splicing factors and stop the mRNA translation preventing the recruitment of ribosomes. The last discoveries allowed highlighting the possibility to design and synthesize specific antisense oligonucleotides for hitting non-coding RNAs and toxic RNAs involved in disease pathogenesis of interest, expanding the potential pharmacological range of action of these compounds. This new class of molecules showed high specificity and ability to hit targets usually unreachable with traditional therapeutical molecules, and a good selectivity index due to the limited systemic exposure. For these reasons, ASOs have generated great interest in the treatment of neurological disorders, even though the requirement to be administrated by intrathecal or intraventricular routes for their inability to cross the blood-brain-barrier (BBB), still represents the biggest obstacle for a clinical use.¹²³

ASO-based therapies are principally used for neurological and hepatic genetically well-defined rare diseases. However, the development of the galactosamine-*N*-acetyl (GalNAc) ASO conjugated used for a target delivery system to hepatocytes, has been proven to be effective also in cardiovascular diseases such as dyslipidaemia and non-alcoholic steatohepatitis (NASH). The versatile efficacy and the broad therapeutic use of ASOs are due to the multiple mechanisms of action by which these derivatives modulate gene expression: enzymatic cleavage or steric blocking, splicing modulation of mRNA that leads to a correction or alteration of the target sequence, and binding to inhibitory elements of transcription or translation to upregulate specific gene expression. *In vivo* pharmacokinetic studies have demonstrated the tendency of ASOs to distribute mostly to the liver, kidneys, spleen, and bone marrow. Although the biggest efforts to upgrade the new derivatives and improve their pharmacological profiles, the presence of negative charges and the size of ASOs limit the distribution across BBB after a systemic administration. Moreover, unmodified oligonucleotides undergo rapid degradation in biological matrices that limits their clinical use. The possibility to design and synthesize ASOs to target genes, modulate RNA processing or protein production, and the specific MoA through which the ASO acts, determine the type and the position of chemical modification applied. As described below,

several chemicals and backbones modifications have been made to improve metabolic stability, and RNA-binding affinity, and to enhance oligonucleotide drug delivery.¹²⁴

Chemicals and backbones modifications

The first *in vivo* administration of ASOs demonstrated the rapid and massive degradation of the unmodified phosphoribose backbone by endonucleases and exonucleases. Thus modifications to improve the pharmacokinetics, pharmacodynamics, and biodistribution of these promising compounds had to be made. A relevant improvement of the resistance of ASOs to the degradative action of nucleases and the binding to proteins both in plasma and within cells has been obtained by incorporating a phosphorothioate (PS) backbone, in which sulfur atoms replace the non-bridging oxygen of the inter-nucleotide phosphate group. Major interactions with plasma proteins like albumin increase the circulation time reducing renal clearance and resulting in improved drug pharmacokinetics. However, when the binding between PS-containing gapmer ASOs and plasma α 2-macroglobulin (A2M) occurs, it results in a loss of efficacy. Additionally, the PS modifications improve the interaction with intracellular proteins such as nucleolin, promoting the ASOs accumulation in the nucleus, the target site of action for splice-switching oligonucleotides. Other backbone modifications, such as boranophosphate, are less commonly used than PS backbone modifications that represent a good strategy for improving weaknesses without disrupting RNase H activity. Although these alterations have permitted higher half-lives of ASOs in serum, a disadvantage is the reduced binding affinity of ASOs for their target that can be compensated for by additional types of modification. A schematic representation of how RNA nucleotides can be chemically modified is reported in Figure 40; backbone, nucleobase, ribose sugar, and 2'-ribose substitutions can be made.

1. ***Stereochemistry.*** Modifications on the PS backbone are realized by introducing additional sulfur atoms resulting in the creation of a chiral centre at each phosphorus atom and two possible stereoisomers, S_p and R_p . The presence of stereocentre brings different physicochemical properties for each of them, such as target affinity, resistance to the degradative action of nucleases, hydrophobic character, or RNase H activity. The difficulty in separating and identifying the most active stereoisomers in

the racemic mixture of oligonucleotides would represent a step forward in the development of more efficacious ASOs. At the same time, the presence of both stereoisomers S_p and R_p in the mixture seems to be required to guarantee stability and efficient silencing activity.

2. **Nucleobase modifications.** Modifications into the nucleobase chemistry have been also investigated; the pyrimidine methylation, introducing 5-methylcytidine or 5-methyluridine/ribothymidine, represents the common incorporation into ASOs, able to increase the melting temperature of oligonucleotides. Moreover, abasic nucleotides have been developed to avoid the miRNA-like silencing while maintaining the target slicer activity.

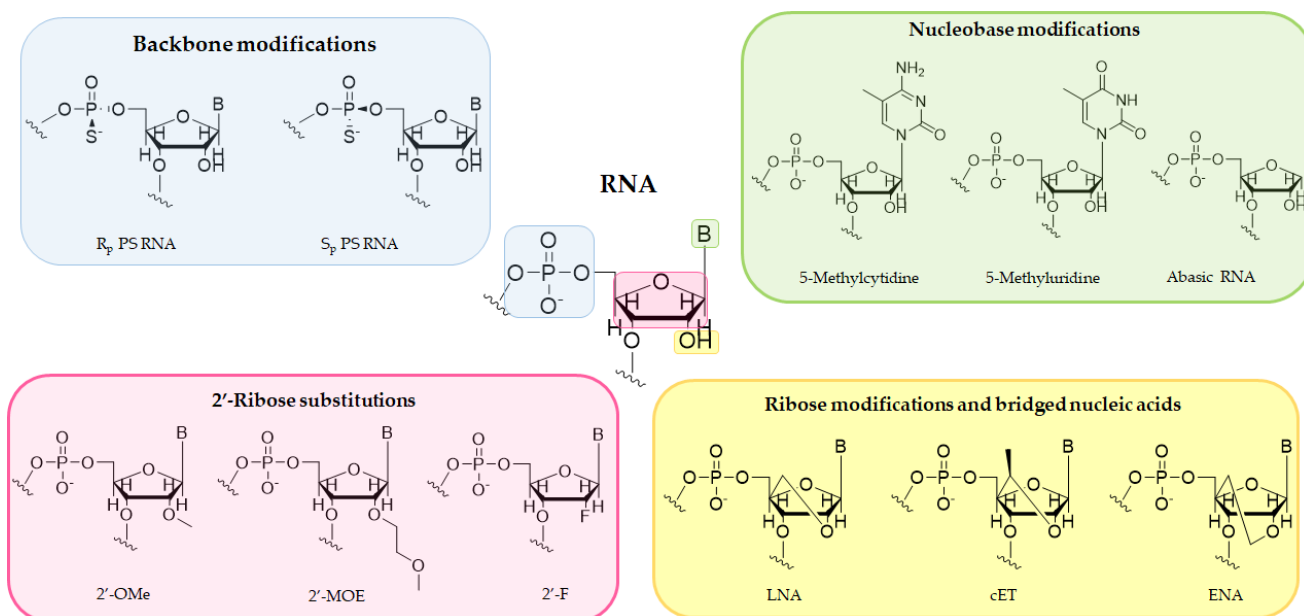


Figure 40

Chemical modifications. Schematic representation of an RNA nucleotide and the possible chemical modifications that could be realized to improve stability of oligonucleotides such as on the backbones (blue), on the nucleobase (green), on the 2'-ribose moiety (pink), or introducing bridge nucleic acids (yellow).

3. **Terminal modifications.** The 5' terminus of the siRNA guide strand needs to be phosphorylated to maintain its activity and potency because the phosphate group is required for the binding in the domain of AGO2. The additional introduction of a 5'-(E)-vinylphosphonate moiety acting as a phosphate without being a phosphatase substrate, prevents the exonuclease degradation and allows an enhanced silencing activity.

4. **Ribose sugar modifications.** These types of modifications occur in the 2' position of the ribose sugar. 2'-O-methyl (2'-OMe), 2'-O-methoxyethyl (2'-MOE), and 2'-Fluoro (2'-F) represent the most common substitutions on the ribose sugar able to increase the ASO stability towards nuclease degradative action by replacing the nucleophilic hydroxyl group of the unmodified RNA. Increased plasma stability, prolonged tissue half-lives, and enhanced ASOs effects are other advantages obtained with 2'-ribose substitutions. Furthermore, these modifications lead to a higher binding affinity of ASOs for the complementary RNA by promoting a 3'-endo pucker conformation of the sugar.
5. **Bridged nucleic acid (BNA) modifications.** BNAs are nucleotides in which the pucker of the ribose sugar is blocked in the 3'-endo conformation for the presence of a bridge connecting the 2' and 4' carbon atoms. Locked nucleic acid (LNA), 2',4'-constrained 2'-O-ethyl (cET), and 2'-O,4'-C-ethylene bridged nucleic acid (ENA) are the most used variations used. BNAs are used for their capability to enhance both the ASOs nuclease resistance and the affinity towards the target RNA by increasing the melting temperature of 3-8 °C per modified nucleotide, in the case of LNA. Otherwise, BNAs cannot undergo the RNase H-mediated cleavage remaining excluded from the DNA gap region.^{123,125}

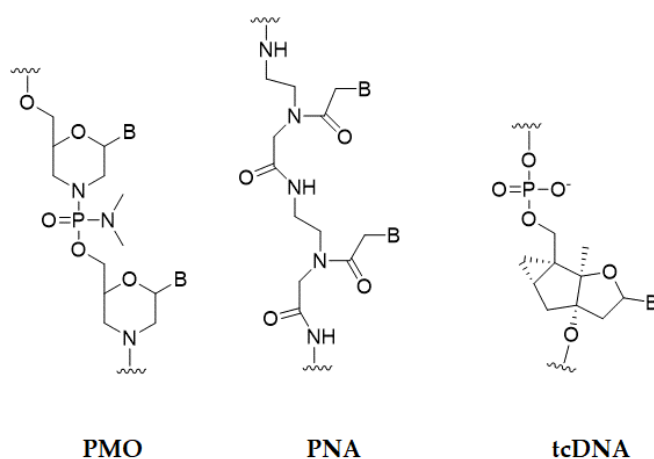


Figure 41

Alternative chemistries for ASOs. Different archetypes can be used to synthesize ASOs: the phosphorodiamidate morpholino oligonucleotide (PMO), peptide nucleic acid (PNA), and tricyclo-DNA (tcDNA).

As seen before, the majority of novel ASOs come from RNA or DNA, but alternative chemistries (Figure 41) have been developed for overcoming ASOs limits.

Charge-neutral nucleic acid chemistry allows the synthesis of the phosphorodiamidate morpholino oligonucleotide (PMO) characterized by the presence of a six-membered morpholine ring instead of a five-membered ribose heterocycle. Although FDA approved two PMOs for targeting exon 51 and 53 of the dystrophin mRNA, PMO drugs are racemic mixtures due to the presence of chiral centers in the backbone linkage, and today the effect of each stereoisomer has not been defined yet. The PNA chemistry has been used as an alternative way for creating a peptide polymer backbone that mimics the PO backbone of DNA and RNA. The lack of charges that characterized the nucleic acids both in PMOs and PNAs limits their interaction with plasma proteins leading to massive clearances and reduced half-lives. A third alternative synthetic scheme has been investigated for developing new ASO derivatives, using constrained DNA analogues able to increase the stability of the complex made by RNA target and ASO: tricyclo-DNA (tcDNA). *In vivo* studies demonstrated the ability of these derivatives to cross BBB, reach the brain, and display their activity. Unfortunately, the unnatural structure of PMO, PNA, and tcDNA does not allow them to be suitable for RNase H and RNAi uses, but they find important application in steric block oligonucleotides and for splice correction.¹²⁵

Delivery challenges

Another way to improve the pharmacokinetic profile of ASOs is represented by the covalent conjugation of oligonucleotides with moieties able to facilitate intracellular uptake, deliver the drug to specific cells and tissues, and reduce clearance prolonging plasmatic circulation. The most developed bioconjugation strategies include the use of sugar, aptamers, and antibodies; an advantage is represented by the relatively simple high-scale synthesis, the exact stoichiometry, and the favourable pharmacokinetic profile of bioconjugates. From a chemical point of view, into the oligonucleotides' structure, can be identified four termini to which conjugates can be attached.

Numerous strategies in the development of new bioconjugated oligonucleotides have been devised to improve the biodistribution of ASOs to specific target cells/tissues and the intracellular bioavailability of these new conjugates. In fact, being polyanionic big molecules, diffuse freely across membranes it has never been their main feature. Thus, using targeted delivery ASOs conjugated with selected ligands able to recognize selectively target receptors on the cell surface is the widest strategy to improve the *in vivo* efficacy and therapeutic index of ASOs.¹²⁵⁻¹²⁷

- **Sugar conjugates.** Delivery systems made by ASOs conjugated with different ligands able to target receptors on cell surfaces represent a validated strategy to improve the ASOs efficacy and therapeutic index. This approach allows also to increase the ASOs biodistribution in other tissues where naturally they do not tend to accumulate, such as the liver. The clinical application of an ASO conjugated to *N*-acetyl galactosamine (GalNAc), a carbohydrate moiety binding the overexpressed asialoglyco protein receptor 1 (ASGPR) and facilitating the uptakes of ASOs into hepatocytes by endocytosis, represents a milestone in the development of new targeting approaches (Figure 42).

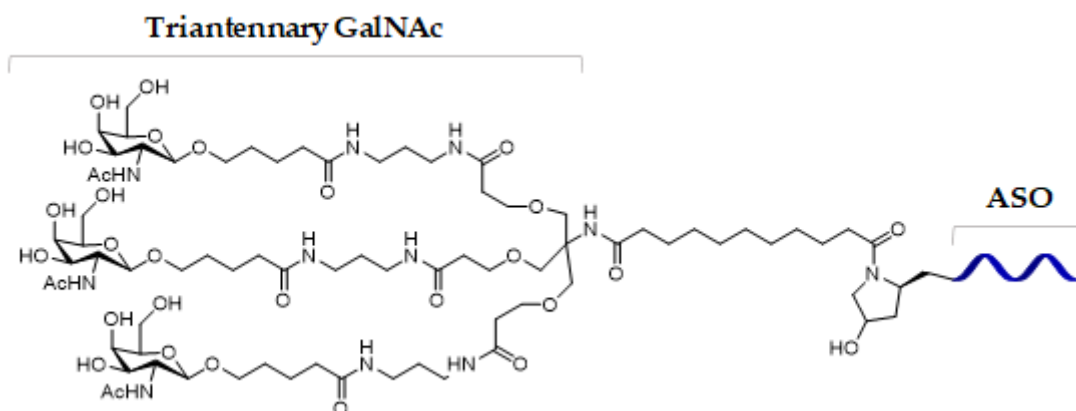


Figure 42

Sugar-ASO conjugates. A successful delivery strategy is represented by the conjugation of ASOs with a sugar moiety, such as Triantennary GalNAc.

The interaction between GalNAc and ASGPR is driven by pH changes, such that the dissociation of the receptor and the ASO occurs during the acidification of the

endosome. GalNAc-ASOs are preferentially delivered to hepatocytes and after enzymatic degradation of the carbohydrate moiety, the oligonucleotide is released.¹²⁸

- **Peptides** are attractive ligands capable to display cell-targeting, cell-penetrating (like CPPs) and endosomolytic properties when conjugated to therapeutic ASOs. CPPs are short proteins transduction domains typically made of less than 30 amino acids; usually, these amphipathic or cationic peptides are obtained from naturally occurring protein translocation motif or made of polymerized basic amino acids such as arginine and lysine. Recent applications of CPPs involve their use as a tool for the delivery of proteins covalently conjugated to oligonucleotides; the ideal cargo for charged CPPs is represented by neutral-charged backbone compounds that can exploit the CPPs ability to cross plasma membranes through specific peptide-mediated uptake mechanisms. Electrostatic interactions can occur when anionic chemistries are combined with cationic CPPs, leading to subsequence aggregation and possible reduction of efficacy.^{129,130}
- **Antibody & Aptamer conjugates.** The strategy to target cell surface receptors typically used by antibody-drug conjugates (ADC) can be adapted also to the oligonucleotides; studies in this field are still in the early stages of development, but the specific interaction between an antibody and cell surface receptors opens to the possibility of targeting tissues or cells subpopulation inaccessible with the other technologies. Several receptors have been targeted both for siRNA and ASOs delivery; the HIV gp160 protein, HER2, CD7, and CD44, EPHA2, EGFR, respectively. Usually, the antibody is chemically attached to the DNA carrier strand of a duplex structure of ASO, allowing the degradation of the DNA passenger strand inside cells and releasing the ASO from the complex. The conjugation of ASOs to nucleic acids aptamers has also been studied for improving and targeting the delivery of oligonucleotides. Aptamers can be defined as chemical antibodies able to bind with high affinity to their targets, but with the advantages to be easier to be synthesized, smaller and lower immunogenic than antibodies.¹²⁵
- **Nanocarriers.** Progress made in nanotechnology science represents a potential advantage for the delivery of oligonucleotides overcoming the problems of crossing

biological barriers and reaching the intracellular compartment. Mostly nanoparticles drug-delivery systems allow a bespoke optimization of the biophysical and biological properties.

- *Lipoplexes and liposomes*. Lipid formulations still represent the most common approach to improve nucleic acids' delivery; mixing polyanionic oligonucleotides with lipids can be obtained nanoparticles sufficiently large and favourably charged that trigger the uptake of nucleic acids by endocytosis. Lipoplexes are heterogeneous and unstable complexes made by the electrostatic interaction between anionic nucleic acid and cationic lipid; usually prepared before use, lipoplexes are successfully used for local delivery therapies. On the contrary, the most stable liposomes are made of a lipid bilayer constituted of cationic fusogenic lipids, promoting the endosomal escape, cholesterol PEGylated lipids, and an aqueous core where nucleic acids accumulate.
- *Exosomes*. Heterogeneous lipid bilayer-encapsulated vesicles, exosomes are generated by the inward budding of the multivesicular bodies. Probably released by cells in the extracellular compartment, exosomes can favourite intercellular communication via the cargo transferred. Several advantages characterize exosomes such as traversing biological membranes, included BBB, protecting from phagocytosis for the presence of CD47, and increasing circulation time. Moreover, exosomes are non-toxic, can be produced autologously and display pro-regeneration and anti-inflammatory properties.
- *Spherical nucleic acids (SNA)*. SNA consist of a hydrophobic core nanoparticle made of gold, silica or other materials and decorated on the surface with hydrophilic oligonucleotides anchored with thiol linkages. Thus oligonucleotides are exposed outwards from the protective core structure, but simultaneously they are protected from nucleolytic degradation.¹²⁵

Cellular uptake and trafficking

PS-ASOs, modified with phosphorothioate (PS) linkages and 2' modifications, have been studied both as drugs and research tools for altering gene expression. Modifications that occurred on the ASO backbone allowed them to penetrate cell membranes without additional formulations, to mediate sequence-specific cleavage of different RNAs targeted by endogenous RNase H1. ASOs' targets can be located both in the cytoplasm and nucleus, and the different subcellular localization can affect their therapeutic potency. As better described below, ASOs can be distinguished into two categories based on the specific mode of action (MoA). On one hand can be found ASOs synthesized as gapmer containing a central deoxynucleotide moiety with modified ribonucleotides ends, able to bind RNase H1 through which degrade target RNAs; on the other hand, ASOs can be designed as steric blockers used for modulating or splicing avoiding RNA degradation. Recent studies have elucidated specific uptake pathways for ASOs but have underlined the different abilities of cell types to bind oligonucleotides. Cancer cells, keratinocytes, and other rapidly growing cells uptake more efficiently ASOs than slow-growing ones. Furthermore, also B and T cells uptake increased rates of ASOs, highlighting how the physiological status of cells can modify the internalization of oligonucleotides. The cellular uptake process can be distinguished into adsorption and internalization. Adsorption is a rapid, saturable process that does not require energy; ASOs can compete with each other for associating with specific membrane receptors leading to a non-productive or productive internalization resulting in a pharmacological effect. Receptor-mediated uptake usually tends to promote the antisense activity of ASOs, suggesting that membrane receptors are involved in productive pathways. Similarly, clathrin- and caveolin-dependent entry mechanisms are considered to be productive. Scavenger receptors, G-protein-coupled receptors and integrins are some of the cell surface proteins involved in ASOs uptake, highlighting the ability of oligonucleotides to penetrate membranes also by alternative mechanisms. Although several studies demonstrated that ASOs enter cells using receptor-mediated or fluid-phase endocytotic mechanisms, only a small fraction of intracellular ASO seems to be entered through a productive pathway. The major limitation in the development and use of ASOs is

represented by the bigger uptake of these compounds via non-productive pathways, resulting in ASOs accumulation and entrapment in late endosomes and lysosomes, resulting in a reduction of therapeutical efficacy. For this reason, the efforts of medicinal chemistry researchers are directed to improve the productive cellular uptake by conjugation with ligands targeting selective receptors, lipophilic moiety, peptides, and sugar, or developing drug-delivery systems, or studying new methodologies allowing ASOs to escape from endosomes. In order to investigate the localization of ASOs inside cells, fluorescent microscopy was used to visualize fluorescently labelled ASOs; unfortunately, the high amount of labelled oligonucleotide required, the semiquantitative method, the capability to identify only punctate labelling accumulates of ASOs, and the inability to determine the stoichiometry of ASOs bound to cellular proteins result in an urgent need of new technologies to co-localize and quantify intracellular ASOs. Although these technical limits, in the 90s, microinjected labelled ASOs were found to accumulate primarily in the nucleus. The relatively low sensitivity of fluorescent technology limits the detection of ASOs in the nucleus after free uptake; in fact, has been detected ASOs accumulation in punctate structures in early and late endosomes, lysosomes, Golgi vesicles, and perinuclear area. It has also been demonstrated the rapid migration of ASOs from early and late endosomes to lysosomes and the slower accumulation in the cytoplasm, demonstrating how difficult could be the release of ASOs from these endocytic organelles and how limiting this step could be, and the importance of research to improve the release from organelles and enhance ASOs efficacy.¹³¹

Whatever the form, as a conjugate or assembled in delivery systems, a therapeutic oligonucleotide enters inside cells and undergoes the random trafficking process that is used by cells to transport endogenous and exogenous materials to many intracellular destinations. Endosomes (early, recycling, and late ones), lysosomes, the Golgi apparatus, and the endoplasmic reticulum are usually involved in the trafficking process. Unfortunately, therapeutic oligos tend to remain entrapped into these intracellular delivery vesicles, thus the manipulation of endocytotic and trafficking pathways can help attain this aim. The trafficking process can be divided into four steps: (a) a coated vesicle is released by the larger plasma donor membrane; (b) after the uncoating, the vesicle displays the

binding and fusion proteins; (c) by actin- or tubulin-based cytoskeletal structures, the vesicle reaches its final destination; (d) binding proteins recognize the target membrane compartment and SNARE proteins complete the fusion step allowing the delivery the cargo to the target destination. Intracellular trafficking mechanisms cannot be detailed discussed without talking about the Rab proteins, a large family of GTPases regulating multiple steps of intracellular trafficking. In the active GTP-loaded form, Rabs modulate downstream proteins, while in the inactive GDP-loaded form, they bind Rab-GDI proteins (Rab GDP dissociation inhibitor) and together act as chaperones regulating the cytosolic and membrane-bound Rab. These proteins are involved in the vesicles uncoating step, moving along cytoskeletal tracks and regulate membranes fusion. Another advantage of Rabs is their high specificity; Rab5 governs the movement of the clathrin-coated vesicles to early endosomes, Rab4 of early and recycling endosomes to the plasma membrane, Rab7 of late endosomes and lysosomes, Rab 9 of late endosomes and Golgi apparatus, and Rab11 regulates movements in the perinuclear endomembrane compartment. Also, binding proteins allow selective interaction between vesicles and their final target membrane compartment, probably acting as a bridge between membranes and promoting fusion by binding both Rab and SNARE proteins. SNARE proteins (soluble N-methylmaleimide sensitive factor attachment protein receptors) mediate the fusion process previously described, interacting with each other to form a four-helix bundle able to induce membrane fusion after conformational changes.¹³²

Mechanism of Action

ASOs are single-stranded oligonucleotides generally made by 16-20 nucleotides designed to target complementary RNA through Watson-Crick base pairing (C-G, A-T) and to avoid relevant off-target toxicity. ASOs can modulate the stability, processing, or activity of target RNA through different mechanisms, but generally can be distinguished two main mechanisms of action (MoA) of ASOs: RNA cleavage and RNA blockage (Figure 43). The majority of ASOs investigated and approved by FDA for therapeutic use, are RNase H-dependent oligonucleotides able to induce the degradation of the target RNA. With this mechanism, ASOs can target the specific RNA sequence and form with them

heterocomplexes that will act as substrates for the RNase H. RNase H is a ubiquitous enzyme that cleaves phosphodiester bonds of RNA when it is present in an RNA-DNA duplex form. There are two types of this enzyme: RNase H1 degrades the RNA of the RNA-DNA complex and the R-loop RNA-DNA hybrid formation that play a key role in the RNA Pol II transcription termination; RNase H2 mainly exploits a ribonuclease H activity in mammalian cells and cleaves ribonucleotides. With this MoA, ASOs can exploit their function reaching around 90% of silencing targeted RNA expression.^{133,134}

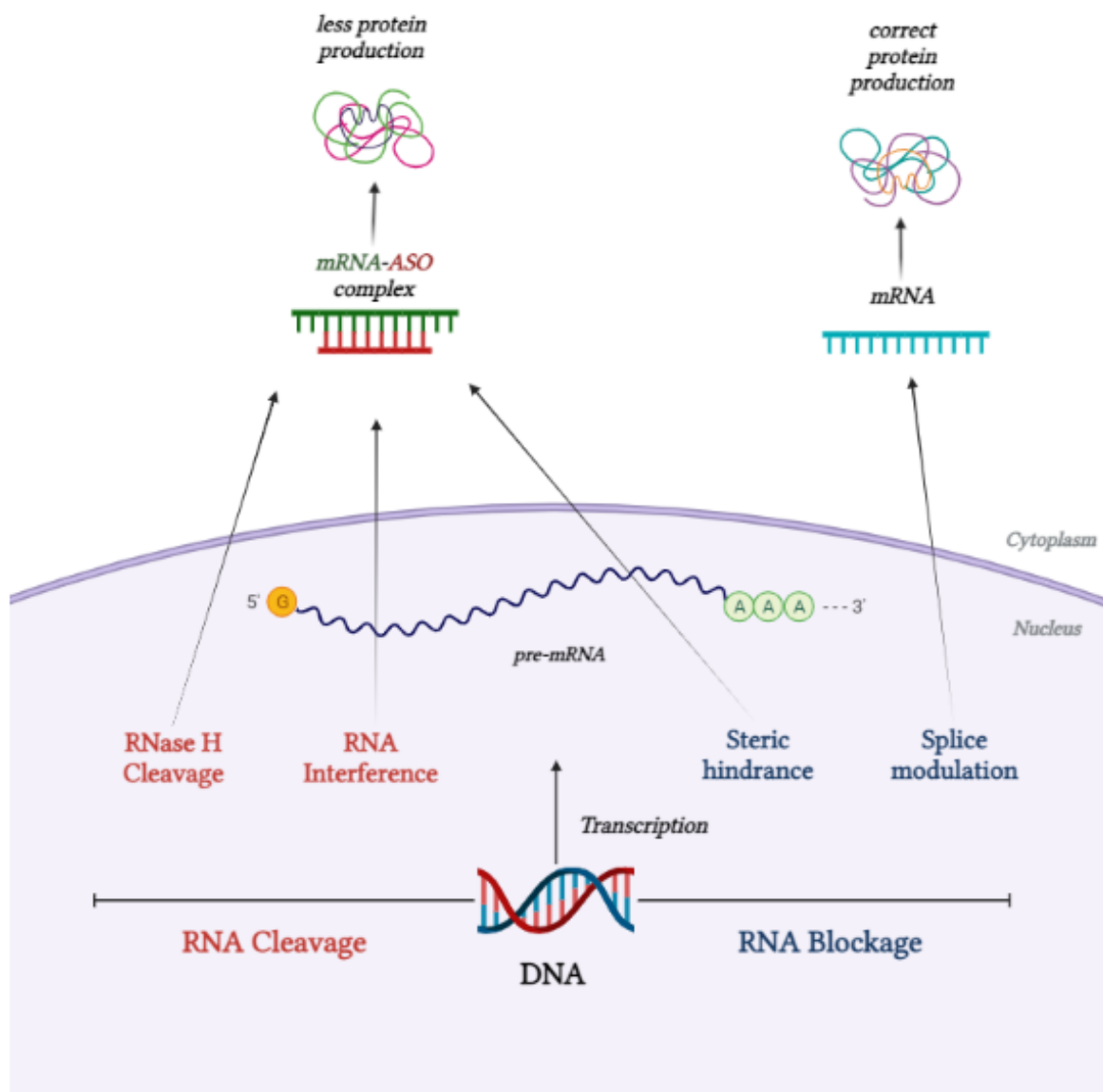


Figure 43

Mechanisms of action of antisense oligonucleotides (ASOs). Mainly can be distinguished two principal MoA RNA cleavage and RNA blockage, distinguished into RNase H cleavage and interference and steric hindrance and modulation, respectively.

The RNA steric blockage occurs when physically ASOs prevent or inhibit the progression of splicing or the translational machinery. These groups of ASOs after binding to the target RNA sequence inhibit their interaction with the 40S ribosomal subunit and prevent their assembly with 40S and 60S ribosomal subunits. Thus, the translational arrest is due to a steric hindrance. These classes of oligonucleotides do not provoke the cleavage mediated by RNase H and allow the retainment of pre-mRNA structure. The increased binding affinity of ASOs with the target results in a major hybridization with the RNA and a followed translational arrest. In fact, the steric hindrance and ASOs binding affinity are directly correlated. Another MoA adopted by ASOs is the splice-switching used to modulate the pre-mRNA target during mRNA maturation. Splice modulation occurs in two modalities: exon skipping and exon inclusion. Usually, frameshift mutations of pre-mRNA result in abnormal production of proteins or an arrest of the translational process. ASOs acting in exon skipping, bind the pre-mRNA transcripts and correct the altered reading frame leading to the production of the functional protein. While in exon inclusion ASOs after binding to the target pre-mRNA site, block the access to the transcript site to the spliceosome and other splicing factors.¹³⁵

Pharmacokinetics of therapeutic oligonucleotides

The pharmacokinetic properties of therapeutic oligonucleotides are primarily influenced by the chemistry of the backbones. PK and biodistribution are usually influenced by plasma protein binding limiting the glomerular filtration and urinary excretion of oligonucleotides. PS-ASOs, if compared to unmodified ones, display higher plasma stability, a major binding to plasma proteins and consequently, a better tissue bioavailability. PS-ASOs are broadly distributed mostly in the liver, kidneys, bone marrow, adipocytes, and lymph nodes. Although their big sizes and the presence of negative charges prevent the passage across the BBB, after an intrathecal administration in the cerebrospinal fluid (CSF), ASOs can broadly distribute in brain tissues. After *iv* administration, ASOs' plasma concentrations rapidly decrease following a multiexponential way characterized by a fast distribution to tissues and a slower elimination phase from them (up to weeks). If considered PS-ASOs, their elimination is facilitated by endonucleases and exonucleases that metabolize the

compounds in small fragments without activity and unable to bind plasma proteins in order to escape from the glomerular filtration and elimination in the urine. When combined with sugars, ASOs result to be more stable against the metabolizing action of these enzymes that degrade ASOs slowly allowing clearance on the order of 2-4 weeks. Conversely, ASOs lack charges or weakly bound to plasma proteins, such as morpholinos or peptides derivatives, are characterized by a more rapid clearance. Also for the ASOs, the toxicity is dose-dependent. Their potential toxicities can be distinguished into hybridization dependent or independent. If ASOs toxicity is hybridization dependent, means that can be due to the massive pharmacological effect induced by the hybridization of non-target RNAs. The off-target effects can be reduced by developing new oligonucleotides with high-affinity modifications to the specific target sequence and improving the informatics analyses to identify targets that perfectly match. A second potential toxicity can be provoked by the interaction between ASOs and proteins and depends on the ASOs' chemistry and the proteins they bind. Effects of coagulation, complement activation and immune cells activation are examples of these kinds of side effects. Over the last two decades, several antisense oligonucleotides have been approved for clinical trials for the treatment of a broad variety of diseases. The PS-ASO Fomivirsen has been approved for the treatment of cytomegalovirus retinitis, an opportunistic infection in HIV patients. In several different therapeutic areas, ASOs can be found in clinical trials or already approved for cardiovascular, infection, inflammation and autoimmune diseases, cancer therapy, and neurology.¹³⁶

MALAT1: a long non-coding RNA

Long non-coding RNAs (lncRNAs) are an important class of transcripts being involved in a wide range of cellular functions. lncRNAs are transcribed by RNA polymerase II and are made of the typical promoter and enhancer elements. Many of lncRNAs undergo alternative pre-mRNA splicing, cleavage or polyadenylation leading to several isoforms of the same locus. lncRNAs have been also characterized by their poor sequence level conservation; despite the large number of lncRNAs, the majority show a low expression level, few transcripts per cell, most of them limited to few cell types or specific conditions and

development stages. Moreover, some of the lncRNAs can be distinguished on their intracellular localization, being some localized in the cytoplasm while others in the nucleus, or associated with specific organelles, such as polycomb bodies, stress granules, nuclear speckles, and paraspeckles. *Metastasis Associated Lung Adenocarcinoma Transcript 1* (*MALAT1*) is a widely studied nuclear lncRNAs that gained much attention for its abundance, ubiquitous expression, and for being involved in several various diseases.¹³⁷. *MALAT1*, known also as *Nuclear Enriched Abundant Transcript 2* (*NEAT2*), was first identified in patients with non-small cell lung cancer (NSCLC) and upregulated in different tumors with a higher propensity to metastasize. *MALAT1* is almost 8.7 knt long gene transcribed by RNA polymerase II and its promotes has an accessible open chromatin structure; this lncRNA has a high expression level almost comparable to highly transcribed housekeeping genes, like β -Actin. Moreover, *MALAT1* is ubiquitously expressed in tissues with an expression around 150 TPM (transcripts per million) and higher expression levels (almost 290 TPM) in ovaries.

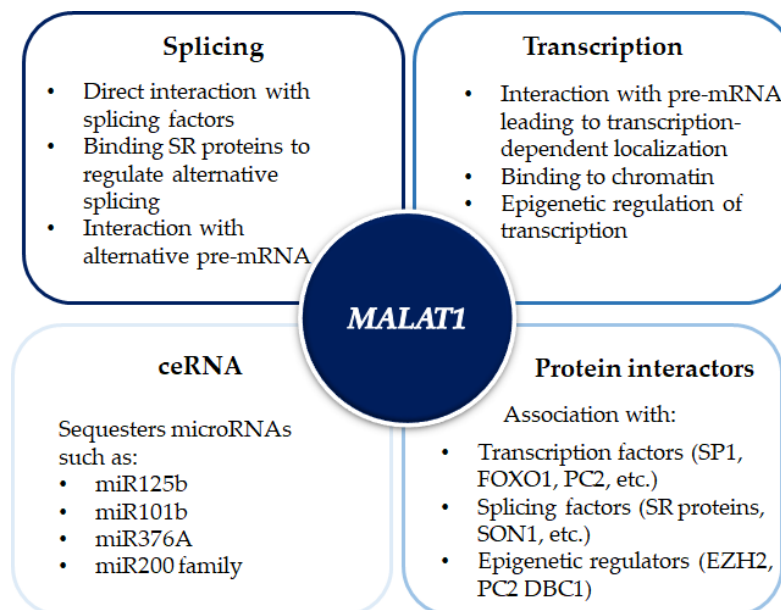


Figure 44

Molecular mechanism of MALAT1 function. The lncRNA *MALAT1* is involved in several functions, such as splicing, and transcription; it can bind and sequester microRNAs or associate with splicing or transcription factors and epigenetic regulators.

The post-processing nuclear *MALAT1* results in a 3' end not polyadenylated, but with a genomically-encoded poly(A)-rich stretch which adopts a triple-helical conformation after

pairing with an upstream U-rich domain. This particular confirmation gives *MALAT1* notable stability and increased nuclear retention and localization. *MALAT1* is a nuclear-retained RNA localized around the nuclear speckles, enriched in pre-mRNA processing and transcription factors, that coordinate the transcriptional and post-transcriptional gene regulation. In these nuclear domains, *MALAT1* seems to be localized mostly in the external part, while the pre-mRNA splicing factors are localized more internally. Although its localization, *MALAT1* has no influence on the formation of nucleus speckles, in regulating the assembly, number and size, or in the distribution and maintenance of them. Additionally, *MALAT1* shows a discrete ability to bind other pre-mRNA splicing factors enriched in nuclear speckles, i.e., SRF1, SON1, hnRNPC, etc, and it has been demonstrated how it can recruit splicing factors to actively transcribing loci, resulting in the regulation of alternative pre-mRNA splicing of a large number of pre-mRNAs. Moreover, *MALAT1* has been demonstrated to be associated with chromatin. Several studies have shown how *MALAT1* was able to coordinate the relocation of genes from polycomb bodies to transcriptionally active sites; this mechanism is probably due to binding between *MALAT1* and several polycomb proteins, such as PC2, EZH2, and DBC1 (Figure 44).¹³⁸

Molecular Function of MALAT1

As previously seen, several mechanisms have been proposed to explain the role of *MALAT1* in a wide range of diseases and physiological conditions. Due to its nuclear localization, *MALAT1* may be directly or indirectly involved in transcription as well as regulates alternative pre-mRNA splicing. This splicing pre-mRNA role of *MALAT1* is strictly due to its localization in the nuclear speckles, naturally enriched in pre-mRNA splicing factors. Moreover, it may regulate the phosphorylation status of SR splicing factors also regulating their speckle localization and the role in alternative pre-mRNA splicing, in which *MALAT1* may directly participate by recruiting factors to the pre-mRNA. In fact, it has been demonstrated the binding between *MALAT1* and several SR proteins, such as SRSF-1, -2, -3. Thanks to *in vivo* cross-linking studies, it has been elucidated the interaction between *MALAT1* and chromatin of actively transcribing genes, and the following regulation of their expression. Moreover, *MALAT1* also interacts with other transcriptional factors and

transcriptional co-activators like FOXO1, PC2, HMGA2, etc. It can increase proliferation and migration in breast cancer cells by binding the promoter EEF1A1 and overexpressing it epigenetically, in multiple myeloma cells can promote activators of proteasome subunit genes, and after binding to DBC1 induces deacetylation of p53 and induce cell proliferation and inhibition of the apoptosis. Additionally to its influence in splicing and transcriptional processes, *MALAT1* acts also as a competing endogenous RNA (ceRNA) sequestering miRNAs; an example is represented by miR-125b that binds *MALAT1* inducing downregulation of the gene and inhibiting bladder cancer development.¹³⁸ Since its identification in patients with NSCLC, *MALAT1* was considered a sort of paradigm as its relevant role in a wide range of tumors. In stage I and II NSCLC primary tumors high expression of *MALAT1* means contributing to metastasis, in particular in the brain by promoting epithelial-mesenchymal transition (EMT). Also in esophageal squamous cell carcinoma (ESCC), *MALAT1* induces tumor progression and metastasis (Figure 45). In pancreatic cancer, it can be an unfavourable predictor, promoting cell growth, migration, and invasion, while in hepatocarcinoma its overexpression means a higher risk of recurrence. Poor diagnosis and worse cancer progression are correlated to high levels of *MALAT1* in clear cell renal carcinoma, while its silencing inhibits invasion, migration, and proliferation in renal cancer cells. Moreover, *MALAT1* is involved in breast cancer where has been demonstrated how the inhibition of migration and cell proliferation after the treatment with 17 β -estradiol was directly dependent on the downregulation of *MALAT1*. It is associated with melanoma metastasis and the progression of osteosarcoma via the phosphoinositide 3-kinase (PI3K)/Akt pathway. Due to the relevant role as an oncogenic gene in the proliferation of several cancers, *MALAT1* can be potentially used as a promising diagnostic biomarker.¹³⁷ An altered expression of *MALAT1* has been found in several physiological stresses such as inflammation or hypoxia; its overexpression enhances glycolysis inhibiting gluconeogenesis via elevated translation of the transcription factors TCF7L2. *MALAT1* was found as an upregulated non-coding transcript upon hypoxia in breast cancer and seems to be regulated by HIF1 α , the transcription factor involved in the hypoxic process. Its key role in hypoxic stress and its ability to induce the proangiogenic isoforms of VEGFa lead to induction of metastasis and angiogenesis.

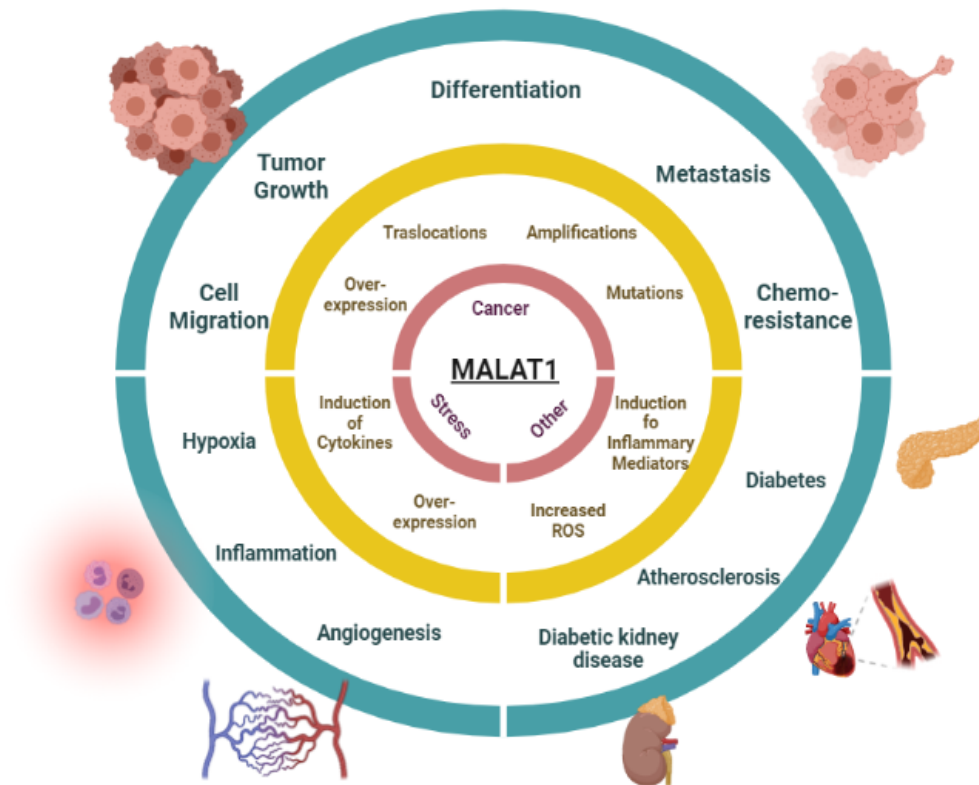


Figure 45

MALAT1 implication in different diseases. Primarily involved in the proliferation, migration, and metastasis of broad types of cancer, MALAT1 plays a relevant role in diabetes, atherosclerosis, and oxidative stress inducing hypoxia and inflammation.

Studies have demonstrated the direct implication of *MALAT1* in the development of diabetes and insulin signaling; its upregulation in endothelial cells was due to the high glucose levels and was also found to play a key role in regulating insulin sensitivity altering the NRF2 activity and downregulating JNK signaling while simultaneously insulin-inducing phosphorylation of Akt. Furthermore, *MALAT1* is involved in diabetes-related complications, such as cerebral ischemic reperfusion injury, diabetic retinopathy, atherosclerosis, and diabetic kidney disease. It mediates the production of the inflammatory cytokines tumor necrosis factor alfa (TNF- α) and interleukin 6 (IL-6) induced by glucose in the endothelial cells and regulates the expression of inflammatory transcripts by associating with the components of the PRC2 complex. *MALAT1* is strictly involved in the development and acceleration of diabetic atherosclerosis acting as an inflammatory factor and being highly expressed in macrophages (Figure 45).^{138,139}

Aim of the work

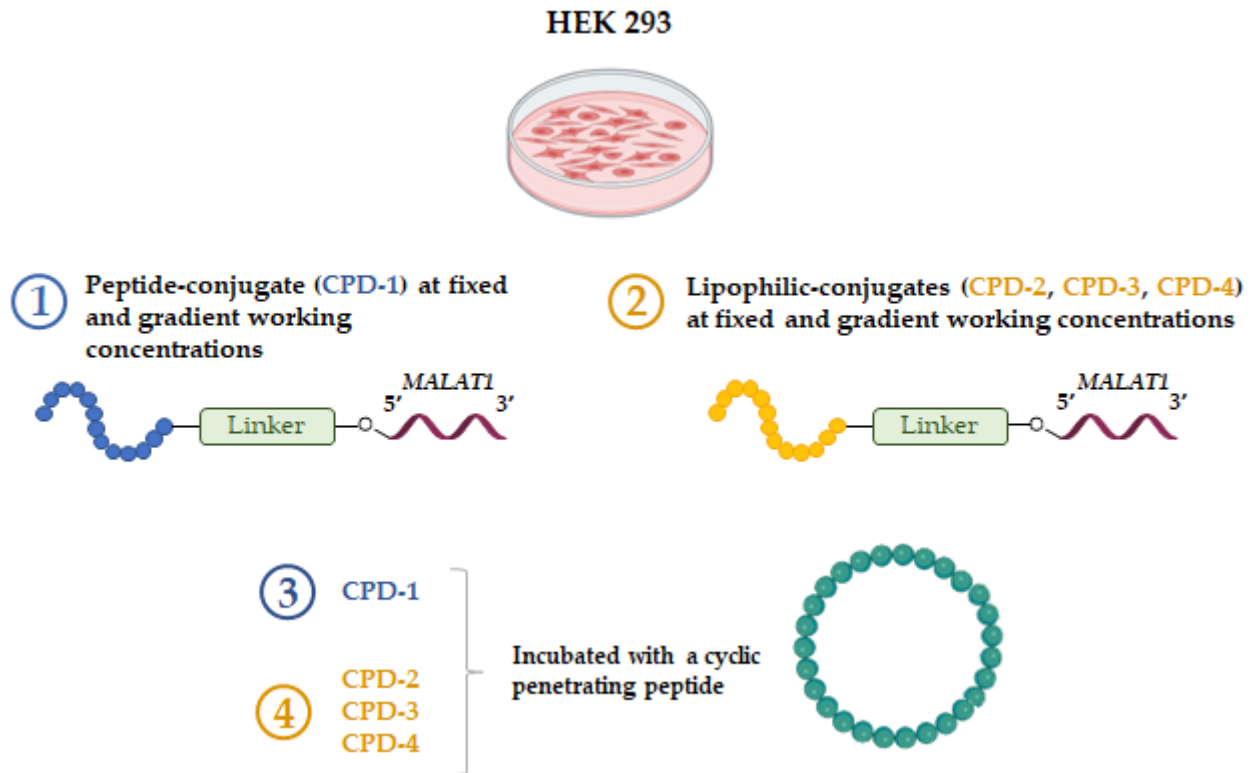


Figure 46

Graphical abstract of the project.

During my exchange period at Professor Artursson's research group in the Department of Pharmacy at Uppsala University (Sweden), I have been involved in the investigation of *MALAT1* silencing efficiency of antisense oligonucleotide (ASO) conjugates. *MALAT1* has been selected as model target for these studies.

Due to their negative charged backbone, ASOs cannot efficiently cross membranes without remaining entrapped within endosomes. Thus, in this Ph.D. project, it has been investigated the efficiency of different ASOs conjugates (CPD-1, CPD-2, CPD-3, and CPD-4) with four strategies of treatments reported in the graphical abstract (Figure 46). The work aimed to identify the best delivery strategy between the ones selected, to overcome the ASOs limit and improve their biological efficacy. For confidentiality reasons it is not possible to show more information regarding the type of conjugates developed, the synthetic process applied, the target receptor selected for the drug delivery system, and the structure of the cyclic cell penetrating peptide used for the studies.

Experimental Section

Biological evaluation

Cell Culture

HEK293 Wild-Type (WT) and HEK293 overexpressing a target G-protein coupled receptor cells (purchased from AstraZeneca) were grown in Dulbecco's Modified Eagle's Medium (DMEM) enriched with 10% of fetal bovine serum (FBS) in the presence of 10000 units/mL Penicillin/Streptomycin (everything purchased from ThermoFisher) at 37°C and 5% CO₂ atmosphere. Cells were passaged or harvested for experiments at 100% confluency.

For splitting cells, DMEM 10% was removed, and cells were washed with 8 mL of PBS. To allow the detachment from the flask, 2 mL of 1x Trypsin (from ThermoFisher) in PBS was added and put back the flask at 37°C to facilitate the passage. The trypsin has been neutralized using 8 mL of DMEM 10%. After centrifugation at 1500 × g for 5', the supernatant was removed and the pellet of cells was resuspended in 13 mL of medium. Flasks returned to the incubation conditions of 37°C and 5% CO₂ atmosphere.

For counting cells, the protocol followed was the same reported for splitting them; after centrifugation and removal of the supernatant, the cell pellet was resuspended in a 6 mL of DMEM 10% and mixed well by pipetting. 20 µL of cellular suspension was mixed with an equal volume of ViaStain AOPI Staining Solution (purchased from Nexcelom Bioscience); then 20 µL of the solution was added to Cellometer disposable counting chambers and vials cells counted using the Cellometer Vision CBA Image Cytometer (from Nexcelom Bioscience).

Stimulation with ASOs conjugates

In this project, different stimulation with the peptide-conjugated ASO (CPD-1) and lipophilic-conjugated ASOs (CPD-2, CPD-3, CPD-4) at fixed and gradient time points and working concentrations, were conducted in the presence and absence of CPP in order to evaluate the silencing efficacy of ASOs derivatives.

For all experiments, 2×10^5 cells/well were seeded in 24-well plates pre-treated with a Poly-D-Lysine (from ThermoFisher) solution diluted in PBS 1:1 _{v/v} (from ThermoFisher) until the final concentration of 0.05 mg/mL. After 30' incubation, the Poly-D-Lysine solution was removed from wells and the coated culture wells were let dry uncovered under a laminar hood. After 24 hrs of incubation at 37°C and 5% CO₂ atmosphere, stimulations with different ASOs were conducted. The experiments have been conducted in duplicates.

1. *Stimulation with CPD-1 at fixed and gradient working concentration.*

CPD-1 was used to stimulate both HEK293 cell lines at the working concentration of 0.5 μ M in Opti-MEM I reduced serum medium (from ThermoFisher) for different time points (0 hrs and 48 hrs). Moreover, another stimulation was conducted, after seeding cells in the same conditions seen before, using a gradient working concentration of **CPD-1** (0.5 μ M, 2.5 μ M, and 5 μ M) in Opti-MEM I reduced serum medium for 0 and 48 hrs. Stimulations were conducted in the presence of two negative controls, **Naked-MALAT1** and **Scrambled-MALAT1**, at the same working concentrations of **CPD-1**.

2. *Stimulation with CPD-1 at a fixed concentration in the absence and presence of a gradient concentration of CPP.*

The day after seeding, treatments were performed using **CPD-1** at 0.5 μ M in Opti-MEM I reduced serum medium in the absence and presence of CPP in a gradient working concentration of 5 μ M, 10 μ M, and 15 μ M, for 0 and 48 hrs. **Naked-MALAT1** and **Scrambled-MALAT1** were used as negative controls and were incubated at 0.5 μ M in the absence and presence of CPP at a fixed concentration of 10 μ M.

3. *Stimulation with lipophilic-ASOs (CPD-2, CPD-3, CPD-4) at fixed and gradient working concentration.*

The treatments were conducted on HEK293 WT, after 24 hrs from the seeding, with **CPD-2**, **CPD-3**, and **CPD-4** at the working concentration of 2.5 μ M in Opti-MEM I reduced serum medium, for 0-24-48 hrs. Moreover, other stimulations were conducted, in the same conditions seen before, using a gradient working concentration of the same lipophilic-conjugated ASOs (0.5 μ M, 2.5 μ M, and 5 μ M) in

Opti-MEM I reduced serum medium for 0-24-48 hrs. Both treatments were conducted in the presence of two negative controls, **Naked-MALAT1** and **Scrambled-MALAT1**, at the same working concentrations of lipophilic-conjugated ASOs.

4. *Effect on CPP on lipophilic-conjugated ASOs.*

To investigate a possible additive effect on the efficacy of lipophilic-conjugated ASOs, HEK293 WT cells were seeded following the protocol described above. The treatments were conducted using the most promising lipophilic-ASOs, **CPD-2** and **CPD-3**, at the fixed concentration of 2.5 μM in Opti-MEM I, in the absence and presence of CPP at a final concentration of 5 μM . CPP was added both together with lipophilic-ASOs and after 4 hrs from the beginning of the stimulation. The treatments were conducted at two time points of 0 and 48 hrs. **Naked-MALAT1** and **Scrambled-MALAT1** were used as negative controls and were incubated at 2.5 μM in the absence and presence of CPP.

5. *Comparison between lipophilic-conjugated ASOs and the peptide-conjugated ASO in the absence and presence of CPP.*

In order to evaluate differences in efficacy between ASOs derivatives on both HEK293 cell lines, lipophilic-conjugated ASOs, **CPD-2**, **CPD-3**, and **CPD-4**, and the peptide conjugate, **CPD-1**, were tested at the final concentration of 2.5 μM in Opti-MEM I reduced serum medium at 0 and 48 hrs. The experiments regarding lipophilic-ASOs were conducted in the absence of CPP, while **CPD-1** was assayed at the final concentration of 2.5 μM in Opti-MEM I reduced serum medium both in the absence and presence of CPP 5 μM for 0 hrs and 48 hrs. **Naked-MALAT1** and **Scrambled-MALAT1** have been used as negative controls at the same working conditions described above.

RNA extraction & quantification

At specific time points, the stimulation solutions were removed and wells were washed with PBS. RNA extraction was performed using the RNeasy Mini QIAcube Kit (purchased from Qiagen). An appropriate volume (350 μL) of lysate buffer RLT enriched with 10 $\mu\text{l}/\text{mL}$ β -mercaptoethanol (β -ME), was added to every well; after 5' of incubation 350 μL of 70%

ethanol were added. Mixing well by pipetting, up to 700 μL of samples were transferred to the RNeasy spin columns supplied with the kit and centrifuged for 15 s at 8000 \times g. 700 μL of the stringent washing buffer RW1 were added to the columns and centrifuged as previously reported. The last two washes, useful to remove traces of salts, have been done using 500 μL of the mild washing buffer RPE (previously implemented with 4 volumes of ethanol 99.9%) and centrifugated firstly for 15 s at 8000 \times g, and secondly for 2' at 8000 \times g. To extract RNA from samples, 40 μL of RNase-free water were placed directly on the spin column membranes; the RNA was eluted after 1' centrifugation at 8000 \times g.

RNA concentration/purity was measured using the spectrophotometer NanoDrop ND-1000 (from ThermoFisher). The A260/280 and A260/230 ratios were used to assess RNA purity along with the nucleic acid concentrations expressed in ng/ μL .

RT-PCR and qPCR assays.

PCR assays were conducted using 1 μg of total RNA which was reverse-transcribed into complementary DNA (cDNA) using a High-Capacity cDNA Reverse Transcription Kit (from ThermoFisher). 10 μL of RNA [1 μg] were added into PCR plates with 10 μL of master mix solution made of 2 μL 10X RT buffer, 2 μL 10X RT random primers, 0.8 μL 25X dNTP mix (100 mM), 1 μL multiscribe reverse transcriptase (50 U/ μL), and 4.2 μL DEPC treated water (kit purchased from ThermoFisher).

PCR assays were run using an Eppendorf Mastercycler PRO S Thermal Cycler Model 6325. Thermal cycler conditions applied were:

- 25°C for 10 minutes;
- 37°C for 120 minutes;
- 85°C for 5 minutes and then 4°C.

After diluting cDNA with DEPC treated water 1:100 v/v , qPCR plates were assembled using 6 μL of TaqMan fast advanced master mix (from ThermoFisher), 0.6 μL of primer, and 3.4 μL of DEPC treated water in the presence of 2 μL of cDNA.

The primers used for qPCR were as follows: human MALAT1 (Hs00273907_s1, from ThermoFisher) and human GAPDH (Hs04420632_g1, from ThermoFisher). qPCR assays have been run using a CFX Connect Real-Time PCR Detection System.

Thermal cyclers conditions applied were:

- 50°C for 2 minutes;
- 95°C for 10 minutes;
- 40 cycles of 95°C for 15 seconds;
- 60°C for one minute.

All PCR and qPCR assays have been conducted in triplicates.

qPCR results have been expressed as differences in the expression levels between the gene of interest (*MALAT1*) and the housekeeping gene (*GADPH*) for each sample, then by the difference of the average of Cq threshold cycle of the reference gene with the Cq of the gene of interest, resulting in the so-called ΔCq . Data have been normalized both with the average of **0 hrs** and **Scrambled-MALAT1** values resulting in the $\Delta\Delta Cq$ values that were calculated for each sample by subtracting the ΔCq of the gene of interest from the average ΔCq calculated for the housekeeping gene. The foldchange values have been expressed as $2^{-\Delta\Delta Cq}$. Data have been analysed using Excel and the averages and standard deviations of the biological foldchanges have been plotted using GraphPad Prism 8 software. Two-way ANOVA and Tukey test for multiple comparisons have been conducted and p values determined; the most significant p values have been reported in each graph following presented.

Results and Discussion

Our first aim was to investigate if ASOs' efficiency could be improved using the targeted delivery system represented by the peptide-conjugated ASO, **CPD-1**. The effect of **CPD-1** was studied by measuring the efficiency in knocking down *MALAT1* gene expression in both HEK293 cell lines (Figure 47 A-B).

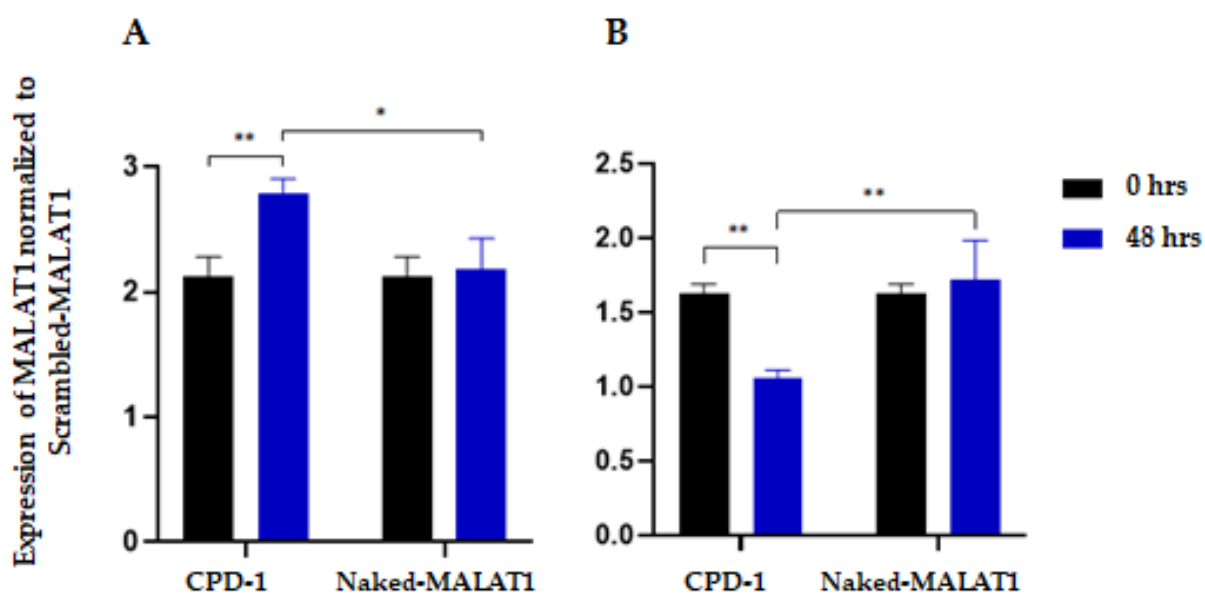


Figure 47

*Expression of MALAT1 gene after treatment of HEK293 WT (A) and HEK293 receptor overexpressing cells (B) with CPD-1 at 0.5 μ M for 0 and 48 hrs. Data are presented as MALAT1 expression normalized to Scrambled-MALAT1. Data display mean \pm STDEV; n = 2. **p<0.01; *p<0.05.*

As expected, **CPD-1** showed significant efficacy in silencing the target gene after 48 hrs, if compared to 0 hrs of treatment and **Naked-MALAT1**, on HEK293 receptor overexpressing cells (Figure 47. B), while on HEK293 WT cells (Figure 47. A) did not explicate any activity in knockdown gene expression. In fact, data obtained from HEK293 WT cells showed a significant decrease in efficacy of **CPD-1** after 48 hrs of treatment, in comparison with 0 hrs and **Naked-MALAT1**. On both cell lines, **Naked-MALAT1** displayed no significant difference in silencing *MALAT1* expression after 48 hrs of treatment.

In order to assess if 0.5 μ M would have been the best concentration to be used for obtaining the major down-regulation of *MALAT1* expression, the efficiency of **CPD-1** was also tested

on both cell lines at a gradient concentration of 0.5 μM , 2.5 μM , and 5 μM for 0 and 48 hrs (Figure 48). Results obtained showed how, by increasing **CPD-1** concentration from 0.5 μM to 2.5 μM , the efficiency in knocking down *MALAT1* gene expression was improved in HEK293 receptor overexpressing cells. Unfortunately, at 5 μM has not been possible to appreciate the same trend; in fact, the efficiency of **CPD-1** decreased.

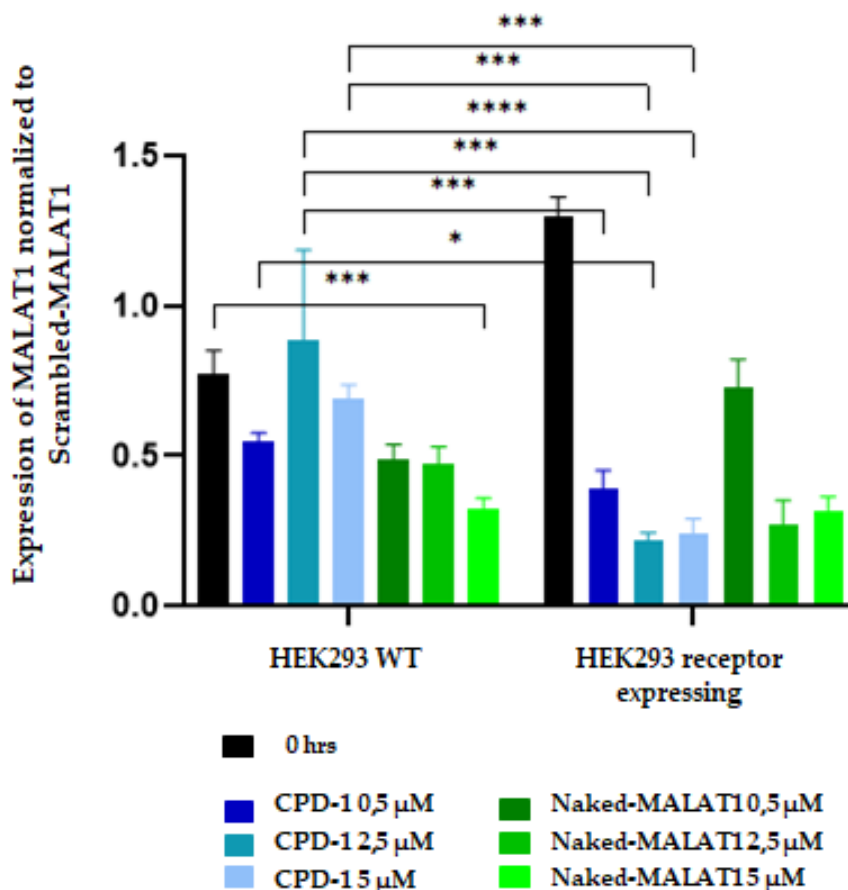


Figure 48

*Evaluation of efficacy of CPD-1 at gradient working concentration of 0.5-2.5-5 μM on HEK293 WT and receptor overexpressing cells after 48 hrs of treatment. Data are presented as MALAT1 expression normalized to Scrambled-MALAT1. Data display mean \pm STDEV; n = 2. ****p<0.0001; ***p<0.001; **p<0.01; *p<0.05.*

From these results has been possible to confirm the selective action of **CPD-1** on HEK293 receptor overexpressing cells, confirming the assumption that target delivery systems can facilitate the cellular uptake step, probably overcoming the ASOs entrapment into endolysosomes. Data obtained allowed us to select the best concentration for further experiments; in fact, looking at the efficacy of **CPD-1** on HEK293 receptor overexpressing

cells, it was clear that 0.5 μM resulted in a too low concentration for explicating a right answer, while between 2.5 μM and 5 μM the first concentration resulted to be the best. For these reasons, 2.5 μM has been chosen as the working concentration more suitable to obtain efficient results in gene silencing. Moving from the idea that higher intracellular bioavailability of ASOs can be achieved by overcoming the endosomal entrapment phenomena, CPD-1 was also tested at the lowest concentration of 0.5 μM in the presence of CPP using the gradient working concentration of 5-10-15 μM (Figure 49).

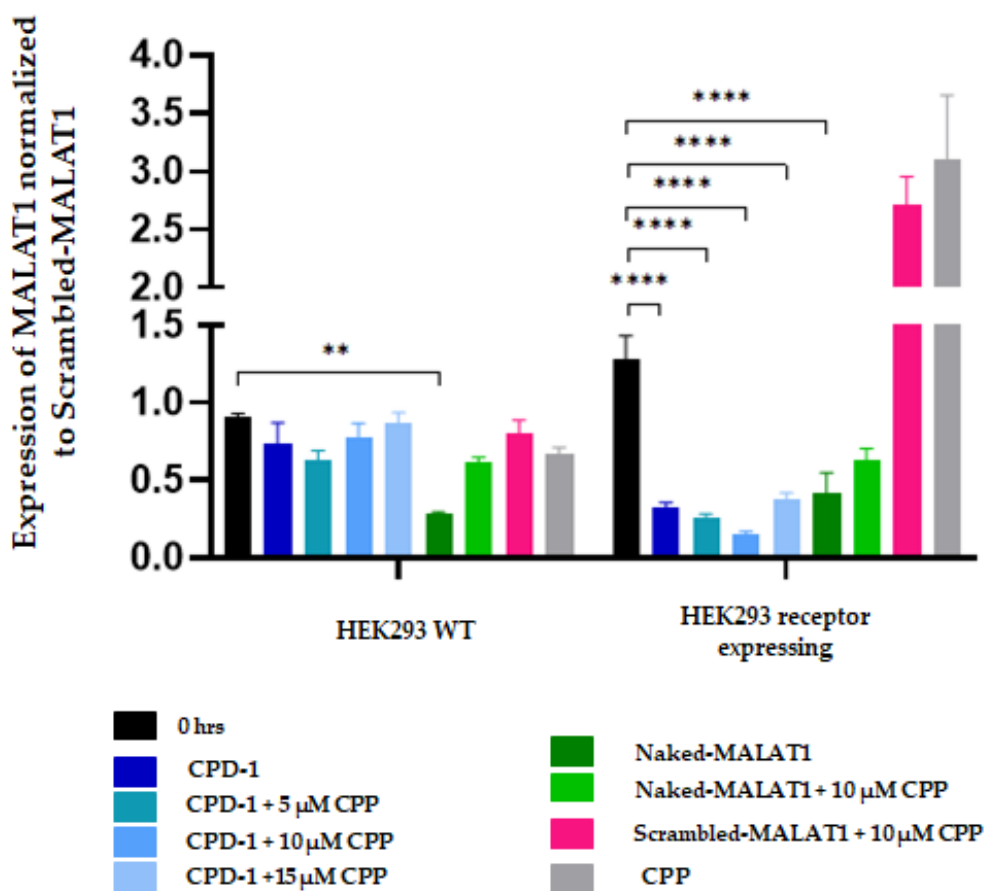


Figure 49

Evaluation of efficacy of CPD-1 at a fixed working concentration of 0.5 μM on both HEK293 cell lines in the absence and presence of CPP (5-10-15 μM) after 48 hrs of treatment. Data are presented as MALAT1 expression normalized to Scrambled-MALAT1. Data display mean \pm STDEV; $n = 2$. **** $p < 0.0001$; ** $p < 0.01$.

Combining two different forms of delivery systems the hypothesis was to appreciate a significant additive effect of CPD-1; in fact, for this reason, the ASO derivative was tested at the lower concentration (0.5 μM) to better evaluate a possible increase in the efficacy of the compound. Results obtained on HEK293 receptor expressing cells demonstrated only a

slight, but not significant, improvement in silencing *MALAT1* gene expression when **CPD-1** was co-incubated with CPP 10 μ M. Otherwise, in the presence of 5 μ M and 15 μ M of CPP, **CPD-1** activity showed no improvement when compared to the ASO alone. Additionally, with the higher concentration of CPP, **CPD-1** capacity in knockdown the expression of *MALAT1* decreased. The lack of significant activity on HEK293 WT cells of **CPD-1** in comparison to **Naked-MALAT1** was confirmed. The same trend of decreased efficiency could be appreciated in both cell lines also when **Naked-MALAT1** was incubated in the presence of 10 μ M of CPP; in fact, also from this experiment a loss of efficacy has been detected. The lack of sensitive increase in the gene silencing activity and the decreased efficiency of ASOs, when incubated with CPP, could be probably due to possible aggregation phenomena occurring between the ASOs negatively charged and CPP positively charged.

Our second aim was to evaluate if the endosomal escape could be better overcome using alternative ASO-conjugates.

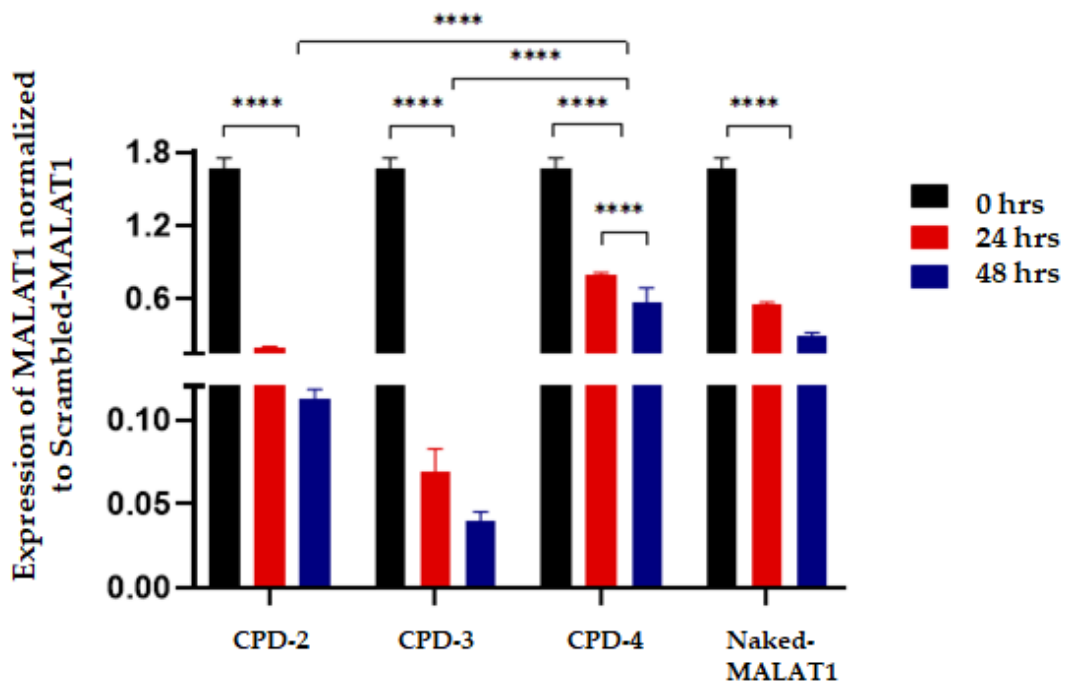


Figure 50

Evaluation of efficacy of CPD-2, CPD-3, and CPD-4 at a final working concentration of 2.5 μ M on HEK293 WT after 24 and 48 hrs of treatment. Data are presented as *MALAT1* expression normalized to Scrambled-*MALAT1*. Data display mean \pm STDEV; n = 2. ****p<0.0001.

We investigated the efficacy of CPD-2, CPD-3, and CPD-4 at the working concentration of 2.5 μM in silencing *MALAT1* expression on HEK293 WT cells after 0, 24, and 48 hrs of treatment (Figure 50). Among the three conjugates assayed, CPD-3 showed the best result with an efficacy close to 95% at 48 hrs. CPD-2 has significantly silenced gene expression in comparison to 0 hrs. Otherwise, CPD-4 was characterized by a decreased activity if compared to Naked-MALAT1 and most of all to CPD-3.

We also performed a second experiment on HEK293 WT cells, to investigate ASOs' behaviour using a gradient working concentration (0.5-2.5-5 μM) at the same time points previously tested (Figure 51).

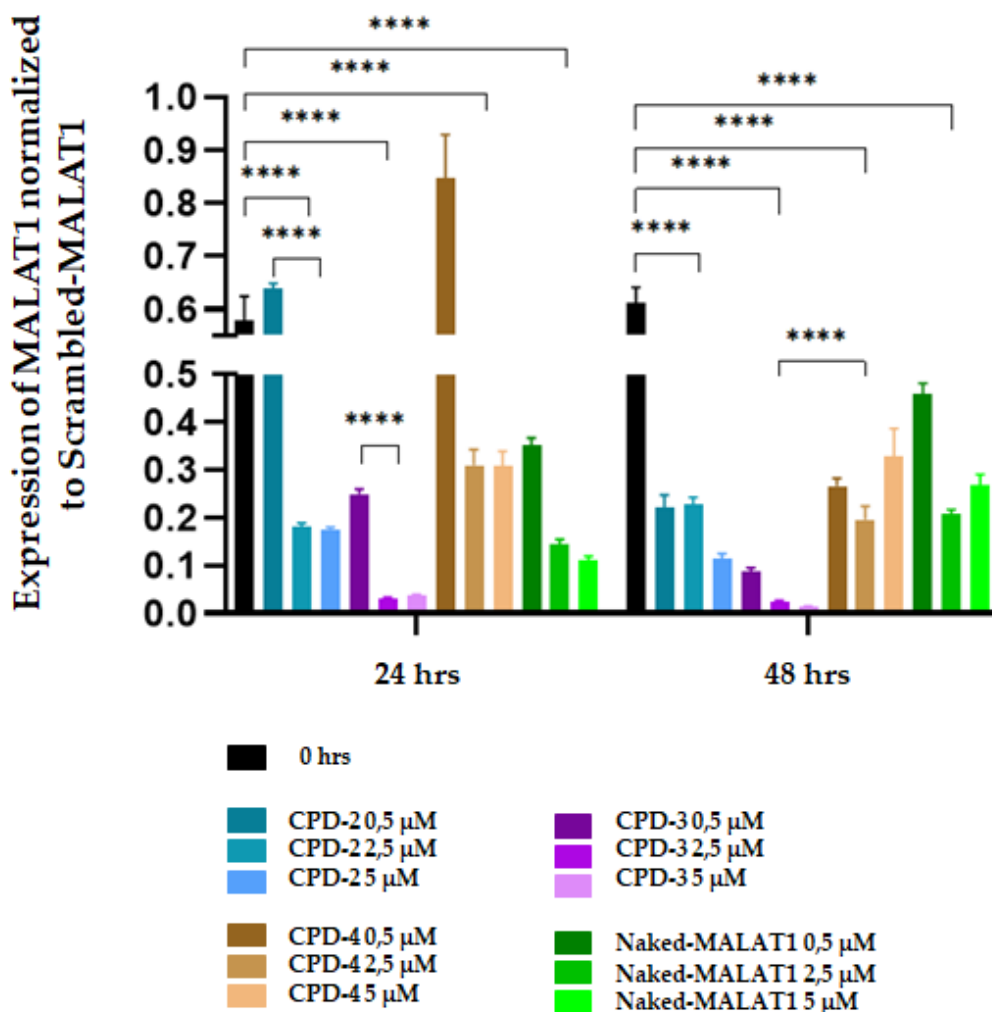


Figure 51

Evaluation of efficacy of CPD-2, CPD-3 and CPD-4 at gradient working concentration of 0.5-2.5-5 μM on HEK293 WT after 24 and 48 hrs of treatment. Data are presented as MALAT1 expression normalized to Scrambled-MALAT1. Data display mean \pm STDEV; n = 2. ****p<0.0001.

Analysing results could be appreciated the significant efficiency in silencing *MALAT1* expression of **CPD-3**. If at 24 and 48 hrs **CPD-3** has reduced the gene expression to less than 10 and 5% respectively, **CPD-2** at 24 hrs improved its efficacy in silencing gene from the lowest (0.5 μ M) to the highest concentrations (2.5-5 μ M), although no significant improvements were highlighted at 48 hrs between the three different concentrations. Something similar happened also to **CPD-4**, which showed an efficacy profile of minor interest when compared with other lipophilic conjugates or **Naked-MALAT1** at both time points of 24 and 48 hrs. As expected, **CPD-2** and **CPD-3**, displayed higher capability in silencing the target gene if compared to **CPD-1** activity on HEK293 WT.

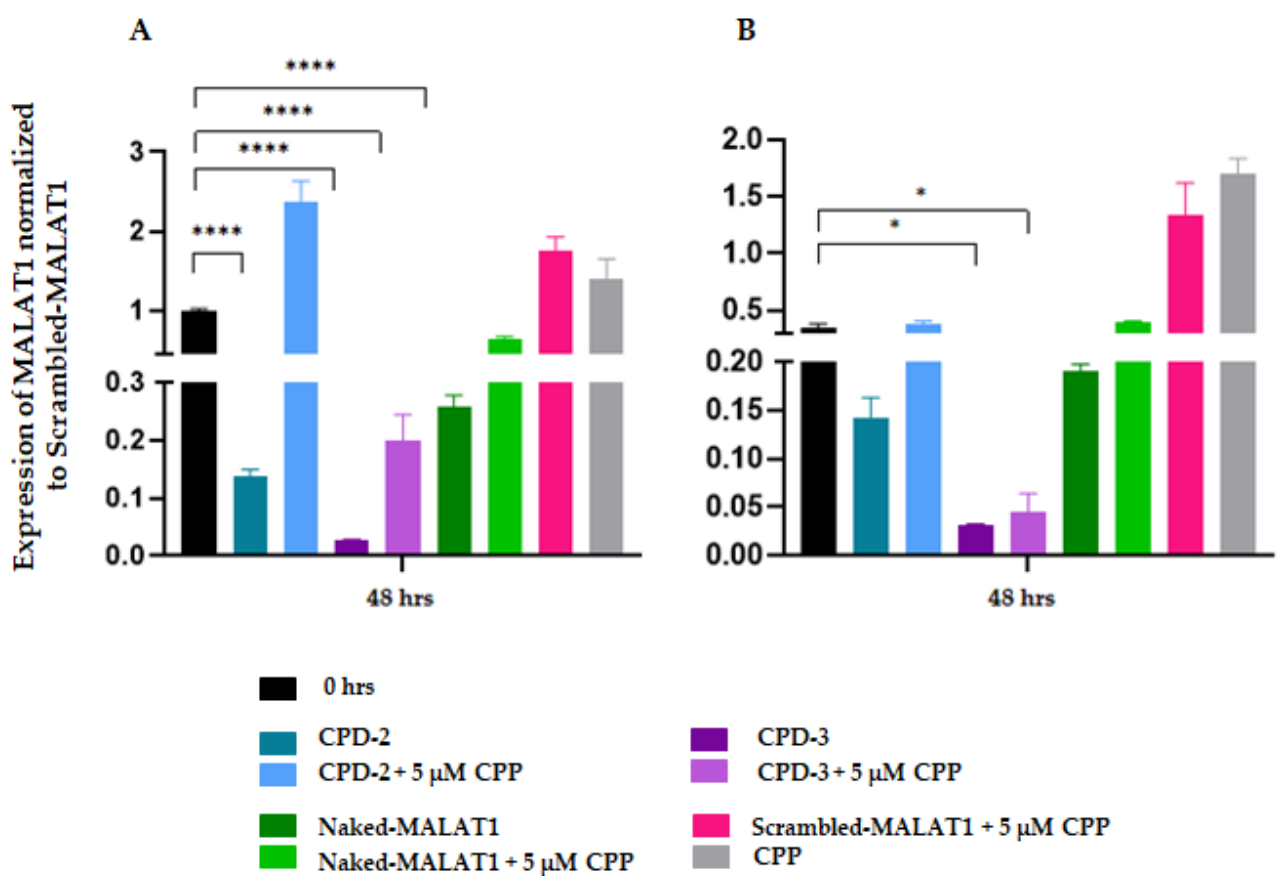


Figure 52

Evaluation of the effect of CPP (5 μ M) added simultaneously (A) and after 4 hrs (B) of treatment with CPD-2 and CPD-3 at a fixed concentration of 2.5 μ M on HEK293 WT. Time points 0-48 hrs.

Data are presented as MALAT1 expression normalized to Scrambled-MALAT1. Data display mean \pm STDEV; $n = 2$. **** $p < 0.0001$; * $p < 0.05$.

In order to study the endosomal escape mechanism and investigate if a higher intracellular bioavailability could be directly connected to the higher efficiency of oligonucleotides, the

next step was to evaluate the potential additive effect of CPP when incubated with the most promising lipophilic-ASOs: **CPD-2** and **CPD-3**.

Both ASOs were incubated on HEK293 WT for 48 hrs at the fixed concentration of 2.5 μ M in the absence and presence of CPP at 5 μ M (Figure 52. A). Results obtained, confirmed the trend seen before; the efficiency in knocking down the gene expression sensitively decreased when CPP was added. These results also supported the initial hypothesis that phenomena of aggregation could happen involving ASOs and CPP. To further investigate the role of co-incubation time of samples in the aggregation phenomena, another experiment was performed adding 5 μ M of CPP after 4 hrs of treatment with only lipophilic-ASOs at 2.5 μ M (Figure 52. B). Even if a decrease in terms of silencing *MALAT1* expression after the addition of CPP has been detected, probably fewer aggregation phenomena took place letting ASOs cross membranes, reach the target, and knock down the gene expression without remaining completely blocked in an aggregate with CPP. In fact, as could be seen by comparing the graphs reported in Figure 52. A-B, **CPD-2** and **CPD-3** efficacies were reduced when CPP was added after 4 hrs, but less than when ASOs and CPP were incubated together from the beginning of the experiment.

Finally, a comparison between all ASO conjugates assayed, in the absence and presence of CPP was conducted on both HEK293 cell lines. As expected, on HEK293 WT cells (Figure 53. A), **CPD-2**, **CPD-3**, and **CPD-4** displayed the same trend seen before, with a gene silencing efficiency of **CPD-3** close to 95% after 48 hrs of treatment. **CPD-2** was confirmed to have higher activity on downregulation gene expression than **CPD-4** whose efficacy resulted closer to **Naked-MALAT1**. Regarding the **CPD-1** effect on HEK293 WT, its activity was lower than the other ASO-conjugates. These data were expected due to the lack of target receptors on HEK293 WT cell surface; relevant is the result obtained when **CPD-1** was incubated in the presence of CPP. In this case, **CPD-1** efficacy in silencing *MALAT1* expression was significantly increased, arriving to be closer to **CPD-2** activity. On HEK293 receptor overexpressing cells (Figure 53. B), **CPD-3** once again showed the best result in downregulating gene expression levels. From these data was found that the efficiency of **CPD-2** decreased concerning **CPD-4**.

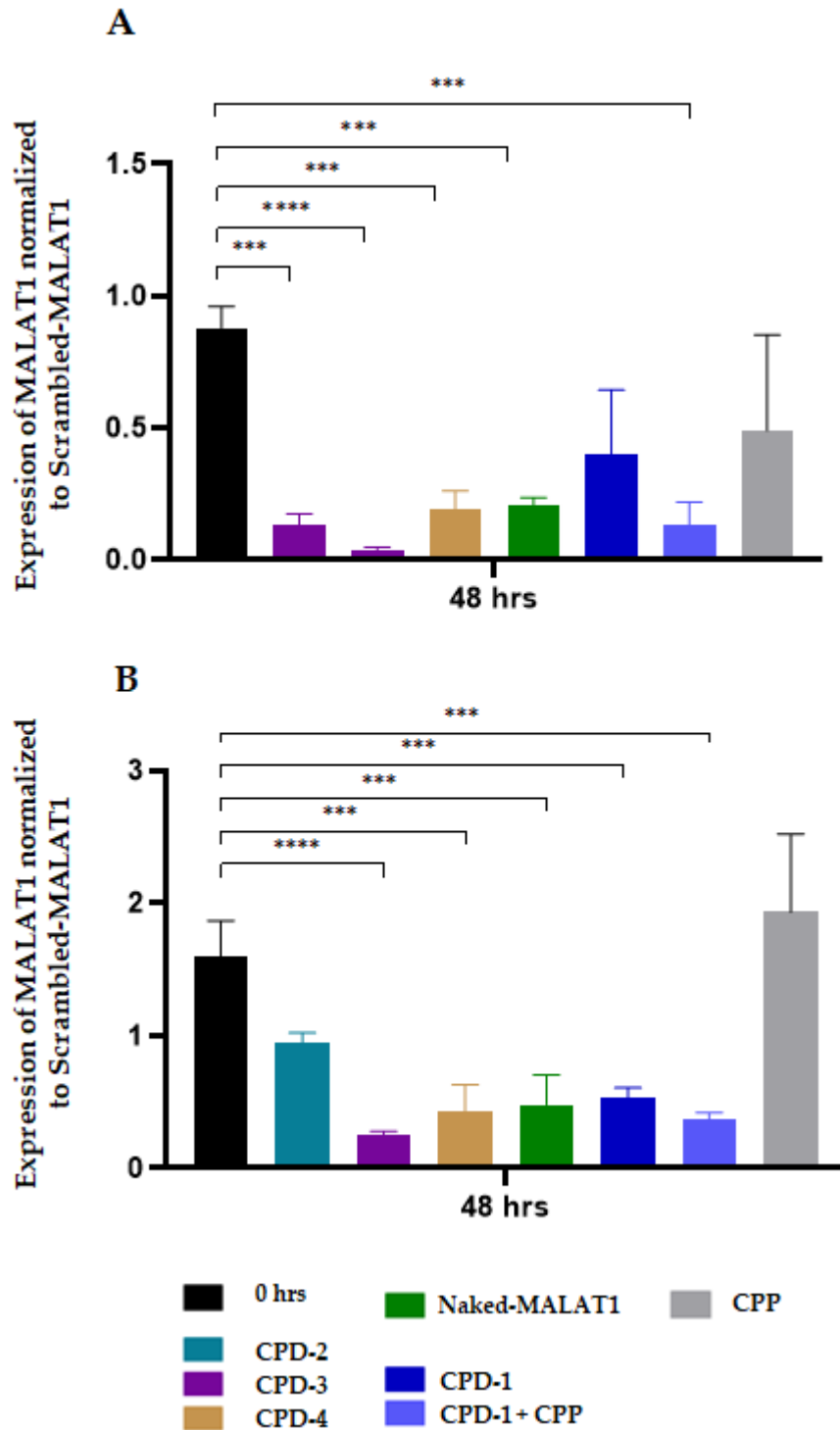


Figure 53

Comparison between ASO-conjugates (CPD-2, CPD-3, CPD-4) at 2.5 μ M, and peptide-ASO (CPD-1), at 2.5 μ M in the absence and presence of CPP (5 μ M), on HEK293 WT (A) and HEK293 receptor overexpressing cells (B) after 48 hrs of treatment. Data are presented as MALAT1 expression normalized to Scrambled-MALAT1.

Data display mean \pm STDEV; n = 2. **** p <0.00001; *** p <0.001.

For what concerns CPD-1 in the absence and presence of CPP, something has changed from the previous experiments. In fact, could be appreciated how the efficiency in silencing

MALAT1 expression was increased when **CPD-1** was incubated in presence of CPP. This result could be due to the higher concentration (2.5 μ M) of **CPD-1** used for this experiment concerning 0.5 μ M used in the previous one. Even if aggregation phenomena could not be completely excluded, the increased concentration of **CPD-1** allowed part of it to escape aggregation phenomena.

Conclusions

We investigated the effect of different antisense oligonucleotides (ASOs) on HEK293 WT and receptor overexpressing cells.

When lipophilic-conjugated ASOs were tested on HEK293 WT cells, was appreciated a relevant capability of silencing target gene expression for all of them both for the lowest concentration of 0.5 μM and the higher of 2.5 and 5 μM , after 24 and 48 hrs of treatment. Even if improvements were appreciated for **CPD-4** from the lowest to the highest concentration, its capability of silence gene expression was the lowest between lipophilic-ASOs.

CPD-2 and **CPD-3** followed the same trend with significant improvement of efficacy in knocking down *MALAT1* expression. For both, no significant change in their capability to silence gene expression was found moving from 2.5 to 5 μM , while from 0.5 to 2.5 μM relevant improvements in their efficacy have been demonstrated. These data highlighted that the concentration of 0.5 μM was probably too low to allow us to appreciate the real effect of ASOs, underestimating it, while 5 μM was probably a too high concentration that could have induced some cytotoxic effects leading to a partial loss of cells and genetic material.

When co-incubated with CPP, **CPD-2** and **CPD-3** were characterized by a significant reduction in the effectiveness of gene silencing if compared to the treatment in the absence of CPP. The hypothesis beyond these results was the possible aggregation phenomena; for that reason, another experiment was conducted incubating CPP after 4 hrs of treatment with lipophilic-ASOs. As expected, the trend confirmed that something happened between ASOs and CPP but adding the cyclic peptide after 4 hrs lets ASOs explicate their action and the decrease of efficacy was sensitively reduced if compared to the previous experiment.

CPD-1 was chosen as a delivery system to specifically target a cell surface receptor and enhance its intracellular bioavailability; when HEK293 receptor overexpressing cells were treated with **CPD-1**, important results have been obtained, with a significant improvement of efficacy with respect to HEK293 WT. Moving from the lowest (0.5 μM) to the highest

concentrations (2.5 and 5 μM) on HEK293 receptor expressing cell line, **CPD-1** capability to silence gene expression resulted significantly improved, mostly at 2.5 μM .

A similar trend was found out also for lipophilic-ASOs; thus, from these results, we hypothesised that 2.5 μM could be the most effective concentration of ASOs to be used to appreciate a significant response to pharmacological stimulations.

In order to evaluate if an increased intracellular bioavailability could be directly correlated to a major downregulation of the target gene, **CPD-1** was co-incubated with a gradient concentration of CPP. The experiment conducted revealed that only using the middle concentration (10 μM) of CPP could be appreciated a little increase in knocking down the *MALAT1* expression. As seen before for lipophilic-ASOs in the presence of CPP, the lack of a significant increase in terms of downregulation of *MALAT1* expression could be correlated to possible aggregation phenomena. When **CPD-1** was incubated at a higher concentration of 2.5 μM with CPP, its efficacy in silencing the gene expression was slightly increased.

In summary, my results indicated that among all tested ASOs, **CPD-3** showed the highest efficiency in knocking down gene expression on HEK293 WT and, **CPD-1**, gave the best result on HEK293 receptor overexpressing cells. Moreover, the addition of CPP, although could bring an increase in the intracellular bioavailability of the ASOs, did not enhance their efficacy, but on the contrary, decreased that.

Appendix I

Publications:

1- Efficient optimization of pyrazolo[3,4-*d*]pyrimidines derivatives as c-Src kinase inhibitors in neuroblastoma treatment.

Alessio Molinari, Anna Lucia Fallacara, Salvatore Di Maria, Claudio Zamperini, Federica Poggialini, Francesca Musumeci, Silvia Schenone, Adriano Angelucci, Alessandro Colapietro, Emmanuele Crespan, Miroslava Kissova, Giovanni Maga, Maurizio Botta.

Bioorganic & Medicinal Chemistry Letters; DOI: [10.1016/j.bmcl.2018.09.024](https://doi.org/10.1016/j.bmcl.2018.09.024)

2- *In vitro* characterization, ADME analysis, and histological and toxicological evaluation of BM1, a macrocyclic amidinourea active against azole-resistant *Candida* strains.

Francesco Orofino, Giuseppina I Truglio, Diego Fiorucci, Ilaria D'Agostino, Matteo Borgini, Federica Poggialini, Claudio Zamperini, Elena Dreassi, Laura Maccari, Riccardo Torelli, Cecilia Martini, Micaela Bernabei, Jacques F Meis, Nitesh Kumar Khandelwal, Rajendra Prasad, Maurizio Sanguinetti, Francesca Bugli, Maurizio Botta.

International Journal of Antimicrobial Agents; DOI: [10.1016/j.ijantimicag.2019.105865](https://doi.org/10.1016/j.ijantimicag.2019.105865)

3- (Thia)calixarenephosphonic Acids as Potent Inhibitors of the Nucleic Acid Chaperone Activity of the HIV-1 Nucleocapsid Protein with a New Binding Mode and Multitarget Antiviral Activity.

Nicolas Humbert, Lesia Kovalenko, Francesco Saladini, Alessia Giannini, Manuel Pires, Thomas Botzanowski, Sergiy Cherenok, Christian Boudier, Kamal K Sharma, Eleonore Real, Olga A Zaporozhets, Sarah Cianférani, Carole Seguin-Devaux, Federica Poggialini, Maurizio Botta, Maurizio Zazzi, Vitaly I Kalchenko, Mattia Mori, Yves Mély.

ACS Infectious Diseases; DOI: [10.1021/acsinfecdis.9b00290](https://doi.org/10.1021/acsinfecdis.9b00290)

4- Synthesis and Antiproliferative Activity of Nitric Oxide-Donor Largazole Prodrugs.

Matteo Borgini, Claudio Zamperini, Federica Poggialini, Luca Ferrante, Vincenzo Summa, Maurizio Botta, Romano Di Fabio.

ACS Medicinal Chemistry Letters; DOI: [10.1021/acsmchemlett.9b00643](https://doi.org/10.1021/acsmchemlett.9b00643)

5- Tyrosine kinase inhibitor Si409 has in vitro and in vivo anti-tumor activity against Diffuse Large B-cell Lymphoma.

Enrico Rango, Salvatore Di Maria, Claudio Zamperini, Federica Poggialini, Emmanuele Crespan, Cecilia Perini, Samantha Sabetta, Simona Saponara, Fabio Fusi, Giovanni Maga, Adriano Angelucci, Eugenio Gaudio, Francesco Bertoni, Silvia Schenone, Lorenzo Botta, Elena Dreassi, and Maurizio Botta.

Pharmaceutical Chemistry Journal; (Accepted)

6- Antibacterial Alkylguanidino Ureas: Molecular Simplification Approach, Searching for Membrane-Based MoA.

Ilaria D'Agostino, Claudia Ardino, Giulio Poli, Filomena Sannio, Massimiliano Lucidi, Federica Poggialini, Silvia Filippi, Daniela Visaggio, Enrico Rango, Elena Petricci Paolo Visca, Lorenzo Botta, Jean-Denis Docquier, and Elena Dreassi.

European Journal of Medicinal Chemistry; DOI: [10.1016/j.ejmech.2022.114158](https://doi.org/10.1016/j.ejmech.2022.114158)

7- The Pyrazolo[3,4-*d*]Pyrimidine Derivative Si306 Encapsulated into Anti-GD2-Immunoliposomes as Therapeutic Treatment of Neuroblastoma.

Enrico Rango, Fabio Pastorino, Chiara Brignole, Arianna Mancini, Federica Poggialini, Salvatore Di Maria, Claudio Zamperini, Giulia Iovenitti, Anna Lucia Fallacara, Samantha Sabetta, Letizia Clementi, Massimo Valoti, Silvia Schenone, Adriano Angelucci, Mirco Ponzoni, Elena Dreassi, and Maurizio Botta.

Biomedicines; DOI: [10.3390/biomedicines10030659](https://doi.org/10.3390/biomedicines10030659)

Appendix II

Conferences

- Poster presentation on “**Evaluation of *in vitro* and *in vivo* pharmacokinetics of Novel Broad-Spectrum antiviral compounds against enveloped viruses**”, Merck Young Chemists' Symposium 2019, (SCI Giovani), November 2019.
- Flash communication and poster presentation on “**Evaluation of *in vitro* and *in vivo* pharmacokinetics of Novel Broad-Spectrum antiviral compounds against enveloped viruses**”, 11th Symposium on Pharmaceutical Profiling in Drug Discovery and Development, Virtual meeting, January 27, 2022.

Bibliography

1. World Health Organization. The top 10 causes of death. <https://www.who.int/news-room/fact-sheets/detail/the-top-10-causes-of-death>. Published 2020.
2. Cagno V, Tintori C, Civra A, et al. Novel broad spectrum virucidal molecules against enveloped viruses. *PLoS One*. 2018;13(12):1-18. doi:10.1371/journal.pone.0208333
3. Peetermans WE, De Munter P. Emerging and re-emerging infectious diseases. *Acta Clin Belg*. 2007;62(5):337-341. doi:10.1179/acb.2007.051
4. World Health Organization. Zoonoses. <https://www.who.int/news-room/fact-sheets/detail/zoonoses>. Published 2020.
5. Palombi N, Brai A, Gerace M, Di Maria S, Orofino F, Corelli F. Viral Envelope Membrane: A Special Entry Pathway and a Promising Drug Target. *Curr Med Chem*. 2021;28:1-20. doi:10.2174/0929867328666210218182203
6. Pillay D, Zambon M. Antiviral drug resistance. *Br Med J*. 1998;317(7159):660-662. doi:<https://doi.org/10.1136/bmj.317.7159.660>
7. Wisskirchen K, Lucifora J, Michler T, Protzer U. New pharmacological strategies to fight enveloped viruses. *Trends Pharmacol Sci*. 2014;35(9):470-478. doi:10.1016/j.tips.2014.06.004
8. Racaniello V, Rey GU. When viruses get naked. 4 July. <https://www.virology.ws/2019/07/04/when-viruses-get-naked/>. Published 2019.
9. Zhou HZ. Structures of viral membrane proteins by high-resolution cryoEM. *Physiol Behav Opin Virol*. 2019;176(3):139-148. doi:10.1016/j.coviro.2014.04.001.Structures
10. Ciuffari B, Henderson E. What are Spike Proteins? News Medical Life Sciences. <https://www.news-medical.net/health/What-are-Spike-Proteins.aspx>. Published 2021.
11. Ryu W-S. Virus Life Cycle. In: *Molecular Virology of Human Pathogenic Viruses*. Vol 3. ; 2017:31-45. doi:<https://dx.doi.org/10.1016%2FB978-0-12-800838-6.00003-5>

12. Mercer J, Schelhaas M, Helenius A. Virus entry by endocytosis. *Annu Rev Biochem.* 2010;79:803-833. doi:10.1146/annurev-biochem-060208-104626
13. White JM, Whittaker GR. Fusion of Enveloped Viruses in Endosomes. *Traffic.* 2016;17(6):593-614. doi:10.1111/tra.12389
14. Jentsch TJ. *CLC Chloride Channels and Transporters: From Genes to Protein Structure, Pathology and Physiology.* Vol 43.; 2008. doi:10.1080/10409230701829110
15. Lafourcade C, Sobo K, Kieffer-Jaquinod S, Garin J, van der Goot FG. Regulation of the V-ATPase along the endocytic pathway occurs through reversible subunit association and membrane localization. *PLoS One.* 2008;3(7). doi:10.1371/journal.pone.0002758
16. Harrison SC. Viral membrane fusion. *Virology.* 2015;479-480:498-507. doi:10.1016/j.virol.2015.03.043
17. Ripa I, Andreu S, López-Guerrero JA, Bello-Morales R. Membrane Rafts: Portals for Viral Entry. *Front Microbiol.* 2021;12(February). doi:10.3389/fmicb.2021.631274
18. Deng F. Advances and challenges in enveloped virus-like particle (VLP)-based vaccines. *J Immunol Sci.* 2018;2(2):36-41. doi:10.29245/2578-3009/2018/2.1118
19. WHO. Dengue and severe Dengue. <https://www.who.int/news-room/fact-sheets/detail/dengue-and-severe-dengue> Published 2021.
20. World Health Organization (WHO). Coronavirus disease (COVID-19): Vaccines.
21. Pardi N, Hogan MJ, Porter FW, Weissman D. mRNA vaccines — a new era in vaccinology. *Nat Publ Gr.* 2018;17(4):261-279. doi:10.1038/nrd.2017.243
22. Salazar G, Zhang N, Fu TM, An Z. Antibody therapies for the prevention and treatment of viral infections. *npj Vaccines.* 2017;2(1):1-12. doi:10.1038/s41541-017-0019-3
23. Andreano E, Nicastri E, Paciello I, et al. Article Extremely potent human monoclonal antibodies from COVID-19 convalescent patients II Article Extremely potent human monoclonal antibodies from COVID-19 convalescent patients. *Cell.* 2021;184(7):1821-

1835.e16. doi:10.1016/j.cell.2021.02.035

24. Verma J, Subbarao N, Rajala MS. Envelope proteins as antiviral drug target. *J Drug Target*. 2020;28(10):1046-1052. doi:10.1080/1061186X.2020.1792916
25. Chen X, Si L, Liu D, et al. Neoechinulin B and its analogues as potential entry inhibitors of influenza viruses, targeting viral hemagglutinin. *Eur J Med Chem*. 2015;93:182-195. doi:10.1016/j.ejmech.2015.02.006
26. Mckimm-Breschkin JL. Influenza neuraminidase inhibitors: Antiviral action and mechanisms of resistance. *Influenza Other Respi Viruses*. 2013;7(1 SUPPL.1):25-36. doi:10.1111/irv.12047
27. Davis LE. Influenza Virus. *Encycl Neurol Sci*. 2014;2:695-697. doi:10.1016/B978-0-12-385157-4.00381-X
28. James SH, Whitley RJ. 172 - *Influenza Viruses*. Fourth Edi. Elsevier Ltd doi:10.1016/B978-0-7020-6285-8.00172-6
29. National Center for Immunization and Respiratory Diseases. Past Pandemics. <https://www.cdc.gov/flu/pandemic-resources/basics/past-pandemics.html>. Published 2018.
30. National Center for Immunization and Respiratory Diseases. Types of Influenza Viruses. <https://www.cdc.gov/flu/about/viruses/types.htm>. Published 2019.
31. Nuwarda RF, Alharbi AA, Kayser V. An overview of influenza viruses and vaccines. *Vaccines*. 2021;9(9). doi:10.3390/vaccines9091032
32. Dou D, Revol R, Östbye H, Wang H, Daniels R. Influenza A virus cell entry, replication, virion assembly and movement. *Front Immunol*. 2018;9(JUL):1-17. doi:10.3389/fimmu.2018.01581
33. Martin K, Helenius A. Transport of incoming influenza virus nucleocapsids into the nucleus. *J Virol*. 1991;65(1):232-244. doi:10.1128/jvi.65.1.232-244.1991
34. Samji T. Influenza A: Understanding the viral life cycle. *Yale J Biol Med*. 2009;82(4):153-

159.

35. Zanin M, Baviskar P, Webster R, Webby R. The Interaction between Respiratory Pathogens and Mucus. *Cell Host Microbe*. 2016;19(2):159-168. doi:10.1016/j.chom.2016.01.001
36. Reperant LA, Kuiken T, Grenfell BT, Osterhaus ADME, Dobson AP. Linking Influenza Virus Tissue Tropism to Population-Level Reproductive Fitness. *PLoS One*. 2012;7(8). doi:10.1371/journal.pone.0043115
37. Ibricevic A, Pekosz A, Walter MJ, et al. Influenza Virus Receptor Specificity and Cell Tropism in Mouse and Human Airway Epithelial Cells. *J Virol*. 2006;80(15):7469-7480. doi:10.1128/jvi.02677-05
38. Principi N, Camilloni B, Alunno A, Polinori I, Argentiero A, Esposito S. Drugs for Influenza Treatment: Is There Significant News? *Front Med*. 2019;6(May):1-7. doi:10.3389/fmed.2019.00109
39. De Clercq E. Antiviral agents active against influenza A viruses. *Nat Rev Drug Discov*. 2006;5(12):1015-1025. doi:10.1038/nrd2175
40. Pierson TC, Diamond MS. The continued threat of emerging flaviviruses. *Nat Microbiol*. 2020;5(6):796-812. doi:10.1038/s41564-020-0714-0
41. Qureshi A. Flavivirus. In: Qureshi A, ed. *Zika Virus Disease: From Origin to Outbreak*. Academic Press; 2018:47-61. doi:10.1016/B978-0-12-812365-2.00004-4
42. Ryu W-S. Flaviviruses. In: Ryu W-S, ed. *Molecular Virology of Human Pathogenic Viruses*. Academic Press; 2017:165-175. doi:10.1017/CBO9780511541728.010
43. Mukhopadhyay S, Kuhn RJ, Rossmann MG. A structural perspective of the Flavivirus life cycle. *Nat Rev Microbiol*. 2005;3(1):13-22. doi:10.1038/nrmicro1067
44. Cruz-Oliveira C, Freire JM, Conceição TM, Higa LM, Castanho MARB, Da Poian AT. Receptors and routes of dengue virus entry into the host cells. *FEMS Microbiol Rev*. 2015;39(2):155-170. doi:10.1093/femsre/fuu004

45. World Health Organization (WHO). Zika virus. <https://www.who.int/news-room/fact-sheets/detail/zika-virus>. Published 2018.
46. Kazmi SS, Ali W, Bibi N, Nouroz F. A review on Zika virus outbreak, epidemiology, transmission and infection dynamics. *J Biol Res*. 2020;27(1):1-11. doi:10.1186/s40709-020-00115-4
47. Tang H, Hammack C, Ogden SC, et al. Zika virus infects human cortical neural progenitors and attenuates their growth. *Cell Stem Cell*. 2016;18(5):587-590. doi:10.1016/j.stem.2016.02.016
48. Guzman MG, Gubler DJ, Izquierdo A, Martinez E, Halstead SB. Dengue infection. *Nat Publ Gr*. 2016;2:1-26. doi:10.1038/nrdp.2016.55
49. Wang W, Nayim A, Chang MR, et al. Dengue hemorrhagic fever e A systemic literature review of current perspectives on pathogenesis , prevention and control. *J Microbiol Immunol Infect*. 2020;53(6):963-978. doi:10.1016/j.jmii.2020.03.007
50. Zhao R, Wang M, Cao J, et al. Flavivirus: From structure to therapeutics development. *Life*. 2021;11(7):1-25. doi:10.3390/life11070615
51. Farfan-Morales CN, Cordero-Rivera CD, Reyes-Ruiz JM, et al. Anti-flavivirus Properties of Lipid-Lowering Drugs. *Front Physiol*. 2021;12(October):1-22. doi:10.3389/fphys.2021.749770
52. Fenwick C, Amad M, Bailey MD, et al. Preclinical profile of BI 224436, a novel hiv-1 non-catalytic-site integrase inhibitor. *Antimicrob Agents Chemother*. 2014;58(6):3233-3244. doi:10.1128/AAC.02719-13
53. Tintori C, Corradi V, Magnani M, Manetti F, Botta M. Targets looking for drugs: A multistep computational protocol for the development of structure-based pharmacophores and their applications for hit discovery. *J Chem Inf Model*. 2008;48(11):2166-2179. doi:10.1021/ci800105p
54. Rinaldi M, Tintori C, Franchi L, et al. A Versatile and Practical Synthesis toward the Development of Novel HIV-1 Integrase Inhibitors. *ChemMedChem*. 2011;6(2):343-352.

doi:10.1002/cmdc.201000510

55. Tiberi M, Tintori C, Ceresola ER, et al. 2-Aminothiazolones as anti-hiv agents that act as gp120-cd4 inhibitors. *Antimicrob Agents Chemother.* 2014;58(6):3043-3052. doi:10.1128/AAC.02739-13
56. Tintori C, Iovenitti G, Ceresola ER, et al. Rhodanine derivatives as potent anti-HIV and anti-HSV microbicides. *PLoS One.* 2018;13(6):1-19. doi:10.1371/journal.pone.0198478
57. Kramer SE, Routh JI. The binding of salicylic acid and acetylsalicylic acid to human serum albumin. *Clin Biochem.* 1973;6(C):98-105. doi:10.1016/S0009-9120(73)80018-9
58. Lassalas P, Gay B, Lasfargeas C, et al. Structure Property Relationships of Carboxylic Acid Isosteres. *J Med Chem.* 2016;59(7):3183-3203. doi:10.1021/acs.jmedchem.5b01963
59. Pinter T, Jana S, Courtemanche RJM, Hof F. Recognition properties of carboxylic acid bioisosteres: Anion binding by tetrazoles, aryl sulfonamides, and acyl sulfonamides on a calix[4]arene scaffold. *J Org Chem.* 2011;76(10):3733-3741. doi:10.1021/jo200031u
60. Gillis EP, Eastman KJ, Hill MD, Donnelly DJ, Meanwell NA. Applications of Fluorine in Medicinal Chemistry. *J Med Chem.* 2015;58(21):8315-8359. doi:10.1021/acs.jmedchem.5b00258
61. Kansy M, Senner F, Gubernator K. Screening: Parallel Artificial Membrane Permeation Assay in the Description of. 1998;41(7):0-3.
62. Evans D, Yalkowsky S, Wu S, Pereira D, Fernandes P. Overcoming the Challenges of Low Drug Solubility in the Intravenous Formulation of Solithromycin. *J Pharm Sci.* 2018;107(1):412-418. doi:10.1016/j.xphs.2017.10.030
63. Li P, Zhao L. Developing early formulations: Practice and perspective. *Int J Pharm.* 2007;341(1-2):1-19. doi:10.1016/j.ijpharm.2007.05.049
64. Pasqua E, Hamblin N, Edwards C, Baker-Glenn C, Hurley C. Developing inhaled drugs for respiratory diseases: A medicinal chemistry perspective. *Drug Discov Today.* 2021;xxx(xx). doi:10.1016/j.drudis.2021.09.005

65. Park SY, Kim JS. A short guide to histone deacetylases including recent progress on class II enzymes. *Exp Mol Med*. 2020;52(2):204-212. doi:10.1038/s12276-020-0382-4
66. Borgini M, Zamperini C, Poggialini F, et al. Synthesis and Antiproliferative Activity of Nitric Oxide-Donor Largazole Prodrugs. *ACS Med Chem Lett*. 2020;11(5):846-851. doi:10.1021/acsmchemlett.9b00643
67. Yoon S, Eom GH. HDAC and HDAC Inhibitor: From Cancer to Cardiovascular Diseases. *Chonnam Med J*. 2016;52(1):1. doi:10.4068/cmj.2016.52.1.1
68. McClure JJ, Li X, Chou CJ. *Advances and Challenges of HDAC Inhibitors in Cancer Therapeutics*. Vol 138. 1st ed. Elsevier Inc.; 2018. doi:10.1016/bs.acr.2018.02.006
69. Dokmanovic M, Clarke C, Marks PA. Histone deacetylase inhibitors: Overview and perspectives. *Mol Cancer Res*. 2007;5(10):981-989. doi:10.1158/1541-7786.MCR-07-0324
70. Ellis L, Pili R. Histone deacetylase inhibitors: Advancing therapeutic strategies in hematological and solid malignancies. *Pharmaceuticals*. 2010;3(8):2441-2469. doi:10.3390/ph3082441
71. Haberland M, Montgomery RL, Olson EN. The many roles of histone deacetylases in development and physiology: Implications for disease and therapy. *Nat Rev Genet*. 2009;10(1):32-42. doi:10.1038/nrg2485
72. Yang X-J, Grégoire S. Class II Histone Deacetylases: from Sequence to Function, Regulation, and Clinical Implication. *Mol Cell Biol*. 2005;25(8):2873-2884. doi:10.1128/mcb.25.8.2873-2884.2005
73. North BJ, Verdin E. Protein family review Sirtuins: Sir2-related NAD-dependent protein deacetylases Gene organization and evolutionary history. *Genome Biol*. 2004;5(224). <http://genomebiology.com/2004/5/5/224>.
74. Tumbarello DA, Turner CE. Hic-5 Contributes to Transformation Through a RhoA / ROCK-dependent Pathway. *J Cell Physiol*. 2006;211(3)(May):736-747. doi:10.1002/JCP
75. Eldridge MJG, Pereira JM, Impens F, Hamon MA. Active nuclear import of the deacetylase Sirtuin-2 is controlled by its C-terminus and importins. *Sci Rep*.

2020;10(1):1-12. doi:10.1038/s41598-020-58397-6

76. Yang W, van de Ven RAH, Haigis MC. *Mitochondrial Sirtuins: Coordinating Stress Responses Through Regulation of Mitochondrial Enzyme Networks*. Elsevier Inc.; 2018. doi:10.1016/B978-0-12-813499-3.00008-3
77. Alhazzazi TY, Kamarajan P, Verdin E, Kapila YL. SIRT3 and cancer: Tumor promoter or suppressor? *Biochim Biophys Acta - Rev Cancer*. 2011;1816(1):80-88. doi:10.1016/j.bbcan.2011.04.004
78. Ardestani PM, Liang F. Sub-cellular localization, expression and functions of Sirt6 during the cell cycle in HeLa cells. *Nucl (United States)*. 2012;3(5):442-451. doi:10.4161/nucl.21134
79. Khan RI, Shahriar S, Nirzhor R, Akter R. A Review of the Recent Advances Made with SIRT6 and its Implications on Aging Related Processes , Major Human Diseases , and Possible Therapeutic Targets. *Biomolecules*. 2018;8(44). doi:10.3390/biom8030044
80. Wang H, Zhu W. Advances in Cellular Characterization of the Sirtuin. *Front Endocrinol (Lausanne)*. 2018;9(November):652. doi:10.3389/fendo.2018.00652
81. Garmpis N, Damaskos C, Garmpi A, Valsami S, Dimitroulis D. *Pharmacoeugenetics of Histone Deacetylase Inhibitors in Cancer*. Vol 5. Elsevier Inc.; 2019. doi:10.1016/B978-0-12-813939-4.00013-9
82. Sahakian E, Woan K, Villagra A, Sotomayor EM. *Epigenetic Approaches : Emerging Role of Histone Deacetylase Inhibitors in Cancer Immunotherapy*. Second Edi. Elsevier; 2013. doi:10.1016/B978-0-12-394296-8.00022-1
83. Hontecillas-Prieto L, Flores-Campos R, Silver A, de Álava E, Hajji N, García-Domínguez DJ. Synergistic Enhancement of Cancer Therapy Using HDAC Inhibitors: Opportunity for Clinical Trials. *Front Genet*. 2020;11(September). doi:10.3389/fgene.2020.578011
84. Glozak MA, Seto E. Histone deacetylases and cancer. *Oncogene*. 2007;26(37):5420-5432. doi:10.1038/sj.onc.1210610

85. Li Y, Seto E. HDACs and HDAC inhibitors in cancer development and therapy. *Cold Spring Harb Perspect Med*. 2016;6(10):1-34. doi:10.1101/cshperspect.a026831
86. Pant K, Peixoto E, Richard S, Gradilone SA. Role of Histone Deacetylases in Carcinogenesis: Potential Role in Cholangiocarcinoma. *Cells*. 2020;9(3):780. doi:10.3390/cells9030780
87. Zhao E, Hou J, Ke X, et al. The roles of sirtuin family proteins in cancer progression. *Cancers (Basel)*. 2019;11(12):1-22. doi:10.3390/cancers11121949
88. Eckschlager T, Plch J, Stiborova M, Hrabeta J. Histone deacetylase inhibitors as anticancer drugs. *Int J Mol Sci*. 2017;18(7):1-25. doi:10.3390/ijms18071414
89. Hu J, Jing H, Lin H. Sirtuin inhibitors as anticancer agents. *Future Med Chem*. 2014;6(8):945-966. doi:10.4155/fmc.14.44
90. B. Kim JH. An Overview of Naturally Occurring Histone Deacetylase Inhibitors. *Curr Top Med Chem*. 2015;14(24):2759-2782. doi:10.2174/1568026615666141208105614.An
91. Yu M, Salvador LA, Sy SKB, et al. Largazole pharmacokinetics in rats by LC-MS/MS. *Mar Drugs*. 2014;12(3):1623-1640. doi:10.3390/md12031623
92. Nasveschuk CG, Ungermannova D, Liu X, Phillips AJ. A Concise Total Synthesis of Largazole, Solution Structure, and Some Preliminary Structure Activity Relationships. *Org Lett*. 2008;10(16):3595-3598. doi:doi:10.1021/ol8013478.
93. Al-awadhi FH, Salvador-reyes LA, Elsadek LA, Ratnayake R, Chen Q, Luesch H. Largazole is a Brain-Penetrant Class I HDAC Inhibitor with Extended Applicability to Glioblastoma and CNS Diseases. *ACS Chem Neurosci*. 2020;11:1937-1943. doi:https://dx.doi.org/10.1021/acchemneuro.0c00093
94. Hong J, Luesch H. Largazole: From Discovery to Broad-Spectrum Therapy. *Nat Prod Rep*. 2012;29(4):449-456. doi:10.1039/c2np00066k.
95. Lee SU, Kwak HB, Pi SH, et al. In vitro and in vivo osteogenic activity of largazole. *ACS Med Chem Lett*. 2011;2(3):248-251. doi:10.1021/ml1002794

96. Liu Y, Wang Z, Wang J, et al. A histone deacetylase inhibitor, largazole, decreases liver fibrosis and angiogenesis by inhibiting transforming growth factor- β and vascular endothelial growth factor signalling. *Liver Int.* 2013;33(4):504-515. doi:10.1111/liv.12034
97. Cole KE, Dowling DP, Boone MA, Phillips AJ, Christianson DW. Structural basis of the antiproliferative activity of largazole, a depsipeptide inhibitor of the histone deacetylases. *J Am Chem Soc.* 2011;133(32):12474-12477. doi:10.1021/ja205972n
98. McCarthy HO, Coulter JA. *Nitric Oxide Methods and Protocols.* (McCarthy HO, Coulter JA, eds.). Humana Press (Springer Science+Business Media); 2011. doi:10.1007/978-1-61737-964-2
99. Förstermann U, Sessa WC. Nitric oxide synthases: Regulation and function. *Eur Heart J.* 2012;33(7):829-837. doi:10.1093/eurheartj/ehr304
100. Korde Choudhari S, Chaudhary M, Bagde S, Gadbail AR, Joshi V. Nitric oxide and cancer: A review. *World J Surg Oncol.* 2013;11:1-11. doi:10.1186/1477-7819-11-118
101. Wang H, Wang L, Xie Z, et al. Nitric Oxide (NO) and NO Synthases (NOS)-Based Targeted Therapy for Colon Cancer. *Cancers (Basel).* 2020;12(7):1881. doi:doi.org/10.3390/cancers12071881
102. Feng CW, Wang LD, Jiao LH, Liu B, Zheng S, Xie XJ. Expression of p53, inducible nitric oxide synthase and vascular endothelial growth factor in gastric precancerous and cancerous lesions: Correlation with clinical features. *BMC Cancer.* 2002;2:1-7. doi:10.1186/1471-2407-2-8
103. Xu W, Liu LZ, Loizidou M, Ahmed M, Charles IG. The role of nitric oxide in cancer. *Cell Res.* 2002;12(5-6):311-320. doi:10.1038/sj.cr.7290133
104. Hu Y, Xiang J, Su L, Tang X. The regulation of nitric oxide in tumor progression and therapy. *J Int Med Res.* 2020;48(2). doi:10.1177/0300060520905985
105. Keefer LK, Nims RW, Davies KM, Wink DA. "NONOates" (1-substituted diazen-1-ium-1,2-diolates) as nitric oxide donors: Convenient nitric oxide dosage forms. In:

106. Mintz J, Vedenko A, Rosete O, et al. Current Advances of Nitric Oxide in Cancer and Anticancer Therapeutics. *Vaccines*. 2021;9(94). doi:10.3390/vaccines9020094
107. Borretto E, Lazzarato L, Spallotta F, et al. Synthesis and biological evaluation of the first example of NO-donor histone deacetylase inhibitor. *ACS Med Chem Lett*. 2013;4(10):994-999. doi:10.1021/ml400289e
108. Duan W, Li J, Inks ES, et al. Design, synthesis, and antitumor evaluation of novel histone deacetylase inhibitors equipped with a phenylsulfonylfuroxan module as a nitric oxide donor. *J Med Chem*. 2015;58(10):4325-4338. doi:10.1021/acs.jmedchem.5b00317
109. Ding Q, Liu C, Zhao C, et al. Synthesis and biological study of class I selective HDAC inhibitors with NO releasing activity. *Bioorg Chem*. 2020;104(June):104235. doi:10.1016/j.bioorg.2020.104235
110. Kaczmarek JC, Kowalski PS, Anderson DG. Advances in the delivery of RNA therapeutics: From concept to clinical reality. *Genome Med*. 2017;9(1):1-16. doi:10.1186/s13073-017-0450-0
111. Gao Y, Patil S, Qian A. The role of microRNAs in bone metabolism and disease. *Int J Mol Sci*. 2020;21(17):1-23. doi:10.3390/ijms21176081
112. Feng R, Patil S, Zhao X, Miao Z, Qian A. RNA Therapeutics - Research and Clinical Advancements. *Front Mol Biosci*. 2021;8(September):1-13. doi:10.3389/fmolb.2021.710738
113. Crooke ST, Witztum JL, Bennett CF, Baker BF. RNA-Targeted Therapeutics. *Cell Metab*. 2018;27(4):714-739. doi:10.1016/j.cmet.2018.03.004
114. Hu B, Zhong L, Weng Y, et al. Therapeutic siRNA: state of the art. *Signal Transduct Target Ther*. 2020;5(1). doi:10.1038/s41392-020-0207-x
115. Karaki S, Clement P, Palma R. Antisense Oligonucleotides, A Novel Developing Targeting Therapy. In: ; 2019. doi:10.5772/intechopen.82105

116. Mayr FB, Knöbl P, Jilma B, et al. The aptamer ARC1779 blocks von Willebrand factor-dependent platelet function in patients with thrombotic thrombocytopenic purpura ex vivo. *Hemostasis*. 2010;50(May):1079-1087. doi:10.1111/j.1537-2995.2009.02554.x
117. Peng H, Latifi B, Chen IA, Lupta A. Self-cleaving ribozymes: substrate specificity and synthetic biology applications. *RSC Chem Biol*. 2021;2:1370-1383. doi:10.1039/d0cb00207k
118. Soo K, Sun X, Aikins ME, Moon JJ. Non-viral COVID-19 vaccine delivery systems. *Adv Drug Deliv Rev*. 2021;169:137-151. doi:10.1016/j.addr.2020.12.008
119. Chaudhary N, Weissman D, Whitehead KA. mRNA vaccines for infectious diseases: principles, delivery and clinical translation. *Nat Rev Drug Discov*. 2021;20(November):817-838. doi:10.1038/s41573-021-00283-5
120. Magadum A, Kaur K, Zangi L. mRNA-Based Protein Replacement Therapy for the Heart. *Mol Ther*. 2019;27(4):785-793. doi:10.1016/j.ymthe.2018.11.018
121. Damase TR, Sukhovshin R, Boada C, Taraballi F, Pettigrew RI, Cooke JP. The Limitless Future of RNA Therapeutics. *Front Bioeng Biotechnol*. 2021;9(March):1-24. doi:10.3389/fbioe.2021.628137
122. Furdon PJ, Dominski Z, Kole R, Cancer L, Hill C. review), methylphosphonate deoxyoligonucleosides (MP-oligos , developed by Miller , Ts ' o *Nucleic Acids Research*. 1989;17(22).
123. Rinaldi C, Wood MJA. Antisense oligonucleotides: The next frontier for treatment of neurological disorders. *Nat Rev Neurol*. 2018;14(1):9-22. doi:10.1038/nrneurol.2017.148
124. Weidolf L, Björkbom A, Dahlén A, et al. Distribution and biotransformation of therapeutic antisense oligonucleotides and conjugates. *Drug Discov Today*. 2021;26(10):2244-2258. doi:10.1016/j.drudis.2021.04.002
125. Roberts TC, Langer R, Wood MJA. Advances in oligonucleotide drug delivery. *Nat Rev Drug Discov*. 2020;19(10):673-694. doi:10.1038/s41573-020-0075-7
126. Geary RS, Norris D, Yu R, Bennett CF. Pharmacokinetics, biodistribution and cell

- uptake of antisense oligonucleotides. *Adv Drug Deliv Rev.* 2015;87:46-51. doi:10.1016/j.addr.2015.01.008
127. Knerr L, Prakash TP, Lee R, et al. Glucagon like Peptide 1 Receptor Agonists for Targeted Delivery of Antisense Oligonucleotides to Pancreatic Beta Cell. *J Am Chem Soc.* 2021;143(9):3416-3429. doi:10.1021/jacs.0c12043
128. Roberts TC, Langer R, Wood MJA. Advances in oligonucleotide drug delivery. *Nat Rev Drug Discov.* 2020;19(10):673-694. doi:10.1038/s41573-020-0075-7
129. Kurrikoff K, Vunk B, Langel Ü. Status update in the use of cell-penetrating peptides for the delivery of macromolecular therapeutics. *Expert Opin Biol Ther.* 2021;21(3):361-370. doi:10.1080/14712598.2021.1823368
130. McClorey G, Banerjee S. Cell-penetrating peptides to enhance delivery of oligonucleotide-based therapeutics. *Biomedicines.* 2018;6(2):1-15. doi:10.3390/biomedicines6020051
131. Crooke ST, Wang S, Vickers TA, Shen W, Liang XH. Cellular uptake and trafficking of antisense oligonucleotides. *Nat Biotechnol.* 2017;35(3):230-237. doi:10.1038/nbt.3779
132. Juliano RL, Ming X, Nakagawa O. Cellular Uptake and Intracellular Trafficking of Antisense and siRNA Oligonucleotides. *Bioconjug Chem.* 2012;23(2):147-157. doi:10.1021/bc200377d.Cellular
133. Cerritelli SM, Crouch RJ. Ribonuclease H: The enzymes in eukaryotes. *FEBS J.* 2009;276(6):1494-1505. doi:10.1111/j.1742-4658.2009.06908.x
134. Dias N, Stein CA. Antisense oligonucleotides: Basic concepts and mechanisms. *Mol Cancer Ther.* 2002;1(5):347-355.
135. Dhuri K, Bechtold C, Quijano E, et al. Antisense oligonucleotides: An emerging area in drug discovery and development. *J Clin Med.* 2020;9(6):1-24. doi:10.3390/JCM9062004
136. Bennett CF, Baker BF, Pham N, Swayze E, Geary RS. Pharmacology of Antisense Drugs. *Annu Rev Pharmacol Toxicol.* 2017;57:81-105. doi:10.1146/annurev-pharmtox-

010716-104846

137. Zhao M, Wang S, Li Q, Ji Q, Guo P, Liu X. Malat1: A long non-coding RNA highly associated with human cancers (review). *Oncol Lett.* 2018;16(1):19-26. doi:10.3892/ol.2018.8613
138. Arun G, Aggarwal D, Spector DL. MALAT1 long non-coding RNA: Functional implications. *Non-coding RNA.* 2020;6(2):1-17. doi:10.3390/NCRNA6020022
139. Gordon AD, Biswas S, Feng B, Chakrabarti S. MALAT1 : A regulator of inflammatory cytokines in diabetic complications. *Endocrinol Diabetes Metab.* 2018;1(2). doi:10.1002/edm2.10

Supporting graphics created with BioRender.com